

THERMAL CONDUCTIVITY OF REFRACTORY BRICK MATERIALS //

BY

JOHN NJOROCE / KIMANI

THIS THESIS HAS BEEN ACCEPTED FOR  
THE DEGREE OF..... MSc 1989 .....  
AND A COPY MAY BE FOUND IN THE  
UNIVERSITY LIBRARY

A thesis submitted in partial fulfilment for  
the award of the degree of Master of Science in  
Physics in the University of Nairobi.

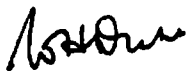
1989

UNIVERSITY OF NAIROBI  
LIBRARY


This thesis is my original work and has not been presented for a degree in any other University.

JOHN NJOROGE KIMANI

This thesis has been submitted for examination with our approval as University Supervisors.



DR. W.H. DRAKE  
Department of Physics,  
University of Nairobi.



DR. ERNEST SARHENE  
Department of Physics,  
University of Nairobi.

### ACKNOWLEDGEMENTS

I owe a lot of gratitude to my major Supervisor, Dr. E. Sarhene who not only introduced me to materials Science but also devoted a lot of time to offer constant guidance and encouragement throughout the course of this work.

I am greatly indebted to my associate supervisor, Dr. W.H. Drake for his continuous guidance and suggestions in the preparation of this thesis.

I wish to sincerely thank members of the Physics Department for the part they played to bring this work to what it is.

Special thanks go to the director and staff, Kenya Industrial Research Development Institute (KIRDI), Chairmen of Geology and Civil Engineering Departments respectively for allowing me access to their facilities, and to the Director Kenya Bureau of Standards for allowing me the use of facilities to calibrate the thermocouples.

My sincere thanks goes to my wife Jennifer Nyambura for her perseverance and encouragement and for proof reading the text. I owe a lot to my son Kimani, who have missed much attention during the preparation of this work.

I thank the Kenya Government and the University of Nairobi who financed the whole project. Thanks also goes to Jane Muhia who patiently typed this thesis.

Last but not least, I wish to thank all friends and relatives who directly or indirectly made this work possible. To Baba Kim, Awimbo, Nyaga, Muthigani, Macharia, Njoka, Gitau and Mate to mention but a few.

## DEDICATION

This thesis is dedicated to my parents,  
Perpetuah Wanjiku and Daniel Kimani for their  
commitment and patience.

C O N T E N T S

|   | <u>PAGE</u> |
|---|-------------|
| Acknowledgements -----  | iii         |
| List of Tables -----  | x           |
| List of Figures -----   | xvi         |
| List of Symbols -----   | xxii        |
| Abstract -----  | xxvii       |
| <br>  |             |
| CHAPTER 1: <u>INTRODUCTION</u> -----  | 1           |
| 1.1.0.        Refractory materials -----  | 3           |
| 1.2.0.        Present work -----  | 10          |
| <br>  |             |
| CHAPTER 2: <u>LITERATURE REVIEW</u>   |             |
| 2.1.0.        Introduction -----  | 13          |
| 2.2.0.        Survey of previous work on<br>thermal conductivity of<br>refractory materials ----- | 13          |
| <br>  |             |
| CHAPTER 3: <u>THEORETICAL BACKGROUND</u>  |             |
| 3.1.0.        Introduction -----  | 23          |
| 3.2.0.        Thermal conductivity -----  | 26          |
| 3.3.0.        Factors influencing thermal<br>conductivity -----                                   | 29          |
| 3.3.1.     Chemical composition -----   | 29          |
| 3.3.2.     Effect of heat treatment -----   | 32          |

|  | <u>PAGE</u> |
|--|-------------|
| 3.3.3. Effect of texture and porosity -----  | 33          |
| 3.3.4. The effect of particle size ---   | 36          |
| 3.3.5. Effect of saturant fluid ----   | 36          |
| 3.3.6. Effect of temperature -----   | 37          |
| 3.4.0. Theory of thermal conductivity measurements -----   | 37          |
| 3.4.1.0. The transient hot wire method -----   | 41          |
| 3.4.1.1. The transient hot wire method of comparison -----   | 44          |
| 3.5.0. Theoretical models for the prediction of thermal conductivity values of heterogeneous porous systems -- | 47          |
| <br><b>CHAPTER 4: <u>EXPERIMENTAL DETAILS</u></b>  |             |
| 4.1.0. Introduction -----  | 58          |
| 4.2.0. Characterisation of samples --  | 58          |
| 4.2.1. Grain size analysis -----   | 58          |
| 4.3.1.1. Sieving -----   | 59          |
| 4.2.1.2. Sedimentation -----   | 59          |
| 4.2.2. Photoanalysis -----   | 60          |
| 4.2.3. Chemical analysis -----   | 61          |

|  | <u>PAGE</u> |
|--|-------------|
| 4.2.4. Measurement of shrinkage on firing -----  | 61          |
| 4.2.5. Measurement of weight loss on firing -----  | 62          |
| 4.2.6. Specific gravity and porosity measurements for the materials in granular form ----- | 63          |
| 4.2.7. Porosity measurements for the bricks -----  | 64          |
| 4.3.0. Preparation of the brick samples -----  | 67          |
| 4.3.1. The mold -----  | 68          |
| 4.3.2. Mixing and pressing -----   | 68          |
| 4.3.3. The heat treatment -----  | 71          |
| 4.3.4. Preparation of samples of varied porosity -----                                     | 72          |
| 4.4.0. Thermal conductivity measurements -----   | 72          |
| <br>   |             |
| CHAPTER 5: <u>EXPERIMENTAL RESULTS AND DISCUSSION</u>                                      |             |
| 5.0.0. Introduction -----  | 76          |
| 5.1.0. Sample characterisation -----   | 76          |
| 5.1.1. Chemical analysis -----   | 76          |
| 5.1.2. Mineralogical Analysis -----  | 79          |

|  | <u>PAGE</u> |
|--|-------------|
| 5.1.3. Optical characterisation -----  | 81          |
| 5.1.4. Particle size distribution ----   | 87          |
| 5.1.5. Specific gravity and porosity<br>measurements for the materials<br>in granular form -----   | 91          |
| 5.2.0. Effect of firing the materials<br>to different temperatures ----  | 92          |
| 5.3.0. Effect of casting pressure ----   | 94          |
| 5.4.0. Effect of porosity variation --   | 95          |
| 5.4.1. Effect of moisture on thermal<br>conductivity at different<br>percentage porosities -----   | 95          |
| 5.4.2. Comparison between experimental<br>results and theoretical<br>prediction of the variation<br>of thermal conductivity with<br>porosity -----                 | 97          |
| 5.5.0. Effect of temperature on<br>thermal conductivity -----  | 102         |
| 5.5.1. Comparison between experimental<br>results with those theoreti-<br>cally predicted for the<br>variation of thermal conduc-<br>tivity with temperature ----- | 102         |



|            | <u>PAGE</u>   |
|------------|---|
| CHAPTER 6: |   |
|            | <u>CONCLUSIONS AND RECOMMENDATIONS</u>  |
| 6.1.0.     | Conclusions ----- 112   |
| 6.2.0.     | Recommendations for future<br>work ----- 116  |
|            | REFERENCES ----- 118  |
|            | APPENDICES ----- 133  |
| APPENDIX : |   |
| A.1.       | Analysis of thermal data ---- 133   |
| A.2.       | Determination of the<br>correction time $t_0$ ----- 137   |
| A.3.       | Calculation of thermal<br>conductivity of the solid<br>phase, $K_s$ ----- 138                                 |
| A.4.       | Thermal conductivity data --- 140   |
| A.5.       | More figures on variation<br>of thermal conductivity<br>with the factors considered<br>in the study ----- 162 |

LIST OF TABLES

|                |  |   |
|----------------|--|---|
| Table 5.1:     | Chemical composition for kaolinite. -----  |   |
| Table 5.2:     | Chemical composition for fireclay. -----   |   |
| Table 5.3:     | Chemical composition for Kisii soap stone. --  |   |
| Table 5.4:     | Chemical composition for Siaya Clay.-----  |   |
| Table 5.5 a&b: | Mineralogical analysis for the materials.-----   |   |
| Table 5.6:     | Particle size distribution for the<br>materials. -----   |   |
| Table 5.7:     | Specific gravity and porosity values for<br>the materials in granular form. -----  |   |
| Table 5.8:     | Thermal conductivity and porosity values<br>for two fireclay bricks, one prepared<br>by hand pressing and the other one by<br>machine pressing to 1000 psi. -----                      |   |
| Table 5.9:     | Comparison between thermal conductivity<br>values obtained from experiment and<br>those from theoretical prediction for<br>a kaolin brick of porosity $p = 38.5$<br>per cent. -----    | 1 |
| Table 5.10:    | Comparison between thermal conductivity<br>values obtained from experiment and<br>those from theoretical predictions for<br>a fireclay brick of porosity $p = 39.5$<br>per cent. ----- | 1 |

|              |  |    |
|--------------|--|----|
| Table 5.11:  | Comparison between thermal conductivity values from experiment and from theoretical predictions for a Siaya clay brick of porosity $p = 38.4$ per cent. -----                    | 10 |
| Table 5.12:  | Comparison between thermal conductivity values obtained from experiment and those from theoretical predictions for Kisii soap stone brick of porosity $p = 7.64$ per cent. ----- | 10 |
| Table A 1.1: | Probe temperature - time data<br>Input voltage = 2.3 v.<br>Current (I) = 0.81 A -----  | 13 |
| Table A 2.1: | Data required for the determination of the correction time $t_0$ . -----   | 13 |
| Table A 4.1: | Comparison between values of thermal conductivity from experimental data with those predicted by theory for kaolin at $113.4^\circ\text{C}$ . -----                              | 14 |
| Table A 4.2: | Comparison between thermal conductivity values obtained from experiment with those predicted by theory for Siaya clay at $105.6^\circ\text{C}$ . -----                           | 14 |
| Table A 4.3: | Comparison between values of thermal conductivity values from experimental -----   |    |

|              |   |     |
|--------------|---|-----|
|              | data and those predicted by theory<br>for fireclay at 100°C. -----  | 142 |
| Table A 4.4: | Variation of thermal conductivity with<br>percentage porosity for fireclay<br>dried and wet samples. Moisture<br>content for the wet samples was 25.6% -- | 143 |
| Table A 4.5: | Variation of thermal conductivity<br>with percentage porosity for Siaya<br>clay dired and moist samples of<br>moisture content of 25.2%. -----            | 143 |
| Table A 4.6: | Variation of thermal conductivity<br>with percentage porosity for Siaya<br>clay at two temperatures A = 105.6°C<br>and B = 632.9°C. -----                 | 144 |
| Table A 4.7: | Variation of therman conductivity<br>with percentage porosity for kaolin<br>dried and wet samples. Moisture<br>content for wet sample was 24.5%. -----    | 144 |
| Table A.4.8: | Variation of thermal conductivity<br>with percentage porosity for kaolin<br>at two different temperatures<br>A = 113.4°C and B = 636.7°C. -----           | 145 |
| Table A 4.9: | Variation of thermal conductivity<br>with percentage porosity for<br>fireclay at two different -----  |     |

|               |   |     |
|---------------|---|-----|
|               | temperatures A = 110.7°C and<br>B = 620.4°C. -----  | 145 |
| Table A 4.10: | Variation of thermal conductivity<br>values with temperature of firing for<br>Siayaclay material (measurements are<br>made at 100°C and porosity = 38.5<br>per cent). ----- | 14  |
| Table A 4.11: | Variation of thermal conductivity with<br>temperature of firing for Kisii soap<br>stone material (measurements are made<br>at 100°C and porosity = 7.64 per cent).--        | 14  |
| Table A 4.12: | Variation of thermal conductivity<br>with temperature of firing for<br>fireclay material (measurements are<br>made at 100°C and Porosity = 39.5<br>per cent). -----         | 14  |
| Table A 4.13: | Variation of thermal conductivity<br>with temperature of firing for kaolin<br>material (measurements were made at<br>100°C, porosity = 38.5 per cent). -----                | 14  |
| Table A 4.14: | Variation of thermal conductivity<br>with temperature for a Siayaclay<br>brick of porosity of p = 29.6.<br>percent. -----   | 14  |

|  | <u>PAGE</u> |
|--|-------------|
| Table A 4.15: Variation of thermal conductivity with temperature for a Siaya clay brick of porosity $p = 32.8$ per cent. ----- | 150         |
| Table A 4.16: Variation of thermal conductivity with temperature for a Siaya clay brick of porosity $p = 34.5$ per cent. --    | 151         |
| Table A 4.17: Variation of thermal conductivity with temperature for a Siaya clay brick of porosity $p = 38.4$ per cent. ----- | 151         |
| Table A 4.18: Variation of thermal conductivity with temperature for a Siaya clay brick of porosity $p = 41.7$ per cent. ----- | 152         |
| Table A 4.19: Variation of thermal conductivity with temperature for a Siaya clay brick of porosity $p = 45.2$ per cent. --    | 152         |
| Table A 4.20: Variation of thermal conductivity with temperature for a fireclay brick of porosity $p = 35.2$ per cent. -----   | 153         |
| Table A 4.21: Variation of thermal conductivity with temperature for a fireclay brick of porosity $p = 39.5$ per cent. -----   | 153         |
| Table A 4.22: Variation of thermal conductivity with temperature for a fireclay brick of porosity $p = 44.5$ per cent. -----   | 154         |

|               |  |     |
|---------------|--|-----|
| Table A 4.23: | Variation of thermal conductivity with temperature for a fireclay brick of porosity $p = 47.8$ per cent. -----       | 154 |
| Table A 4.24: | Variation of thermal conductivity with temperature for a Kisii soap stone brick of porosity $p = 7.64$ per cent. --- | 155 |
| Table A 4.25: | Variation of thermal conductivity with temperature for a kaolin brick of porosity $28.4$ per cent. -----             | 155 |
| Table A 4.26: | Variation of thermal conductivity with temperature for a kaolin brick of porosity $p = 32.6$ per cent. -----         | 156 |
| Table A 4.27: | Variation of thermal conductivity with temperature for a kaolin brick of porosity $p = 35.3$ per cent. -----         | 156 |
| Table A 4.28: | Variation of thermal conductivity with temperature for a kaolin brick of porosity $p = 38.5$ per cent. -----         | 157 |
| Table A 4.29: | Variation of thermal conductivity with temperature for a kaolin brick of porosity $p = 46.0$ per cent. -----         | 157 |

LIST OF FIGURES

|             |   |    |
|-------------|---|----|
| Figure 1.1: | The tetrahedral sheet of a clay molecule.-----  | 6  |
| Figure 1.2: | An octahedral sheet of a clay molecule.-----  | 7  |
| Figure 1.3: | The unit cell of a kaolinite crystal.----   | 8  |
| Figure 1.4: | The unit cell of a dickite crystal. ----  | 9  |
| Figure 2.1: | Comparison of thermal conductivity values from experiment and those from theoretical calculations for a dry sandstone [10]. ----- | 15 |
| Figure 3.1: | Thermal conductivity versus pore size relationship [24].-----   | 34 |
| Figure 3.2: | Model of a structure with interpenetrating components (a) the model (b) the unit cell [ 8 ]. -----                                | 52 |
| Figure 3.3: | Characteristic geometry of the thermal conductance model. -----   | 54 |
| Figure 3.4: | The heat transfer mechanism for a sintered porous material [28] -----   | 55 |
| Figure 4.1. | Various kinds of pores found in a porous material. -----  | 66 |
| Figure 4.2: | Standard split sizes for molding of refractory bricks. -----  | 69 |



|             |   |    |
|-------------|---|----|
| Figure 4.3: | The mold designed and used for moulding the refractory bricks. -----  | 70 |
| Figure 4.4: | The arrangement of the experimental apparatus. The thermal probe and its circuitry. -----   | 73 |
| Figure 5.1: | A photomicrograph of the kaolinite material x 80.<br>The plate shows an almost uniform distribution of almost spherical particles or agglomeration of particle. ---                                 | 83 |
| Figure 5.2: | A photomicrograph of the fireclay material x 20. The plate shows relatively large particles which predicts large interparticulate pores in the molded material. -----                               | 84 |
| Figure 5.3: | A photomicrograph of the Siaya clay material x 20. The plate shows an agglomeration of small particles to form large ones. This predicts low porosities in the molded material. -----               | 85 |
| Figure 5.4: | A photomicrograph of the powdered Kisii soap stone material x 20, showing thread-like patterns of grains. The patterns predict an enhanced conductivity along the grain threads and a relatively -- |    |

|              |  |     |
|--------------|--|-----|
|              | low one along any direction that crosses the grain threads. -----  | 86  |
| Figure 5.5:  | Particle size distribution for the fireclay material. -----  | 88  |
| Figure 5.6:  | Particle size distribution for the kaolinite material. -----   | 89  |
| Figure 5.7:  | Particle size distribution for the Siaya clay material. -----  | 90  |
| Figure 5.8:  | Variation of thermal conductivity with firing temperature for the kaoline material (the measurements were made at 100°C and porosity $p = 38.5$ per cent). - | 93  |
| Figure 5.9:  | Graph of thermal conductivity against percentage porosity for a dry kaolin brick at two temperatures A = 113.4°C and B = 636.7°C. -----                      | 96  |
| Figure 5.10: | Graph of thermal conductivity against percentage porosity for kaolin dried and wet samples of moisture content of 24.5%. -----                               | 98  |
| Figure 5.11: | Comparison between theoretical prediction and experimental data for a fireclay brick at 110.7°C. -----   | 100 |
| Figure 5.12: | Graph of thermal conductivity against temperature for a Siaya clay sample at different percentage porosities. -----  | 101 |

- Figure 5.13: Comparison between variation of thermal conductivity with temperature by experiment and from theoretical prediction (porosity  $p = 38.4$  per cent). --- 1
- Figure A 1.1: Graph of the natural logarithm of the time against the temperature for a fireclay sample at  $71.7^{\circ}\text{C}$ .  
 $V = 2.1 \text{ f}$  and  $I = 0.8\text{A}$ . ----- 1
- Figure A 2.1: Graph of  $dt/dT$  against time,  $t$ , for the determination of the correction time  $t_0$ . ----- 1
- Figure A 5.1: Variation of thermal conductivity with firing temperature for fireclay material (measurements made at  $100^{\circ}\text{C}$  and for porosity  $p = 39.5$  per cent). ----- 1
- Figure A 5.2: Variation of thermal conductivity with firing temperature for Kisii soap stone material (measurements made at  $100^{\circ}\text{C}$  and porosity  $p = 7.64$  per cent). ----- 1
- Figure A 5.3: Variation of thermal conductivity with firing temperature for Siaya clay material (measurements are made at  $100^{\circ}\text{C}$  and porosity  $p = 38.5$  per cent). ---- 1
- Figure A 5.4: Graph of thermal conductivity against percentage porosity for fireclay at

|                |   |     |
|----------------|---|-----|
|                | two temperatures A = 105.6°C and<br>B = 632.9°C. -----  | 161 |
| Figure A 5.6:  | Graph of thermal conductivity against<br>percentage porosity for a dried and<br>wet sample of fireclay at 30°C.<br>Moisture content was 25.6%. -----          | 163 |
| Figure A 5.7:  | Graph of thermal conductivity against<br>percentage porosity for Siayaclay dried<br>and wet samples at 33.3°C moisture<br>content was 25.2% -----             | 164 |
| Figure A 5.8:  | Comparison between theoretical prediction<br>and experimental data for variation<br>of thermal conductivity with porosity<br>for Siaya clay at 105.6°C. ----- | 165 |
| Figure A 5.9:  | Comparison between theoretical<br>prediction and experimental data for<br>variation of thermal conductivity with<br>porosity for kaolin at 113.4°C. -----     | 166 |
| Figure A 5.10: | Graphs of thermal conductivity against<br>temperature for fireclay samples of<br>different percentage porosity. -----   | 167 |
| Figure A 5.11: | Graphs of thermal conductivity against<br>temperature for kaolin samples of<br>different porosities. -----  | 168 |

- Figure A 5.12: Graph of thermal conductivity against temperature for a Kisii Soap stone brick of porosity  $p = 7.64$  per cent. --- 169
- Figure A 5.13: Comparison between experimental data and those predicted by theory for the variation of thermal conductivity of a Kisii soap stone brick of porosity 7.64 per cent. ----- 170
- Figure A 5.14: Comparison between experimental data and that predicted by theory for the variation of thermal conductivity of a kaolin brick of porosity  $p = 38.5$  per cent. ----- 171
- Figure A 5.15: Comparison between experimental data and theoretical predictions for the variation of thermal conductivity for a fireclay brick of porosity 39.5 per cent. ----- 172

LIST OF SYMBOLS

- $a\{m\}$  - Contact-area radius.
- $A\{m^2\}$  - Area of cross-section.
- $b\{m\}$  - Largest dimension of gap in direction of flow of heat.
- $B$  - factor expressing heat transfer through contact and gas microgap at the place of contact of two particles.
- $C\{m\ s^{-1}\}$  - Velocity of light in vacuum.
- $C_k$  - Constant dependent on effective emissivity and geometrical shape of a surface.
- $C_p$  - Specific heat capacity of a material.
- $C_g$  - Geometric parameter related to the void volumetric fraction.
- $d\{m\}$  - particle diameter.
- $G_s$  - Specific gravity.
- $g\{m\ s^{-2}\}$  - Gravitational acceleration.

(xxiii)

- $K\{wm^{-1} \text{ } ^\circ C^{-1}\}$  - Thermal conductivity.
- $K_b\{wm^{-1} \text{ } ^\circ C^{-1}\}$  - Thermal conductivity of bond material.
- $K_e\{wm^{-1} \text{ } ^\circ C^{-1}\}$  - Effective thermal conductivity.
- $K_f\{lm^{-1} \text{ } ^\circ C^{-1}\}$  - Fluid conductivity.
- $K_g\{wm^{-1} \text{ } ^\circ C^{-1}\}$  - Thermal conductivity of gas.
- $K_m\{mw^{-1} \text{ } ^\circ C^{-1}\}$  - Thermal conductivity of a heterogeneous matrix system.
- $K_o\{wm^{-1} \text{ } ^\circ C^{-1}\}$  - Thermal conductivity of reference temperature.
- $K_s\{wm^{-1} \text{ } ^\circ C^{-1}\}$  - Thermal conductivity of material with zero porosity.
- $K_l\{wm^{-1} \text{ } ^\circ C^{-1}\}$  - Thermal conductivity of host component.
- $k\{m^2 \text{ } s^{-1}\}$  - Thermal diffusivity.
- $L\{m\}$  - Characteristic size of an elementary cell.
- $\ell\{m\}$  - A characteristic dimension
- $n$  - An integer.
- $p$  - Porosity percentage.

|                              |  |
|------------------------------|--|
| $Q \{Jm^{-2} s^{-1}\}$       | - Heat flux per unit time.                         |
| $T \{^{\circ}C\}$            | - Temperature                                      |
| $\Delta T \{^{\circ}C\}$     | - Temperature difference.                          |
| $dT/dx \{^{\circ}C/m^{-1}\}$ | - Temperature gradient in x-direction.             |
| $t \{s\}$                    | - Time in seconds.                                 |
| $\mu \{m\}$                  | - Effective thickness of the bond material.        |
| $V \{m^3\}$                  | - Volume   |
| $V_b$                        | Volume fraction of bond material.                  |
| $V_f$                        | - Volume fraction of fluid.                        |
| $V_g$                        | - Volume fraction of gas.                          |
| $V_m$                        | - Volume fraction heterogeneous matrix.            |
| $w \{k_g\}$                  | - Mass of material                                 |
| $Y_w \{k_g m^{-3}\}$         | - Density or unit mass of water.                   |
| $\alpha = \frac{k_g}{k_m}$   | - Ratio of gas conductivity to solid conductivity. |



- $\gamma$  - A coefficient which is a function of the ratio  $K_f/K_m$ , the shape, and the mutual arrangement of particles.
- $\epsilon$  - Emissivity
- $\delta$  {m} - Average pore size
- $\phi$  { $m^{-1}$ } -  $\ell/\delta$ .
- $\sigma$  { $J \text{ } ^\circ K^{-1}$ } - Stefan Boltzmann constant.
- $\xi$  - Parameter governing the importance of heat transfer through the solid in the porous system.
- $\psi$  - Parameter in thermal conductance model which is unity if pores are closed and zero if pores are interconnecting.
- $\tau$  {m} - Optical path length.
- $v$  { $m \text{ s}^{-1}$ } - Terminal velocity reached by particles.
- $\rho$  { $K_g \text{ m}^{-3}$ } - Density.
- $\rho_i$  { $K_g \text{ m}^{-3}$ } - Density of water

- $\rho_s \{K_g m^{-3}\}$  - Density of solid.
- $\lambda \{m\}$  - Mean free path
- $\nabla^2$  - Laplacian operator
- $x, y, z.$  - Rectangular coordinate axes.

ABSTRACT:

Thermal conductivities of refractory bricks made from the materials; fireclay, kaolin, siaya clay and Kisii soap stone have been measured. The thermal conductivities of the bricks in dry air at atmospheric pressure were determined at different porosity percentages and as a function of temperature from room temperature to about 800°C. The effects of particle size distribution, chemical composition, grain structure, firing shrinkage, weight loss on firing, density, casting pressure and firing temperature for each material on the thermal conductivity values were investigated. The thermal conductivity values were determined by an unsteady state method, the transient hot wire method of comparison, which is based on the model of heating a cylinder of a perfect conductor surrounded by an infinite amount of a reference material on one side and on the other side the material whose thermal conductivity is being measured.

The porosities of the prepared bricks ranged; from 23.3 to 56.0 per cent for fireclay, from 21.1 to 56.7 per cent for kaolin and from 21.3 to 57.6 per cent for Siaya clay.

The thermal conductivities of the refractory bricks increased with decreasing percentage porosity. For all the brick materials studied, the thermal conductivity values measured increased with increasing temperature. The rate of increase of these thermal conductivity values was higher at low temperatures below 500°C and lower at higher temperatures above 500°C.

The results obtained from experiment were compared to those predicted by theoretical models of heat transfer in porous materials. The model of Imura et al. gave the best explanation of the variations.

These results are useful to designers who will require to calculate heat losses in refractory material applications.

## C H A P T E R     O N E

### INTRODUCTION:

The knowledge of the mechanism with which heat is transported through matter and also through a vacuum is important in the consideration of many applied and theoretical problems. Most attempts to understand how heat is transferred through refractory materials reduce to attempts to determine the thermal conductivity values of the refractories.

The property of thermal conductivity is of particular importance in the application of refractory materials since in many cases the ability to conduct or not conduct heat is one of primary functions of the refractory. In certain parts of a furnace for example, such as the walls or the roof, a minimum transmission of heat to the outside is desired; hence a refractory with a low thermal conductivity would be necessary for these conditions. On the other hand, such parts as the muffles or underfired hearths require a refractory with a high conductivity value. It will therefore be seen that a furnace designer must have accurate data on the thermal conductivity of his refractories before he can intelligently select his materials or predict the performance of his furnace.

In this study, an attempt is made to measure the thermal conductivities of refractory bricks prepared from locally mined materials in relation to the various conditions of use and the different ways of preparation.

The materials selected for the study were kaolinite, Kisii soap stone, Siayaclay and fireclay. Magnesite and limestone bricks were also initially considered for the investigation, but the two were dropped from the list because they required a kiln that could fire them to their maturing temperature of about 1600°C and this was not immediately available. The reasons behind these choices were mainly due to the availability and the low costs incurred for the purchase of these materials. Except for those people who make use of the fireclay refractory bricks manufactured by Refractories Ltd. of Kahawa in Nairobi, anyone else in the country requiring the use of refractory bricks may only either import the raw material to fabricate them or import ready-made refractory bricks. Should the materials therefore prove to be applicable for certain thermal uses, the study will have gone some way in helping save some foreign exchange.

All the four materials chosen for the study are naturally occurring minerals. Kisii soap stone is

mined in Kisii area of Western Kenya. This is obtained in the form of smooth surfaced hard greyish stones. Its chemical composition compares well with that of the kaolinite mineral whose refractory properties has been investigated on and found to be good [1] (see section 5.1.1. for the chemical compositions). This was an added reason for its choice.

Kaolinite is mined, processed and marketed by Mineral Mining Co-operation (1965) Ltd. of Nairobi (Kenya). It is found mainly at Karatina in Nyeri District and in Machakos and Kitui Districts. The fireclay used was mined from the Kitui area, while the Siayaclay was obtained from Siaya also in Western Kenya. The three minerals are mined by open cast methods.

#### 1.1.0. REFRACTORY MATERIALS:

Of all the materials found in the earths crust, which number over one hundred, only a few have both the abundance and the ability to form refractory compounds. These are Silicon (Si), Aluminium (Al), Carbon (C) and Zirconium (Zr), Magnesium (Mg), Chromium (Cr), and Calcium (Ca). These form the useful oxides  $\text{SiO}_2$ ,  $\text{Al}_2\text{O}_3$ ,  $\text{MgO}$  and  $\text{ZrO}_2$ . The oxide of chromium is volatile and that of calcium is unstable in the atmosphere,

however, they may be combined into useful materials such as with MgO to form dolomite or the basic spinel. Carbon may be used directly after graphitisation, or combined with silicon to form silicon carbide. Fortunately, many of these are found in deposits of sufficient purity to enable direct use. These include clays consisting mainly of Si and Al, ganister mainly consisting of Si, magnesia mainly consisting of mg, dolomite consisting of Mg and Ca and chromite which mainly consist of cr, Fe and Al.

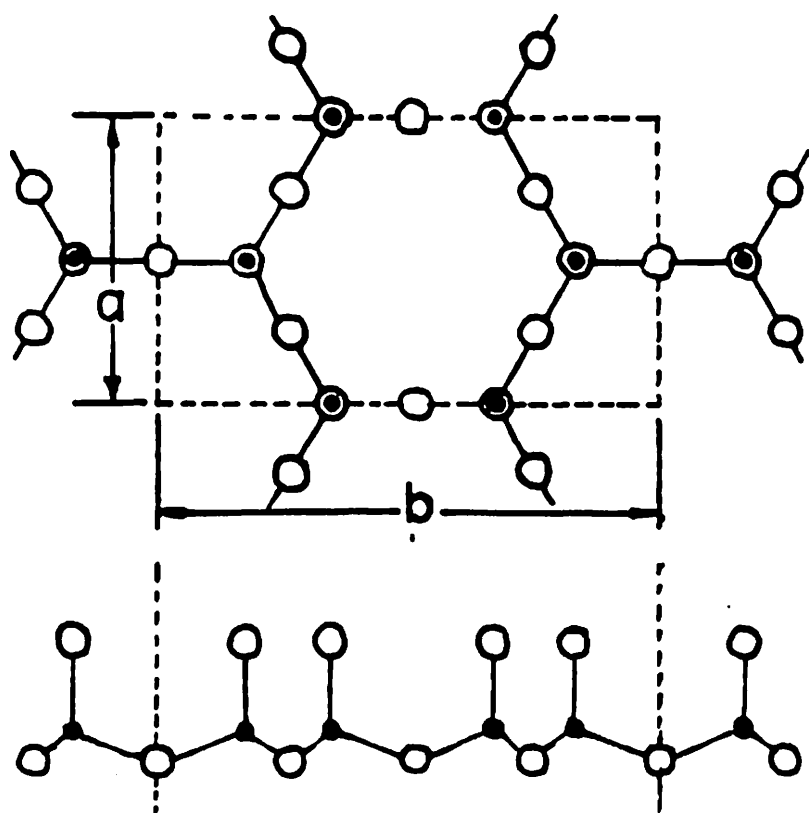
Contrary to the early conception that clay consisted of an amorphous colloid, it is now known from x-ray diffraction studies that substantially all the particles in clay are crystalline [1, 2, 3]. Each atom species has a specific diameter, which in the case of clay minerals can be summarised as  $2.64 \times 10^{-10}$  m. for oxygen,  $1.14 \times 10^{-10}$  m. for aluminium and  $0.78 \times 10^{-10}$  m. for silicon. Because of its large size, the oxygen atom largely determines the type of packing in the crystal [2], the smaller atoms fitting into the interstices. Since the crystals are ionic, then the atoms are charged with the aluminium and the silicon atoms positive and the oxygen atom, negative. These are held together by the resultant attractive forces. The building block in clay minerals is the Si-O sheet



shown in Fig. 1.1. and the Al-OH sheet of Fig. 1.2. When one sheet is transposed on top of the other, they may be fitted together to form the unit cell of Kaolinite as shown in Fig. 1.3. or with a slightly different arrangement to form the unit cell of dickite as shown in Fig. 1.4. These two minerals which comprise the bulk of material found in kaolin have the composition  $Al_2 (Si_2 O_5) (OH)_4$ .

Unless there is a particular need to purify a given sample, refractories are prepared from raw materials which contain a mixture of the oxides of the elements mentioned above. All refractories, with an exception of those which are chemically bonded, are fired to stabilize for strength and performance by formation of ceramic bonds in their structure. It is a generally accepted view that a refractory brick should be stabilised at a temperature as high or higher than the temperature at which it is used.

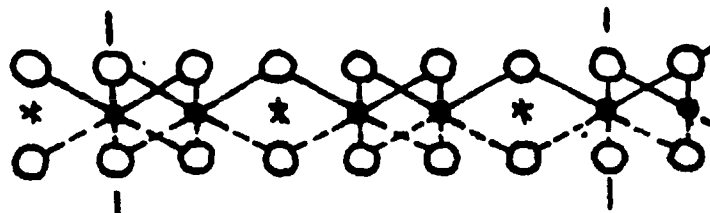
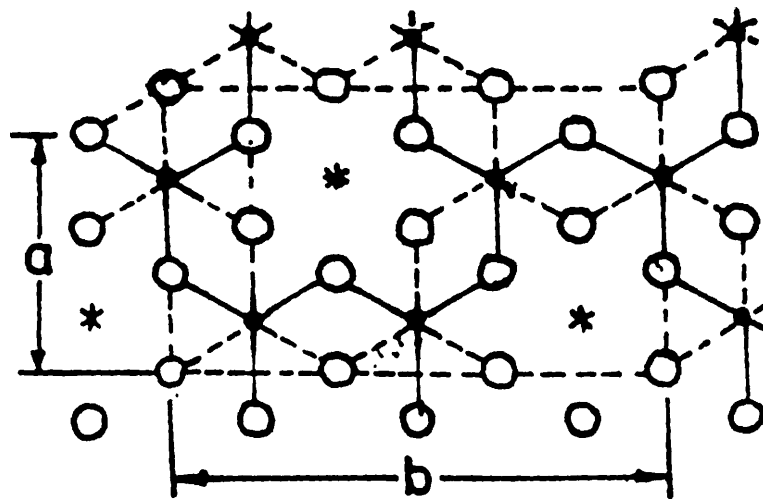
Refractories have technological importance and are of scientific interest because of their application in different industries. Their use has been enhanced in recent years because of the increased awareness to conserve energy through efficient use of fuels, energy saving devices and insulation against heat losses.



O = OXYGEN

● = SILICON

FIGURE 1.1 : THE TETRAHEDRAL SHEET



O-OH

•-ALUMINIUM

\*-VACANT SITES

FIGURE 1-2: THE OCTAHEDRAL SHEET

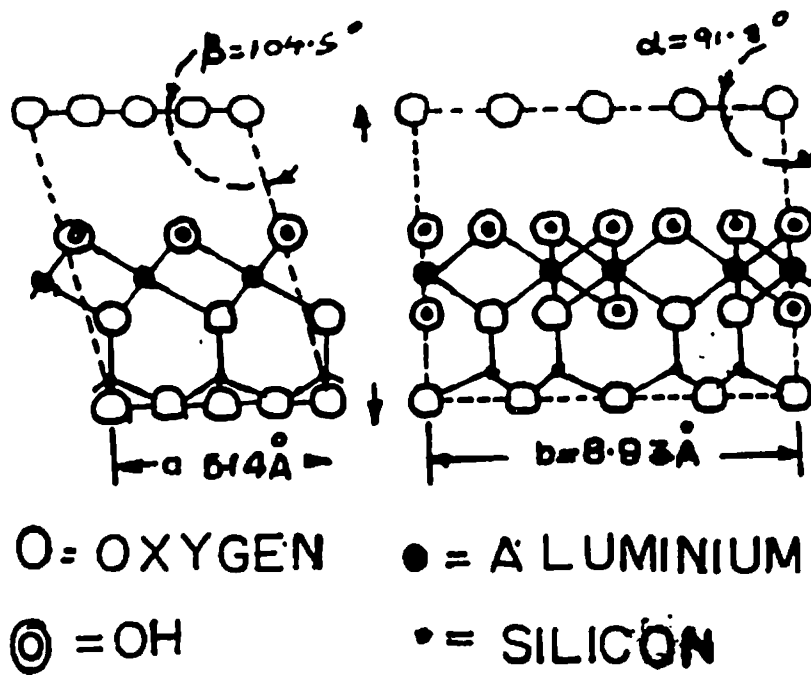
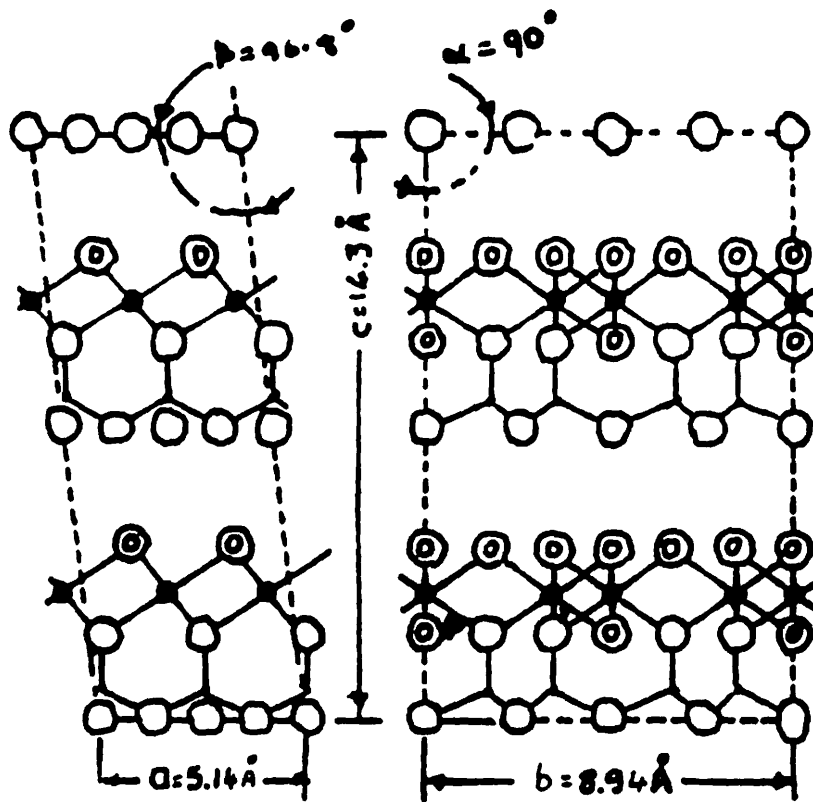


FIGURE 1.3 UNIT CELL OF KAOLINITE.



O = OXYGEN

● = ALUMINIUM

⊙ = OH

FIGURE 1.4 UNIT CELL OF DICKITE

Their applications have been found in such areas like the iron and steel industry and in other non-ferrous producing industries such as copper and copper alloy production, zinc, lead, aluminium and nickel production. Their uses are also found in other ceramic industries. Here they are mainly used in firing kilns, glass smelting, cement and lime industry, tea drying, refuse combustion and in all furnaces. Refractory materials are also used for high pressure steam pipe lagging in steam power generation. Domestically, refractory materials have been used in wood and charcoal stoves, hot water/steam pipe lagging, hot water tank insulation and in cold storage and refrigeration.

#### 1.2.0. PRESENT WORK:

There is a conviction that the behaviour of any ceramic and in this case a refractory, should be determined by the properties of the pure components, the particle parameters i.e. sizes and shapes, and the manner in which the components are combined in the end-product [1]. However, it is difficult to determine which of the pure components' properties and particle parameters or modes of combination are most important and even more difficult to determine how each affects the behaviour of the produced refractory. Much of the

data in the literature on the effective thermal conductivity of refractory materials which appear similar, based on volumetric concentrations and thermal conductivities of the constituents actually vary widely [4, 5]. Although some differences in the values of thermal conductivity reported by Kingery and McQuarrie [4] may be attributed to differences in the methods employed in the measurements, some seem to be due to other factors. Schotte [5a] for example compared five glass beads air systems at temperatures which are not far apart and at the same porosities and found that the conductivities differ by a factor of 2.4. Therefore, one of the principal aims of the present work is to attempt to establish the validity of the notion that such differences in thermal conductivity found in apparent similar systems could easily be real and that they may be explainable in terms of more subtle factors such as the particle size distribution, surface conditions of the ceramic bonds formed etc.

In chapter two, a review of the previous work related to this study has been given. The theoretical background to the study of the thermal conductivity properties of refractory materials and its measurements has been presented in chapter three. Chapter four deals with the experimental details and the techniques used

in this study, while the experimental results and their discussion have been given in chapter five. The conclusions arrived at have been given, together with the recommendations for future work in chapter six.



## C H A P T E R   T W O

### LITERATURE REVIEW

#### 2.1.0. INTRODUCTION

The importance of the property of thermal conductivity in the application of refractory materials has led to a good deal of work being carried out on its measurements by many investigators over the years. Therefore, a substantial amount of work has been reported in the literature on the subject.

As it has been pointed out by Godbee and Ziegler [5], the transport of heat through porous media follows some complex patterns, its literature is therefore large and varied, thus posing a good challenge to its interpretation. The main reason for the varied reports in the literature on the subject is that, different workers have used different methods of measurements in their investigations. The variations have prompted different researchers [5, 6, 7, 8] to work towards reconciling the different findings and also to try and find an accord in the various proposed theoretical models.

#### 2.2.0. SURVEY OF PREVIOUS WORK ON THERMAL CONDUCTIVITY OF REFRACTORY MATERIALS

Notable among the works reported on the refractoriness of some local materials are those on the thermal conductivity of porous insulators, wood-ash and vermiculite [9]. This

study tested the thermal conductivity properties of the materials in powder form and also in consolidated form. The thermal conductivity values were observed to increase with temperature for all the considered cases. An observation also made from this report was that the thermal conductivities increased following a trend that was predicted theoretically by Zumbrunnen [10]. Other studies reported on local materials are those on tests on materials for woodstove linings [11] and also a review of the production of improved jiko stoves in Kenya [8]. A study on thermal shock behaviour has also been reported for cylindrical specimen made from Maragua and Nyeri clays [12].

Experimental results of thermal conductivity values obtained by Sugawara and Yoshizawa for dry sandstone have been compared by Brailsford et al. [13] with expressions for thermal conductivity of a two phase media derived for various types of structures, namely continuous solid phase continuous fluid phase and random assembly. Fig. 2.1. shows the variation of the thermal conductivity as a function of percentage porosity for each type of structure and for the experimental values obtained by the investigators. The conclusions arrived at from this exercise were that; for a natural porous media the fluid component played a more important role at low porosities than would be expected for a purely random assembly. These authors

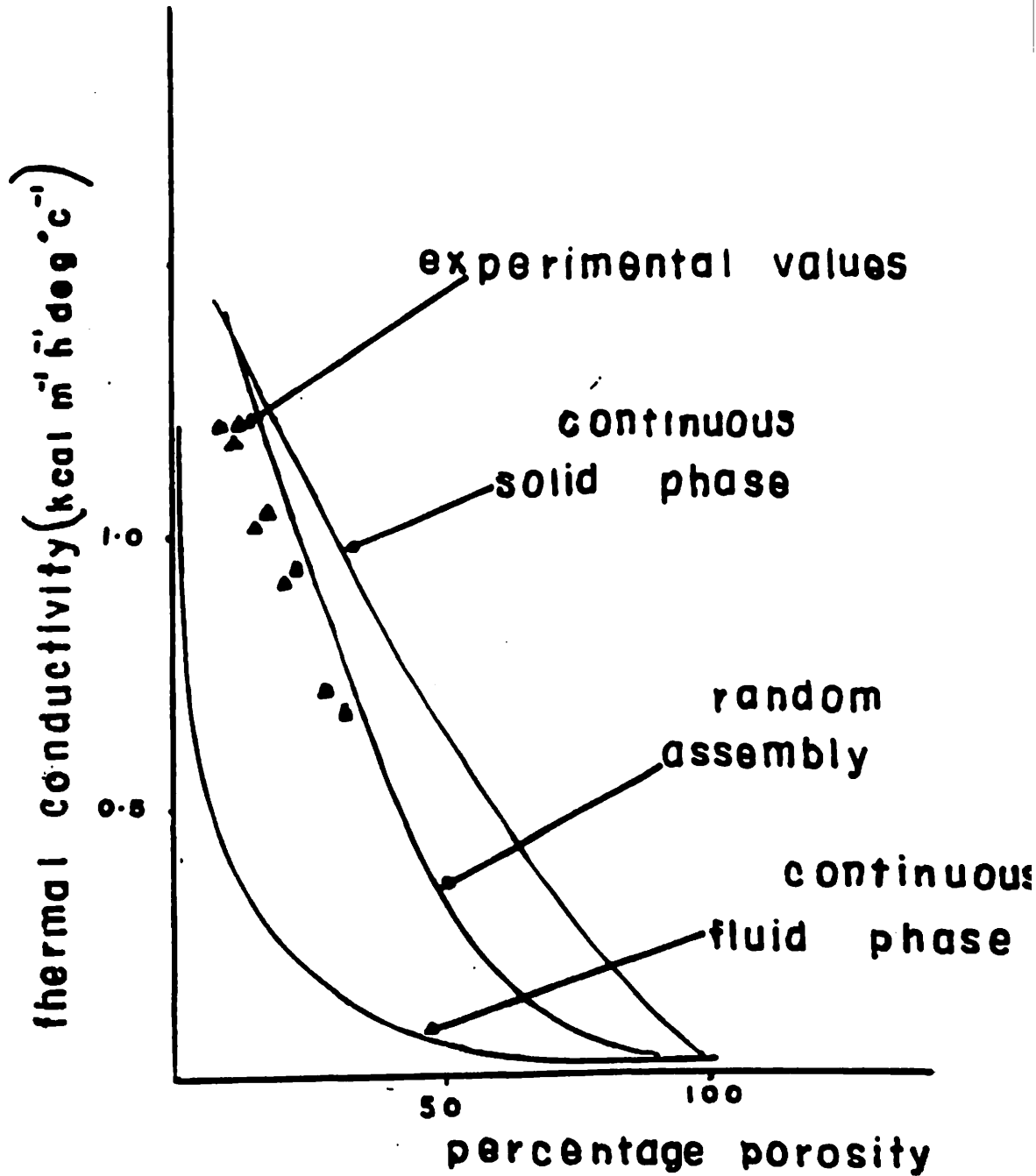


FIGURE 2.1

comparison of thermal conductivity values from experiment and from theoretical calculations for dry sandstone [10].

attributed this to the widely differing mechanical properties of the two phases, which enable the liquid to infiltrate between solid grains, thus playing a significant role in the determination of the thermal conductivity.

The problem of determining the effective thermal conductivity of a two phase system, given the conductivities and volume fractions of the components has been investigated by Woodside et al. [14]. They compared equations which have been proposed as solutions to this problem to the analogous electrical conductivity problem. These equations included those of Maxwell [15], De Vries and Kunii and Smith [16]. Comparison of these equations with experimental effective thermal conductivity values for unconsolidated samples of quartz sand packs showed that; the equations either underestimated the effective thermal conductivity or gave just some fair agreement with the observed values over some ranges of porosities. Nevertheless, the effective thermal conductivity of an unconsolidated pack was observed to increase with the conductivity of a saturating fluid. The increase was almost in direct proportion for the cases where the saturant conductivity was small relative to that of the solid. In another investigation [7], the same authors have reported measurements made for the effective thermal conductivity of porous sandstones. The results are compared with

those previously obtained for unconsolidated sands. In all cases, the samples were observed to exhibit a lower thermal conductivity when saturated with a gas at atmospheric pressure than when saturated with a liquid of the same value of thermal conductivity as the gas. Another noteworthy observation was that the resistor model equation [14, 17] was seen to predict rock thermal conductivities which were in good agreement with those measured, which permits the estimation of sandstone conductivities from the porosities and the conductivity of the saturating fluid.

Thermal conductivity values of some thirteen pure sintered refractory oxides taken from various research works have been reported by Norton [1]. The values have been given for temperatures ranging between 200°C and 1600°C. In all these cases, the thermal conductivity values were observed to decrease with increasing temperature. This trend is confirmed by the Debye expression for thermal conductivities of crystalline solid materials (see eqn. 3.9). Also reported by Norton [1] are the mean thermal conductivity values of some twenty four 'heavy' refractories. The values are given over a temperature range of between 500°F and 2000°F. For nine of these materials the thermal conductivity values increase with increasing temperature while in all the other cases the values decrease with increasing

temperature. The values given for the apparent percentage porosity given for the materials does not seem to explain the differences in trends of variation of thermal conductivity values for these materials. A possible explanation can be given in terms of the structure of the material. That is whether the materials were homogenously crystalline or amorphous. Other thermal conductivity values given by Norton are those for insulating refractory materials over the temperature range between 500°F and 2000°F. Of all these with an exception of one (3300 bubble alumina) the thermal conductivity values increase with increasing temperature.

Studies on the thermal conductivity of some refractory power materials have also thrown some light to the behaviour of thermal conductivity of refractory materials. Those that need to be mentioned are by two investigators Godbee and Ziegler [5]. They carried out measurements on MgO, Al<sub>2</sub>O<sub>3</sub> and ZrO<sub>2</sub> powders up to a temperature of 850°C. Their results showed that the effective thermal conductivity for each of the three powders increased at a decreasing rate with increasing temperature and following an approximately quadratic temperature dependence.

Though there has been some agreement between thermal conductivity values obtained by some different investigators using different methods of measurements, the error introduced

by each method can be considerable and has been considerable for much of the materials reported in the literature as it has been pointed out by Patton and Norton [18, 19]. This has also been shown in a comparative test by six independent investigators for the same material as reported by Kingery and McQuarrie [4]. These reports point out that the greatest difficulty in thermal conductivity measurements is to obtain heat flow patterns that coincides exactly with the one assumed in deriving the mathematical relationship. The two investigators [4] then deduced that the method generally used to ensure that heat flows in a desired path by providing heat guards to maintain the isothermals in a specimen and prevent extraneous heat flow are never perfect, and advocated the use of a specimen that completely surrounds the heat source. This study employs a similar technique.

More work on pure refractory oxides has been reported by McQuarrie [20]. He performed an analysis of variation of thermal conductivity with temperature for alumina ( $\text{Al}_2\text{O}_3$ ), beryllia ( $\text{BeO}$ ) and magnesia ( $\text{MgO}$ ). In his work, he attempted to summarise the thermal conductivity results obtained for these materials over the temperature range from room temperature to  $1800^\circ\text{C}$ , using five different methods of measurements. He arrived at the conclusions that the thermal conductivity for alumina, beryllia and

magnesia has the same general temperature dependence. That is, a decrease with increasing temperature until a minimum is reached at about 1500°C after which there is a sharp increase. The minimum of the conductivity observed in this experiment which is not predicted by any theory was believed to be due to an increase in apparent conductivity at the highest temperature caused by the passage of radiant energy through the translucent specimens.

Data for thermal conductivity measurements for sixteen pure crystalline oxide ceramics have also been reported by Kingery et al. [21]. These were taken for temperature ranges of between 100°C and 1800°C. For all the polycrystalline oxides, except for stabilized Zirconia ( $ZrO_2$ ) and electrical porcelain, the values of the thermal conductivity decreased with increasing temperature. The decrease being very rapid at low temperatures below 600°C but tending to flatten off at higher temperatures above 1000°C.

Some work has also been reported on the study of thermal conductivity of some refractory carbides and Nitrides by Vasilos [22]. The thermal conductivities of TiC, SiC, TiN and ZrN were measured in the temperature range of between 100°C and 1000°C. The thermal conductivities for these materials were observed to decrease with decreasing temperature.



Luikov et al. [6] measured the thermal conductivities of chamote ceramics in different gases at different pressures. The gases that were used included air, helium and freon. The measurements were conducted at temperatures between 100°C and 450°C. The chamote ceramics used were of porosity of 40 per cent. In all the cases considered, the thermal conductivity values increased with increasing temperature. The rate of increase of these values was high at lower temperatures below 200°C, but as the temperature rose, the rate of increase of the thermal conductivity values decreased, almost flattening off at temperatures above 400°C.

More data showing the trends that are followed by thermal conductivity values for ceramics at different temperatures and for different textures are also given in different texts [24, 25, 26]. The general trend from most reports appears to be a decrease of thermal conductivity with increase in temperature for perfectly crystalline materials and an increase with increasing temperature for amorphous materials.

Many investigators have attempted to develop models and have come up with expressions for calculating thermal conductivity for various materials from the theory [6, 7, 10, 13, 14, 17, 20, 21, 22, 27, 28]. This has only been possible for cases where the nature of the material, the chemical composition and the number of

phases involved (i.e. liquid, solid and gaseous phases) are known and well defined. In the cases of fire clay-products, it has not been easy to establish all the above requirements to be able to come up with one thermal conductivity expression for theoretical calculations.

## C H A P T E R   T H R E E

### THEORETICAL BACKGROUND:

#### 3.1.0. INTRODUCTION:

Heat may be thought of as the kinetic energy of motion (translation, rotational or vibrational) of ions or molecules. Although this concept of heat does not lend itself to quantitative manipulation as well as does that one of thermodynamics (where heat is defined as the amount of energy required to raise the temperature of a substance through a definite amount), it aids greatly in understanding the phenomena of heat transfer. It is usual to consider three methods of heat transfer namely, conduction, convection and radiation. In any transfer of heat, two or perhaps all three of these methods may be operative. It is possible however, to devise conditions whereby the amount of heat transferred by one of these methods is much greater than that transferred by the others and then study this case as an example of heat transfer by this method alone.

In conduction, heat energy is transferred by the mechanism of interaction between two particles, such as ions and molecules, one with a greater amount of energy and the other with a lesser amount of energy

in such a way that some energy is passed from one particle to the other. In the case of a gas, one molecule may strike another molecule which has less kinetic energy and impart some of its energy to the second molecule. In the case of a solid, a molecule with a certain amount of vibrational energy will tend to transmit some of its energy to a neighbouring ion with less energy through the bond connecting them.

In convection, heat is transferred by the actual movement of particles with a given amount of energy to another part of the system where the particles have less energy on the average. This type of heat movement is only effective in fluids and may be neglected in solids. This investigation therefore, does not consider heat transfer by convection.

In radiation, heat is transferred by the emission or absorption of radiant energy between particles or surfaces. When heat is transferred between two surfaces one at a temperature  $T_1$  and the other at a temperature  $T_2$  by radiation, the amount of heat,  $Q$ , transferred per unit area of surface in a unit time is given by

$$Q = C_k(T_1^4 - T_2^4) \text{ ----- (3.1.)}$$

where  $C_k$  is a constant dependent on effective emissivity and geometrical shape of the surfaces, and the temperatures  $T_1$  and  $T_2$  are on the absolute scale. This formula has been derived from theoretical considerations and thoroughly tested experimentally [29, 30, 31]. If an observer was to assume that he was measuring heat transfer by a means which obeyed the law of conduction only whereas the heat was really transferred by radiation according to Eqn. 3.1. he would conclude that the conductivity of the material increases as  $T^3$ . This can be seen if we assume that  $T_1$  and  $T_2$  are near enough together so that after factorising equation 3.1. as follows:

$$\begin{aligned} Q &= C_k(T_1^4 - T_2^4) \\ &= C_k(T_1^2)^2 - (T_2^2)^2 \\ &= C_k(T_1^2 - T_2^2)(T_1^2 + T_2^2) \\ &= C_k(T_1 - T_2)(T_1 + T_2)(T_1^2 + T_2^2) \end{aligned}$$

and approximating  $(T_1 + T_2)$  to be equal to  $2T$  and  $(T_1^2 + T_2^2)$  to equal to  $2T^2$ , we get

$$\begin{aligned} Q &= C_k \times 2T \times 2T^2 \times (T_1 - T_2) \\ &= 4 C_k T^3 \Delta T \text{ ----- (3.2)} \end{aligned}$$

From this expression, it can be seen that some heat transmitted in the form of radiation during a heat conduction measurement would introduce a term in  $T^3$  into the equation of thermal conduction heat as a function of temperature.

3.2.0. THERMAL CONDUCTIVITY:

The thermal conductivity coefficient  $K$  of a solid is most easily defined with respect to the steady-state flow of heat down a long rod with a temperature gradient  $dT/dx$  as:

$$Q = - K \frac{dT}{dx} \text{ ----- (3.3)}$$

Here  $Q$  is the flux of thermal energy, or the energy transmitted across unit area per unit time. The law states that the amount of heat flowing per second per unit area is proportional to the temperature gradient and that the proportionality constant  $K$  is the thermal conductivity. There has been some discussion as to whether or not  $K$  is a function of  $Q$ , the amount of heat flowing through the rod. Experimental evidence indicates that the conductivity does not vary with the amount of heat flowing [4] and therefore, equation (3.3) may be said to be verified by experimental evidence. The

differential equation (3.3) applies to a small differential area, but in the case of a few simple shapes it can be integrated to cover the whole of a finite body. In general, the integral equation has the form:

$$QB = - K\Delta T; K = \frac{-(B)(Q)}{\Delta T} \text{-----} (3.4)$$

where B is a factor determined by the geometrical shape of the body,

Q is the total heat per unit time flowing through the body and,

$\Delta T$  is the temperature difference of the two (isothermal) surfaces of the body between which the heat flows.

The basic equation governing the flow of thermal conductivity K is the Laplace's equation for heat flow which, as derived by Carslaw et al. [32] can be written as:

$$\nabla(K \nabla T) = C_p \rho \frac{dT}{dt} \text{-----} (3.5)$$

where  $\nabla$  is the operator nabla which must be evaluated for the particular coordinate system used;

$C_p$  is the specific heat of the material,

$\rho$  is the density of the material  
 $\Delta T$  is the change in temperature and  
 $t$  is the time.

This equation can be simplified by making the assumption that the material under consideration is homogeneous ( $K$  is independent of direction) and that  $K$  is independent of temperature. Then equation 3.5 can be written as,

$$\nabla^2 T = \frac{C_p \rho}{K} \frac{dT}{dt} \text{ ----- (3.6)}$$

For rectangular coordinates,  $x$ ,  $y$ ,  $z$ , this equation becomes;

$$\frac{dT}{dt} = \frac{K}{C_p \rho} \left( \frac{\partial^2 T}{\partial x^2} + \frac{\partial^2 T}{\partial y^2} + \frac{\partial^2 T}{\partial z^2} \right) \text{ ----- (3.7)}$$

The equation serves as a basis for any dynamic test of thermal conductivity where the change in temperature with time at any point is measured. Actually, the quantity  $K/C_p \rho$ , the thermal diffusivity, is measured and the thermal conductivity derived from this and from a knowledge of the heat capacity,  $C_p$ , and density  $\rho$ . If the steady state is reached such that the temperature is independent of time, we may write;

$$\frac{dT}{dt} = 0, \text{ and } \nabla^2 T = 0 \text{ ----- (3.8)}$$



Then, equations (3.3) and (3.4) may be employed for direct measurement of the thermal conductivity.

### 3.3.0. FACTORS INFLUENCING THERMAL CONDUCTIVITY:

The chief factors to be considered in connection with the rate of passage of heat through refractory materials are:

- (a) The chemical composition of the material used.
- (b) The previous heat treatment of the material.
- (c) The texture or the physical conditions of the material.
- (d) The porosity of the material and the sizes and the distribution of the pores.
- (e) The temperature at which the material is used or tested.

### 3.3.1. CHEMICAL COMPOSITION:

A number of attempts have been made to explain the property of thermal conductivity on the basis of theoretical reasoning. It has for instance been pointed out that the basis for almost all considerations of the effect of composition on thermal conductivity is the Debye equation for the thermal conductivity of crystals [33, 34] see eqn. 3.9. This is based on the concept that a solid may be regarded as a system of coupled oscillators which transmit thermoelastic waves.

The thermal conductivity, will then be given by

$$K = \frac{1}{4} \rho C v \lambda \text{ ----- (3.9)}$$

where;

- $\lambda$  is the mean free path of the wave,
- $v$  the average velocity of the wave,
- $\rho$  the density of the material, and
- $C$  is the velocity of light.

Debye considers that when the atomic or ionic groupings within a crystal act as oscillators or vibrators and if their frequencies correspond to those of the thermal wave, then conduction readily proceeds.

For an ideal lattice,  $\lambda$ , would be infinite if the lattice interactions were completely harmonic. However, anharmonic terms in the lattice interactions will decrease  $\lambda$  by coupling together various vibrations of the lattice and will give a distribution of frequencies corresponding to thermal equilibrium. The value of  $\lambda$  will depend on the magnitude of the anharmonic vibrations and the wave amplitude. It thus seems apparent that any factor which decreases the mean free path of the thermoelastic wave will tend to lower the thermal conductivity. On the same basis, highly symmetrical

crystals, where the vibrations are harmonic, will be better conductors of heat than those which are disordered or contain many types of bonds. Whilst this simple concept holds true in general, there are many discrepancies in experimental findings which suggest that other factors may be involved. Another presumption is that, since thermal and electrical conductivities are closely related, the nature of the electron linkages and orbital transfers play a large part in the transfer of heat as they undoubtedly do in electrical conduction.

Apart from the chemical composition of a material determining its thermal conductivity, the ratios of the components say the ratio of the amount of alumina to that of silica for a material indicate the approximate value of the material as a refractory. Similarly, the total content of alkalies in a material will show whether it is likely to have a high melting point or not, though it would not be quite safe to predict the vitrification temperature on the results alone. The reason being that, soda and potash, when in the form of felspar, are more detrimental to the refractoriness of a material than when they are in the form of mica, because the former melts more readily. Sodium silicate is even more easily fusible.

A chemical analysis is also valuable in showing the presence of some deleterious ingredients, such as

(i) lime, which may destroy refractory bricks and tiles made of a material containing it, or (ii) ferric oxide which may either discolour or enhance the beauty of the product, depending on whether a white or red material is desired, or (iii) alumina, which in siliceous refractories greatly reduces the load-bearing capacities at high temperatures.

### 3.3.2. EFFECT OF HEAT TREATMENT:

Materials differ with regard to their thermal conductivity which changes with the heat treatment to which they have been subjected to, just as the temperature and the duration of firing during manufacture modifies other properties of such materials. The change of the thermal conductivity during firing follows the trend of the firing shrinkage.

For most clays, shrinkage starts at 550°C, continuing at a fairly even rate until 950°C is reached, where there is a sudden shrinkage corresponding to the change of metal-kaolin to the spinel structure. Thereafter, there is little shrinkage with increasing temperature until 1100°C is reached. Shrinkage continues rapidly as mullite and cristobalite form together with an even more fluid glassy phase until zero porosity is reached.

### 3.3.3. EFFECT OF TEXTURE AND POROSITY:

The influence of texture and porosity may be considered together because, the principal effect on the thermal conductivity is the relation between the amount of solid and of air which the heat has to traverse in passing through the material. Since air is a much better insulator than any solid material, the larger the proportion of air the greater will be the thermal insulating power of the material. Hence, a fine grained, close-textured material has a much greater thermal conductivity than one with a coarser open-texture. The relation between insulating power and texture or porosity cannot, however be expressed in very simple terms. This is due to the fact that the relation is always modified by the following parameters; (i) the temperature, (ii) the size of the pores and the interstices, (iii) the shape and the orientation of the pores and the interstices and (vi) the position of the interstices relative to each other and the solid matter i.e. the distribution of the interstices.

At high temperature, if the rate of transfer of heat by radiation increase until it equals the rate of conduction through the solid, then the pore spaces ceases to act as insulators. With pores of 0.01 cm diameter, this equality of the rates of heat transfer

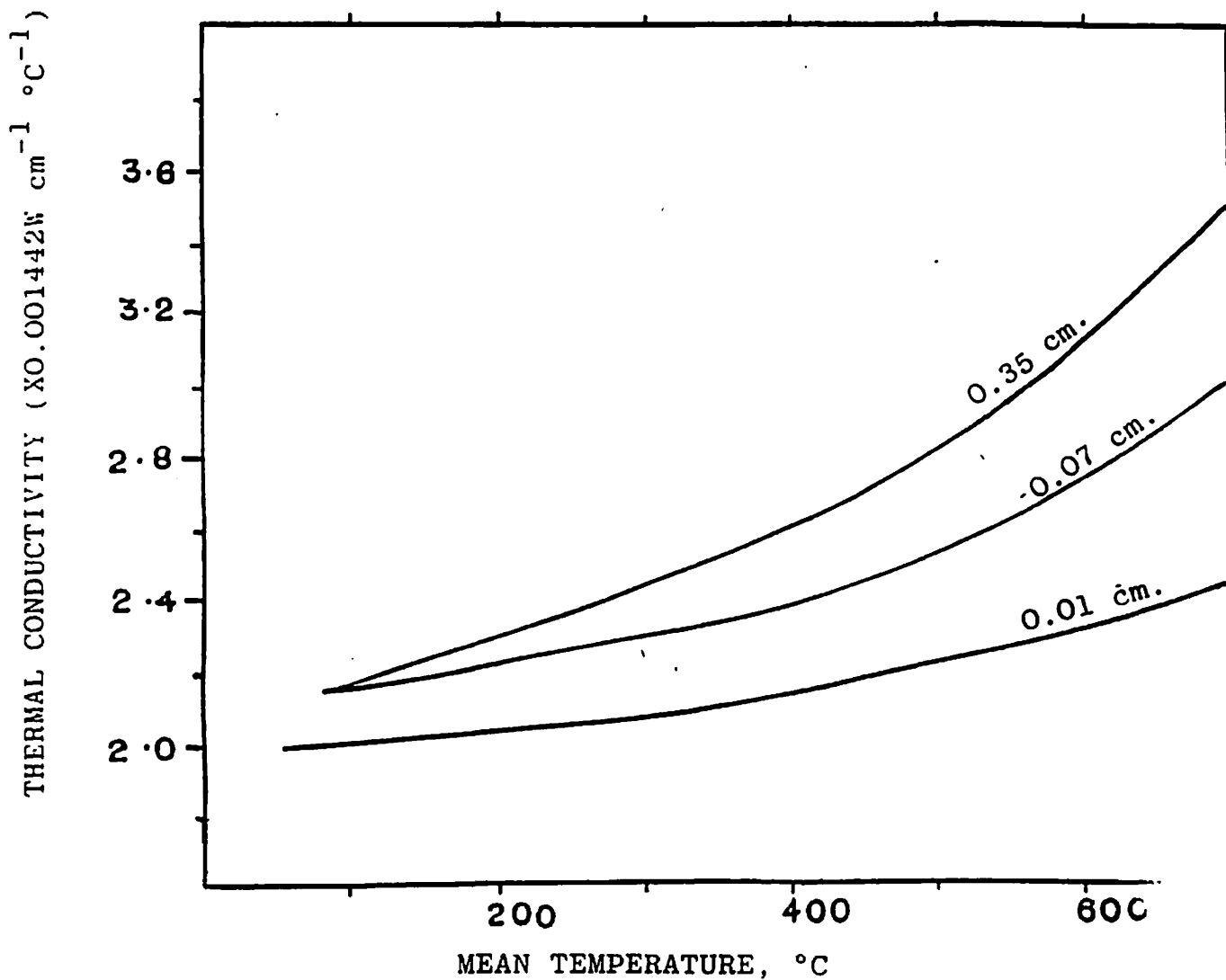


FIGURE 3.1: THERMAL CONDUCTIVITY VERSUS MEAN TEMPERATURES OF SAMPLES WITH VARIOUS POLE SIZES

The values have been equated to a bulk density value of 40 lb/cu. ft. in every case. The average pore size calculated for each specimen is shown in the diagram.

should occur at a temperature of about 3600°C [24]. At low temperatures or with wider pores, the rate of radiation is lower than the rate at which heat passes through the solid material, so that the presence of pores in materials used at these temperatures decreases the thermal conductivity. At temperatures of about 1500°C, the pore spaces lose their insulating properties and transmit heat at about the same rate as the solid matter. This would mean that at temperatures below 1500°C, radiant heat transfer does not affect the heat conduction rate in a refractory material, and therefore, may be neglected in considerations of other factors affecting thermal conductivity.

The thermal conductivity of refractories will in fact not only depend on the total void space but also on the size and the nature of the voids i.e. to whether the voids are closed or interlinked. Although at first sight, a body with large pores might be expected to be more insulating than the one with small pores but with the same total porosity, this is not the case. In a system of small holes the path length  $\lambda$  of equation 3.9 through the solid from the hot face to the cold face must be far less than in the case when only a few large holes are present. For this reason alone, the conductivity of a small pored material would be

less than a large-pored specimen of equal total porosity [24]. Fig. 3.1. demonstrates this point clearly.

#### 3.3.4. THE EFFECT OF PARTICLE SIZE:

At low temperatures and in evaluated systems, the effective thermal conductivity of refractory materials increase with decreasing particle size. This is due to increase in heat transfer through the solid. At elevated temperatures the effective thermal conductivity rises with increasing particle size. This may be attributed to increase in radiant heat transfer through the voids and in the particles [28, 35].

#### 3.3.5. EFFECT OF SATURANT FLUID:

The thermal conductivity of a system is significantly influenced by the saturant fluid within its pores. The presence of the saturant fluid has the effect of increasing the thermal conductivity of the system as compared to that of the solid skeleton alone [17, 36]. The effect is due to a cycle of evaporation-diffusion-condensation during which the heat flux is increased. In general if the fluid wets the particles, then it acts as a binder and thermally couples the particles, thus significantly increasing the effective thermal conductivity.



### 3.3.6. EFFECT OF TEMPERATURE

The effect of temperature on the thermal conductivity of a ceramic material depends on whether the material is dominated by crystalline or amorphous particles.

For crystalline materials, the theory predicts decreasing thermal conductivity with increasing temperature. This may be seen from eqn. 3.9. and has also been observed by experiment [5, 20, 21]. Experimentally, a minimum thermal conductivity at elevated temperatures has been observed [20, 21]. The decrease in  $K$  for crystalline substances is due to an increase in anharmonicity of the lattice vibrations. This decreases the mean free path of eqn. 3.9 by coupling together various lattice vibrations resulting in a decrease of thermal conductivity.

For amorphous granular or loose porous systems the values of  $K$  increase with increasing temperature. This is because the decrease in  $K$  due to the anharmonicity in the vibrations at high temperatures is offset by an increase in transmission of radiant energy and the substantial increase in gas conductivity.

### 3.4.0. THEORY OF THERMAL CONDUCTIVITY MEASUREMENTS:

Many different methods have been applied in the measurement of the thermal conductivities of different

materials. These methods can be classified into two; the steady state methods and the unsteady state methods. Methods employing the former state were developed earlier and have therefore been in application longer and a lot of work has been reported on the subject [1]. These methods are now deemed to have several short comings due to their high costs and complexity. They also require a long duration of time to establish the steady state and therefore are much slower as it has been pointed out by Takegoshi et al. [16, 38].

In steady state methods, the specimen is subjected to a temperature field which is time-invariant, and  $K$  is determined directly by measuring the rate of heat flow per unit area and the temperature gradient at the equilibrium state. The most commonly used steady state methods in the study of thermal conductivity of refractory materials are: (i) the high-temperature method described by Norton [18, 19]. In this method, a uniform parallel flow of heat is set up normal to the faces of a slab and the quantity of heat flowing is measured by a water calorimeter on the cold face of the specimen. The temperature gradient is calculated using the temperatures of the hot and cold faces of the specimen together with the thickness of the specimen, and (ii) the radiant method where heat is generated

inside a hollow cylinder and the temperature drop in the wall measured to obtain the temperature gradient. Other methods are, the Northrup method, the guarded hot plate method, the heat flow-meter, the guarded hot box method and the prolate spheroidal envelope method [39, 40].

In the simplest form, for a steady state apparatus, a sample of uniform cross-sectional area is supplied with a heat flux,  $Q$ , at one end at a known rate. This heat is removed from the other end which is connected to a heat sink. Thermometers are attached to the sample at intervals separated by a distance  $L$  and the temperature difference  $\Delta T$  between any two of them is measured. Using eqn. 3.3, the thermal conductivity,  $K$ , is then calculated from the expression;

$$Q = K A \cdot \frac{\Delta T}{L} \text{ ----- (3.3a)}$$

where;

- A is the cross-sectional area of the specimen,
- Q is the heat flux,
- L is the distance between the two points
- K is the thermal conductivity, and
- $\Delta T$  is the temperature difference between the two points.

Then provided the temperature range is small, the value of  $K$  thus calculated corresponds to the mean temperature of the two thermometers considered.

The most common dynamic methods are the hot wire method [16, 38], the hot strip method [16, 41, 42] and the flash method. In the flash method, the front face of a thin disk sample is supplied with a flash of energy from a flash tube. The temperature-time history at the rear face is recorded. From the knowledge of the sample thickness  $L$ , the time ( $t$ ) at which the back face of the sample reaches half its maximum value, the thermal diffusivity  $k$  is determined. The thermal conductivity  $K$  may then be calculated from the relation

$$K = k C_p \rho \text{ ----- (3.10)}$$

where:

$C_p$  is the specific heat capacity of the sample, and

$\rho$  is the density of the sample.

In this study, the unsteady state, the transient hot wire method of comparison described in Section 3.4.1.1. was employed. The hot strip method mentioned above is quite similar to the hot wire method described in the next section, except that it uses a thin metal foil in the place of a thin wire for a heat source.

3.4.1.0. THE TRANSIENT HOT WIRE METHOD:

The transient hot wire method, in which an infinitely long thin wire inserted in a material is heated stepwise by an electric current at time  $t = 0$ , and the thermal conductivity,  $K$ , of the material of constant density, and specific heat capacity,  $C_p$ , determined from the temperature rise of the hot wire has long been attracting attention for its rapidity and simplicity. The method was suggested theoretically by Schleiemacher [16a] as early as 1888. The possibility of measuring the thermal conductivity experimentally based on this principle was first tested by Stalhane and Pyk [16]. For a difference  $dT$  of the temperature of the wire and its initial temperature, they found that:

$$dT = A \frac{Q}{K} \ln\left(\frac{r_0^2}{t} + B\right) \quad \text{-----} \quad (3.11)$$

where;

- $Q$  is the heat production in Watt/cm
- $2r_0$  is the diameter of the wire in cm
- $A$  and  $B$  are constants, and
- $t$  is the time in seconds.

The empirical formula of Stalhane and Pyk was mathematically deduced by Van der Held and Van Drunen in 1932 [43]. The two investigators measured the

thermal conductivities of liquids, and the errors caused necessarily by experimental apparatus were examined theoretically in detail. They found that in order to find a simple solution of the fourier differential equation at stationary circumstances and for the case that the temperature depends only on one coordinate, the thermal conductivity is given by

$$dQ = - K \frac{dT}{dx} ds dt \quad \text{-----} \quad (3.12)$$

where s is the surface area and with the following given boundary conditions:

$$\left. \begin{array}{l} r = \infty \\ t \neq \infty \end{array} \right\} = 0; \quad \left. \begin{array}{l} r = 0 \\ t = 0 \end{array} \right\} = 0; \quad \left. \begin{array}{l} r \rightarrow 0 \\ t < 0 \end{array} \right\} -2\pi r K \frac{\partial T}{\partial r} = Q = \text{constant}$$

The third boundary condition being a simplifying assumption.

The solution to this mathematical problem is;

$$T = \frac{Q}{4\pi k} \left\{ -E_i \left( -\frac{4kt}{r^2} \right) \right\} \quad \text{-----} \quad (3.14)$$

where;

$$-E_i(-x) = \int_x^\infty \frac{1}{x} \exp(-x) dx = -C_E - \ln x + \frac{x}{1.1!} - \frac{x^2}{2.2!} + \dots, \quad \text{-----} \quad (3.14)$$

and  $C_E = 0.5772$  is the Euler's constant and  $k$  is the thermal diffusivity given by Eqn. 3.10. If  $r^2/4kt$  is very small,  $-E_1(-x)$  can be described by the terms  $-C_E - \ln x$  only; then the temperature at the surface of the wire would be given by

$$T = \frac{Q}{4\pi t} \left( \ln \left( \frac{4kt}{r_0^2} \right) - 0.5772 \right) \text{-----} (3.15)$$

A comparison with the empirical formula of Stalhane and Pyk give the value of  $A = 0.2389/4\pi \log_{10} e = 0.04377$ , which is indeed a constant and was found to be in good agreement with experimental determination [43]. However,  $B$  is not in general a constant since it is given by  $B = -0.5772 \log_{10} e + \log_{10} 4k$ . To avoid this difficulty, the difference in temperature at two times is taken. Then the following expression is obtained.

$$\Delta T(r,t) = T(r,t) - T(0) = \frac{Q}{4\pi K} \ln \left( \frac{4kt}{r^2 \gamma} \right) \text{-----} (3.16)$$

where;

$\gamma = \exp C_E$ , and  $C_E = 0.5772$  the Euler's constant measured by monitoring the resistance of the wire in a wheat stone bridge as described by De Groot et al. [44].

This relation is the base of the non-stationary method of measuring thermal conductivity. We see that

eqn. 3.16 has a linear relationship in  $\Delta T$  versus  $\ln t$  coordinates. Thus by recording the temperature history at the surface of the wire half-way along its length and plotting  $\Delta T$  against  $\ln t$ , we find  $Q/4\pi K$  is equal to the slope of the straight line, from which  $K$ , the thermal conductivity may be calculated, knowing the quantity,  $Q$  of the heat passing through the wire. More contributions to the theory of the hot wire method have been given by Nieto De Castro, Blackwell, Fukui etc. [16, 44, 45, 46, 47].

#### 3.4.1.1. THE TRANSIENT HOT WIRE METHOD OF COMPARISON:

This method has been developed from the transient hot wire method; and it has been used by Takegoshi et al; for instance to determine the thermal conductivity of orthogonal anisotropic materials such as laminated materials [16, 38]. To determine the thermal conductivity of a solid, using this method, the hot wire is sandwiched between two similar plate type specimens. However due to the difficulty in contacting closely the two specimens because of the thickness of the hot wire it has become more desirable to previously fixing the wire on one of the specimen. These are then conveniently used as a kind of probe and measurements may be started immediately on placing it on any plate type specimen.



Takegoshi et al. [16] have shown that if the material on which the hot wire is fixed has a thermal conductivity value,  $K_1$ , and another plate type specimen with which to sandwich the hot wire has a thermal conductivity  $K_2$ , then the thermal conductivity equation for the arrangement is;

$$K_2 = \frac{Q}{2\pi} \frac{d \ln t}{dT} - K_1 \text{ ----- (3.17)}$$

Then if  $K_1$  is known, it may be used as a reference material for determining the thermal conductivity values of other materials. This method of determining values of thermal conductivity of materials employing the use of a known value of thermal conductivity of a reference material is referred to as the transient hot wire method of comparison.

#### 3.4.1.2. TIME CORRECTIONS:

In deriving equation 3.17 some assumptions are made. For example, it is assumed that (i) the materials under consideration are very large (infinitely) and that the hot wire is infinitely long, (ii) that the hot wire is very thin i.e. the thickness of the wire is infinitesimal and therefore the volume of the wire may be ignored, (iii) that there is no thermal resistance

at the boundary between the hot wire and the material and between the two materials, (iv) the thermal properties such as the thermal conductivity or the thermal diffusivity of the material do not change with temperature, and (v) the hot wire is placed exactly at the boundary of the two materials.

The errors involved due to the above assumptions have been theoretically studied by Van der Held [43] and other workers [47, 49]. For example, Knibble [50] showed that the end effect error, which is the error that arises due to the hot wire being finite, and there being a cooling effect at the ends, can be ignored since it can be kept very small by having the right dimensions of the probe.

Due to the uncertainty in fixing the time at the beginning of reading the temperature-time data Van der Held et al., [43] have shown that, if the total correction time is  $t_0$ , and the temperatures of the surface of the hot wire at time  $t_1$  and  $t_2$  are  $T_1$  and  $T_2$  respectively, then we may write equation 3.12 as;

$$T_2 - T_1 = \frac{Q}{4\pi K} \ln \frac{t_2}{t_1} \text{-----} (3.18)$$

considering the correction time  $t_0$ , then we may write equation (3.18) as;

$$T_2 - T_1 = \frac{Q}{4\pi K} \ln \left( \frac{t_2 + t_0}{t_1 + t_0} \right) \text{ ----- (3.19)}$$

The reciprocal of the derivative with respect to  $t$  is

$$\frac{dt}{dT} = \frac{4\pi K}{Q} (t + t_0) \text{ ----- (3.20)}$$

Plotting  $dt/dT$  against  $t$  yields a straight line with a slope  $Q/4\pi K$ . This straight line cuts the  $t$ -axis at  $-t_0$ . The plot permits us to determine  $t_0$  and not necessarily the value of the thermal conductivity  $K$ , since by graphical differentiation, we get a spread of points which is not admissible. The value of  $t_0$  thus obtained is then used to correct the undifferentiated curve.

### 3.5.0. THEORETICAL MODELS FOR PREDICTION OF THERMAL CONDUCTIVITY VALUES OF HETEROGENEOUS POROUS SYSTEMS

In all attempts to derive an expression for calculating the thermal conductivity of a heterogeneous matrix system, the authors have started by considering the following. That the system is composed of several constituents, one of which is a continuous matrix within

which other constituents are embedded in the form of particles or fibres, this distribution being uniform or at least statistically uniform.

Maxwell [15] suggested a formula for calculating the electric conductivity of a heterogeneous system consisting of a homogeneous isotropic medium filled with spherical particles of another substance that are separated by distances much greater than a particle diameter. Eucken used this expression for calculating the effective thermal conductivity  $K_e$  from the thermal conductivity  $K_m$  of the matrix and  $K_f$  of the filler and the volumetric fraction  $V_f$  of the latter, to obtain the expression referred to as the Maxwell-Eucken formula; i.e.

$$K_e = K_m \frac{K_f + 2K_m - 2(K_m - K_f)V_f}{K_f + 2K_m + (K_m - K_f)V_f} \quad \text{-----} \quad (3.21)$$

Burgers and Fricke [51] applied the Maxwell theory to a similar model, in which the non-reacting particles are of ellipsoidal shape and found the expression called the Burgers-Fricke formula

$$K_{ef} = \frac{K_m V_m + \gamma K_f V_f}{V_m + \gamma V_f} \quad \text{-----} \quad (3.22)$$

where  $\gamma$  is a coefficient which is a function of the ratio  $K_f/K_m$ , the shape, and the mutual arrangement of

the particles. For spherical particles, one should assume that;

$$\gamma = \frac{3K_f}{2K_m + K_f}$$

There is also, the Goring-Churchill formula pertaining to systems containing spherical inclusions [6].

$$\frac{K_e}{K_m} = \frac{2 + \frac{K_f}{K_m} - 2V_f \left(1 - \frac{K_f}{K_m}\right)}{2 + \frac{K_f}{K_m} + V_f \left(1 - \frac{K_f}{K_m}\right)} \quad \text{-----} \quad (3.23)$$

The Wiener formula which is applicable for all inclusions and especially extended to the cases of ellipsoids appears as follows:

$$\frac{K_e - K_m}{K_e + 2K_f} = \frac{K_f - K_m}{K_f + 2K_m} \quad \text{-----} \quad (3.24)$$

Odelevskiy [7] examines a heterogeneous matrix system with a filler in the form of equal-diameter particles. On the basis of the formal coincidence between differential equations for steady flows of heat, electric currents and electromagnetic induction, Odelevskiy derived the expression;

$$K_e = K_m \left[ 1 + \frac{V_f}{\frac{1-V_f}{3} + \frac{K_m}{K_f - K_m}} \right] \text{-----} \quad (3.25)$$

An expression differing significantly from the foregoing equations was suggested by Bruggeman [51]. The discrete filler in the Bruggeman model is taken to have the shape of plate particles, ellipsoids and spheroids. The Bruggeman formula for spherical particles has the form;

$$1 - V_f = \frac{K_f - K_e}{K_f - K_m} \left( \frac{K_m}{K_e} \right)^{1/3} \text{-----} \quad (3.26)$$

Another approach to the derivation of an expression to predict the thermal conductivity coefficients of these systems has been to assume that all the inclusions distributed over the system may be replaced by one large cube shaped pore. Starostin [8] on sub-dividing the elementary cell Fig. 3.2 by isothermal planes, perpendicular to the heat flux direction obtained the following expression for the effective thermal conductivity of the system;

$$K_e = K_m \frac{1 + V_g^{2/3} (\alpha - 1)}{1 + (V_g - V_g^{2/3})\alpha - 1}, \quad \alpha = \frac{K_g}{K_m} \text{-----} \quad (3.27)$$

where  $K_m$  and  $K_g$  are the thermal conductivity coefficient of the host material and of the inclusions respectively, and  $V_g$  the volumetric fraction of the inclusions. This was for all models with isolated inclusions.

For the same model, but deviding the cell by adiabatic planes parallel to the heat flux direction, Missenard [8] derived the expression;

$$K_e = K_m \left[ 1 + \frac{V_g (1 - \frac{1}{\alpha})}{1 - V_g^{1/3} (1 - \frac{1}{\alpha})} \right] \text{-----} \quad (3.28)$$

This was for the case of large volumetric concentration of cube-shaped inclusions located in the nodes of a cubic lattice and  $K_g > K_m$ .

A. Loeb [39], using a model with staggered arrangement of cube shaped inclusions and adiabatic subdivision of the elementary cell, obtained the expression

$$K_e = K_m \left[ 1 - V_g + \frac{V_g}{1 - V_g + \frac{V_g}{\alpha}} \right] \text{-----} \quad (3.29)$$

In addition to spherical and cube-shaped inclusions, studies have been carried out for inclusions in the shapes of cylinders, ellipsoids of revolution, pyramids, rhombhedrons etc., all located at the nodes of a

cubic lattice. The effect of the shape of inclusions is taken into account by an additional characteristic, the shape factor. Loeb suggested that for a structure with voids as inclusions the effective thermal conductivity is;

$$K_e = K_m \left[ 1 - v_g + \left( v_g \left( 1 - v_g + \frac{v_g K_g}{4\sigma\epsilon T C_g T^3} \right)^{-1} \right) \right] \text{--- (3.30)}$$

Latter a model of a structure with interpenetrating components was suggested by G.N. Dul'nev [6, 7, 8]. It consists of two interpenetrating cubic lattices made up of bars with constant cross section Fig. 3.2.

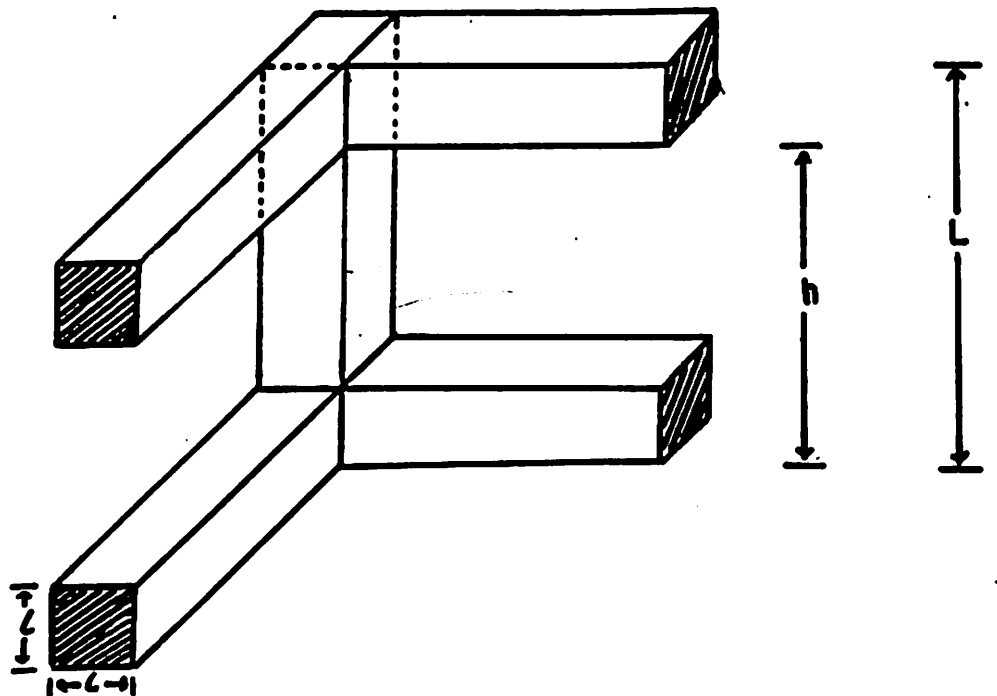


FIGURE 3.2: Model of a Structure with Interpenetrating Components (a) the Model (b) the Unit Cell [8].



He came up with the following expression

$$K_e = K_m \left[ C_g^2 + \alpha(1 - C_g)^2 + \frac{2\alpha C_g(1 - C_g)}{\alpha C_g + (1 - C_g)} \right] \text{ ---- (3.31)}$$

Where  $C_g = \ell/L$  is a geometric parameter (Fig. 3.2b) related to the volumetric fraction  $V_g$  given by

$$V_g = 2C_g^3 - 3C_g^2 + 1$$

Luikov et al. [40] used the same model to derive a similar relationship.

$$\frac{K_e}{K_m} = \frac{1}{(h/L)^2 + A} + \alpha(1 - h/L)^2 + \frac{2}{1 + h/\ell + \frac{1}{\alpha h/L}} \text{ --- (3.32)}$$

Here  $L = \ell + h$  and the value  $A$  expresses heat transfer through contact and gas microgap at the place of contact of two particles, and with no thermal resistance at the joint of two particles,  $A = 0$ .

Zumbrunnen et al. [10] also used a unit cell model Fig. 3.3 to derive the expression;

$$K_e = \left[ \zeta + \Lambda \left( \frac{\beta+1}{\beta} \right) + 1 \right] \left[ \frac{1}{K_m} \left( \frac{\Lambda \psi}{\beta} + \zeta \right) + (1 + \Lambda) \left( Vh_{rv} + \frac{K_t}{\phi} \right)^{-1} \right]^{-1} \text{ ----- (3.33)}$$

where;

$$\zeta = \frac{\Delta}{V} = \frac{(1 + \beta) \left[ \frac{2 + \beta}{1 + \beta} \ln(1 + \beta) + 1 \right]}{\beta \ln(1 + \beta)}$$

and where  $\beta$  is related to the porosity  $p$  by

$$\beta = \frac{p^{1/3}}{1 - p^{1/3}}$$

and  $V$  is the dimensionless parameter,  $4\epsilon\sigma\delta T^3/K_m$ ,  $\sigma$  is the Stefan-Boltzman constant,  $\phi = \lambda/\delta$ ,  $\lambda$  being the effective length for conduction across the pores and  $\delta$  the characteristic pore size,  $\epsilon$  is the emissivity,  $\psi = 0$  or 1 if the pores are interconnecting or closed respectively and  $\Lambda$  is the average number of pores contained in the heat path.

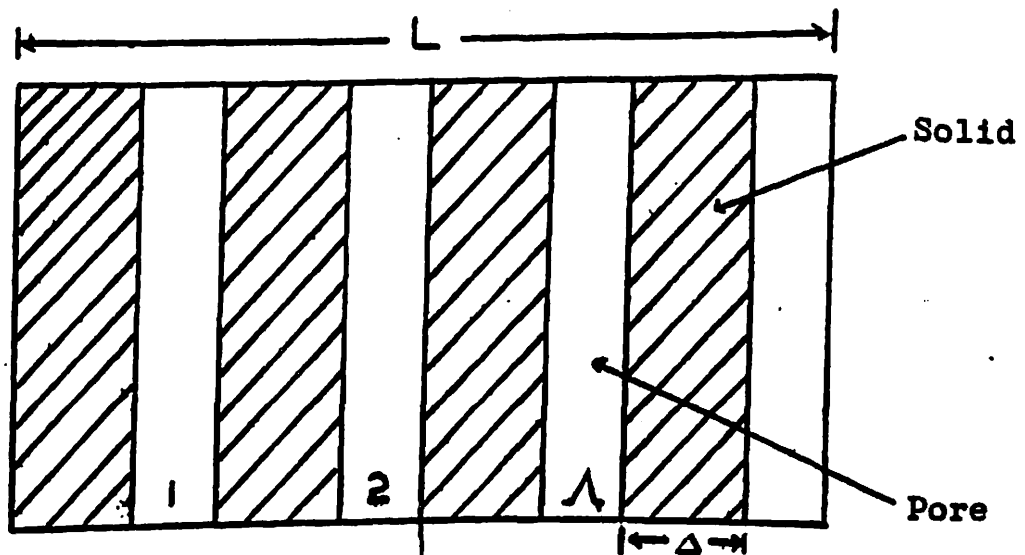


FIGURE 3.3: Characteristic Geometry of the Thermal Conductance Model.

Imura et al. [28] have also derived an expression for the thermal conductivity coefficient of sintered porous materials Fig. 3.4.

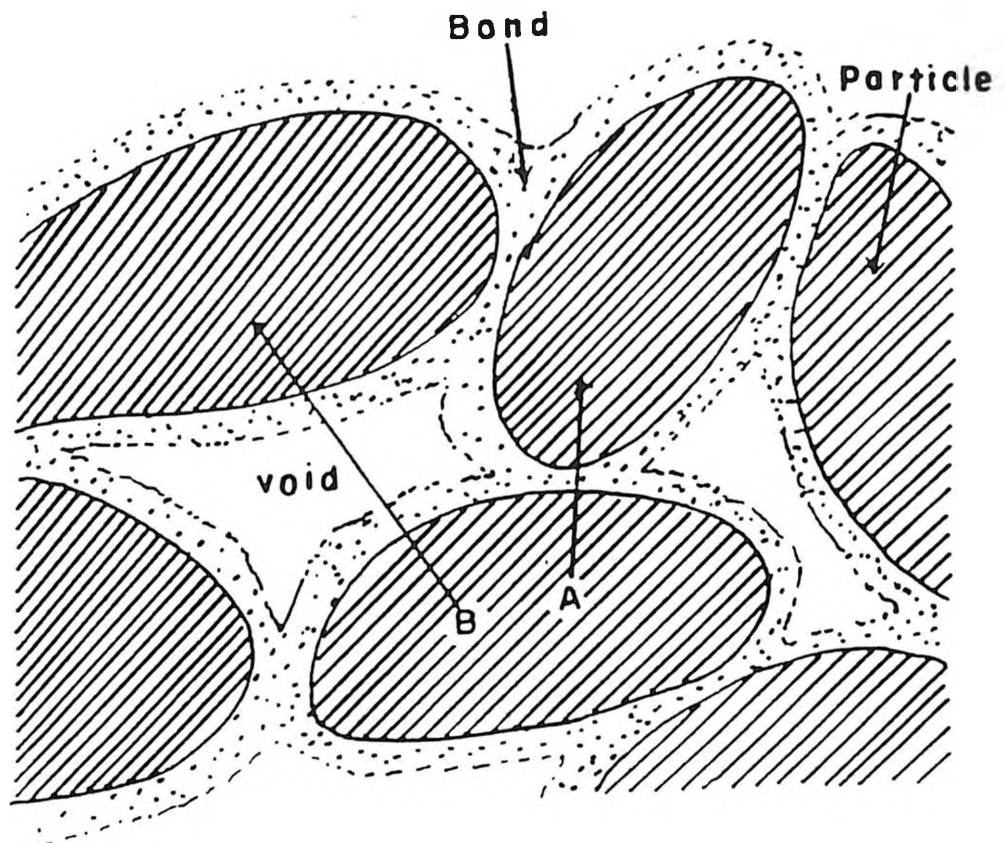


FIGURE 3.1: The Heat Transfer Mechanism for a Sintered Porous Material [28].

They assumed that the heat transfer mechanism as shown by the arrows in the figure is divided into two main paths. In path A, heat flows only through the series path of the solid phases of the particle and bond, and

path B, where heat flows through a path of the solid phases of the particles and the bond and the gas phase in the voids. They came up with the expression for the effective thermal conductivity coefficient;

$$K_e = \frac{(1 - \xi)^2 K_m V_n' + K_b V_b' + K_f V_f'}{\tau \left( \frac{V_m'}{K_m} + \frac{V_b'}{K_b} + \frac{V_f'}{K_f} \right) \left( \frac{K_m}{V_m'} + \frac{K_b}{V_b'} + \frac{K_f}{V_f'} \right) + (1-\tau)(1-\xi)^2} + \frac{\xi}{\frac{1-\mu}{K_m} + \frac{\mu}{K_b}} \quad \text{-----} \quad (3.34)$$

where;

$\xi$  = effective heat conduction area of mechanism of the heat transfer model/total heat conduction area.

$\mu$  = Effective thickness of the bond in mechanism A of the heat transfer model/total heat conduction distance.

$\tau$  = Effective distance of the series arrangement part in mechanism B of the heat transfer model/total heat conduction distance.

$K_b$  is the thermal conductivity of the band,  $V_b$  is the volume fraction of the band,

and  $V'_b = V_b - \xi\mu$

$$V'_m = V_m - \xi(1 - \mu)$$

## C H A P T E R   F O U R

### EXPERIMENTAL DETAILS:

#### 4.1.0. INTRODUCTION:

In this chapter, the procedures used in the characterisation of the materials in terms of particle sizes, chemical composition and porosities are given. This is followed by a description of the techniques used for sample preparation and for thermal conductivity measurements.

#### 4.2.0. CHARACTERISATION OF SAMPLES

##### 4.2.1. GRAIN SIZE ANALYSIS

Many methods exist for determination of particle size distribution of disperse specimen [53, 54, 55]. The merits and demerits of each method depend on the dominant particle size in the sample, the state of the sample, the desired accuracy and the time available.

By microscopy, the size, shape, morphology and colour of the sample may be discerned. The main disadvantages of this method are human fatigue caused by sizing large number of particles at a time, and the difficulty of sizing powders with a broad spectrum of particles. Because of these limitations microscopy

was not used to measure size distribution of the materials under study.

#### 4.2.1.1. SIEVING

This method is used to analyse particle sizes larger than 100 $\mu$ m. A set of 500 $\mu$ m, 250 $\mu$ m, 200 $\mu$ m, and 125 $\mu$ m are arranged and set up in order of decreasing mesh sizes with the coarsest at the top. 100 gms of the dry sample are weighed and placed on the top sieve and the stack gently shaken avoiding spillage. After 10 minutes, the material remaining in each sieve is removed and weighed. These are then recorded as a percentage of the initial sample weight. The results are then plotted as a cumulative percentage frequency curve.

#### 4.2.1.2. SEDIMENTATION:

This method is used to analyse the finer sediments with particle diameters of less than 100  $\mu$ m. The method, unlike the sieve one which employs direct measurement of particle diameter, is based on Stokes law [53], which relates the diameter of a sedimentary particle with its velocity of fall through a viscous medium like water.

About 10 gms of the dry sample is weighed. This together with 10 mls of 0.6 per cent calgon (sodium hexametaphosphate), used to deflocculate the powder,

are placed in an Andreason pipette apparatus and the level raised to the 600 mls mark by adding distilled water and shaking for five minutes. Ten mls of the mixture are then successively drawn, using a pipette, the first one drawn immediately after shaking and the subsequent ones after 3, 6, 12, 24, 48, 90, 150 and 240 minutes. The particle diameters are then calculated from the equation

$$d = \left[ \frac{18\eta v}{(\rho_s - \rho_l)g} \right]^{\frac{1}{2}} \text{----- (4.1)}$$

where  $v$  is the terminal velocity reached by the particles and may be written as  $v = h/t$ , and  $h$  is the height fallen in time  $t$ ,  $\eta$  is the viscosity of water,  $\rho_s$  is the density of the solid,  $\rho_l$  is the density of water and  $g$  is the acceleration due to gravity. The particle diameter values thus obtained are then plotted on a cumulative percentage curve.

#### 4.2.2. PHOTOANALYSIS

The shapes of the grain structures for the materials used to make the refractory bricks were obtained by observing the materials under a Carl-Zeiss transmission microscope. Photomicrographs of the observed structures were then taken using a camera fitted to the microscope.



The colours observed in the materials also gave some information regarding the mineralogy of the materials.

#### 4.2.3. CHEMICAL ANALYSIS

To determine the chemical compositions of the materials, the samples were first dried and ground in an agate mortar to obtain a very fine powder. The samples were then digested by fusing them first to ensure that the silica components would dissolve in acid solution. Fusion was accomplished by mixing the sample intimately with an acid flux of potassium bisulphate ( $\text{KHSO}_4$ ) and heating until the mixture was molten. This was then first cooled and then dissolved in hydrochloric acid ( $\text{HCl}$ ). The chemical analysis was then carried out, using gravimetric methods and also the atomic absorption spectroscopy method as described in various text [24, 56, 57, 58].

#### 4.2.4. MEASUREMENT OF SHRINKAGE ON FIRING

The shrinkage on firing of a clay is of interest because, the greater the shrinkage, the greater the difficulty in holding the finished tolerance. Also, high shrinkages enhance the danger of cracking in the kiln. In general, the more compact the formed brick, the lower the shrinkage. This compaction may either

be inherent in the used material as for example flint clay, or it may be produced by high pressure.

Marks of length 10 cm are made on the surface of the brick in the green state, before firing. The lengths of these marks are then measured again after the bricks are fired. The shrinkage on firing is then determined from the difference between the two measured lengths.

#### 4.2.5. MEASUREMENT OF WEIGHT LOSS ON FIRING

The weight loss on firing is an important characteristic for refractory materials. It includes (i) loss of hygroscopic and absorbed water (ii) loss of water of hydration and absorbed water (iii) loss of colloidal water. These three are for the most part, removed by heating up to 120°C for long periods, say 12 hrs. and are usually classified as the loss of moisture, (iv) loss of combined water, which is part of the structure of minerals, (v) loss of carbon dioxide or carbon monoxide from the burning of carbonaceous materials or the decomposition of carbonates (vi) loss of sulphur dioxide and sulphur trioxide from sulphur compounds, such as pyrites, sulphates, etc. Hydrogen sulphide ( $H_2S$ ), may sometimes be evolved, and (vii) loss of various other gases and volatile substances present in the material.

The weight of a sample of the raw material is measured before being placed into a porcelain crucible. These are then placed into a kiln and fired to 1250°C. The weight of the sample is again taken. The weight loss is then calculated as the percentage of the original weight after calculating the difference between the two weights.

#### 4.2.6. SPECIFIC GRAVITY AND POROSITY MEASUREMENTS FOR THE MATERIALS IN GRANNULAR FORM

To determine the true specific gravity of the materials in the grannular form, the density bottle method, described in the British standards manual [59], was used. The material is first ground into a fine powder in an agate mortar.

The density bottle and stopper were first cleaned, dried and weighed ( $w_1$ ). A sufficient quantity of the dry powder to half fill the bottle is placed in it and the bottle is again weighed ( $w_2$ ). The weight of the powder is thus given by ( $w_2 - w_1$ ). The bottle was then filled with water and freed from all air. Satisfactory results were ensured by evacuating the air and then filling under vaccum with distilled water, which had been boiled to eliminate dissolved air bubbles and then cooled in the absence of air. Excess water overflowing

through the stopper is removed with tissue paper and the bottle and contents weighed ( $w_3$ ). The bottle is then emptied, cleaned, refilled with distilled water and re-weighed ( $w_4$ ). The volume of the bottle is  $(w_4 - w_1)/\rho$ , where  $\rho$  is the density of water or any other fluid used at the temperature of test.

The true specific gravity may now be calculated from the formula

$$G_s = \frac{(w_2 - w_1)\rho}{(w_4 - w_1) - (w_3 - w_2)\rho} \quad \text{-----} \quad (4.2)$$

From this value of the specific gravity, the porosity of the granular material may then be calculated from the expression

$$P = 1 - \eta_s = 1 - \frac{w_d}{V_T G_s Y_m} \quad \text{-----} \quad (4.3)$$

where  $\eta_s$  is the relative volume of solid particles of dry samples,  $w_d$  is the dry weight,  $V_T$  is the bulk volume of the sample,  $G_s$  the specific gravity of the sample and  $Y_m$  the unit mass of water.

#### 4.2.7. POROSITY MEASUREMENTS FOR THE BRICKS:

The porosity of a body is the total proportion of the air space contained between the solid particles

of which the body is composed. The pores in a body may be categorised into six different types [60], (a) closed or 'sealed' pores, (b) channel pores connecting separate pores, (c) blind alloy pores; (d) loop pores, (e) pocket pores - some with narrow necks; and (f) micropores, which are so small as not to be filled with a liquid in any ordinary period of soaking. To these may be added the continuous pores which runs, perhaps with a complex path, from one external face of the body to another. Fig. 4.1. shows these types of pores.

In experiment these different kinds of pores produce two sets of results when the porosity of a material is determined. (a) The true porosity, and (b) the apparent porosity. The true porosity is the ratio between the volume of all voids, both open and closed pores and the total volume of the body. This means that, any closed pores or for that matter, any open ones which are so fine that liquid cannot penetrate into them will not count as void spaces in the determination of apparent porosity.

The usual method of carrying out the determination as described in the British Standards [61], is to take a conveniently sized test piece which is thoroughly

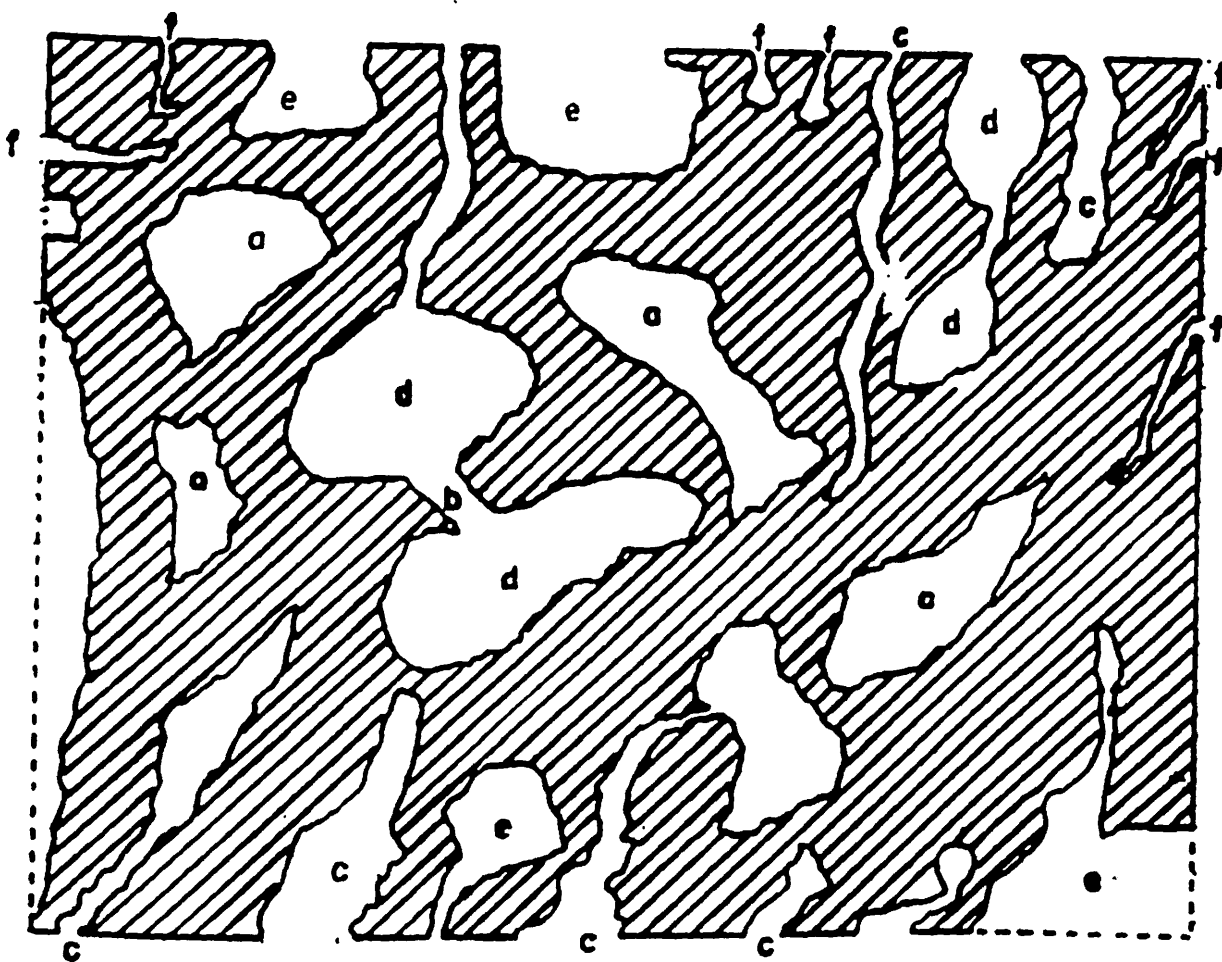


FIGURE 4.1: VARIOUS KINDS OF PORES

- KEY:
- (a) Closed or 'sealed' pores.
  - (b) Channel pores connecting separate pores.
  - (c) Blind alley pores
  - (d) Loop pores.
  - (e) Pocket pores.
  - (f) Micropores.

dried and then weighed ( $w_d$ ). To make sure that liquid completely fills all unsealed pores, the piece is immersed into boiling water for two hours. The saturated sample is then weighed in air to give the weight  $w_s$  by suspending it from a thread attached to the arm of a balance. Finally, the weight of the sample when immersed in water ( $w_{aq}$ ) is measured.

The weight of the liquid absorbed is given by ( $w_s - w_d$ ) gm. provided that water (density = 1) is used for immersion. This figure is also the volume of the open pore spaces in cubic centimeters. The total volume of the test piece is ( $w_s - w_{aq}$ ), i.e. the weight 'lost' on immersion in water, so that the percentage apparent porosity (P), by volume is given by

$$P = \frac{w_s - w_d}{(w_s - w_{aq})\rho} \times 100 \quad \text{-----} \quad (4.4)$$

where  $\rho$  is the density of the liquid used, which is equal to 1 for water.

#### 4.3.0. PREPARATION OF THE BRICK SAMPLES:

The specimens used in the investigation were in the form of refractory bricks. These were made from locally mined samples of the materials listed in section 1.0.0. Except for fireclay which was obtained

both as a raw clay and also as ready-made bricks from Refractories Kenya Ltd., all the other materials were obtained in the form of raw clays and therefore, had to be molded into bricks.

Also required for the preparation of the refractory bricks were the organic binders Dextrin and Starch. These were preferred to the inorganic binders because the organic binders burn off during firing of the bricks, thus leaving behind only the original material to be investigated on.

#### 4.3.1. THE MOLD:

The mold for use in producing the refractory bricks was made as compared to standard sizes of splits of cubic dimensions;  $A = 230$  mm,  $B = 114$  mm and  $C = 32$  mm [62] see Fig. 4.2.

The material used for making the mold was mild steel of thickness 6.0 mm. A metal sheet of the same material was then cut to size and fixed with a handle such that it could slide into the mold to facilitate pressing of the bricks, see Fig. 4.3.

#### 4.3.2. MIXING AND PRESSING:

The recommended water (moisture) content for wet pressing is one of twenty per cent (20%) by weight [24]



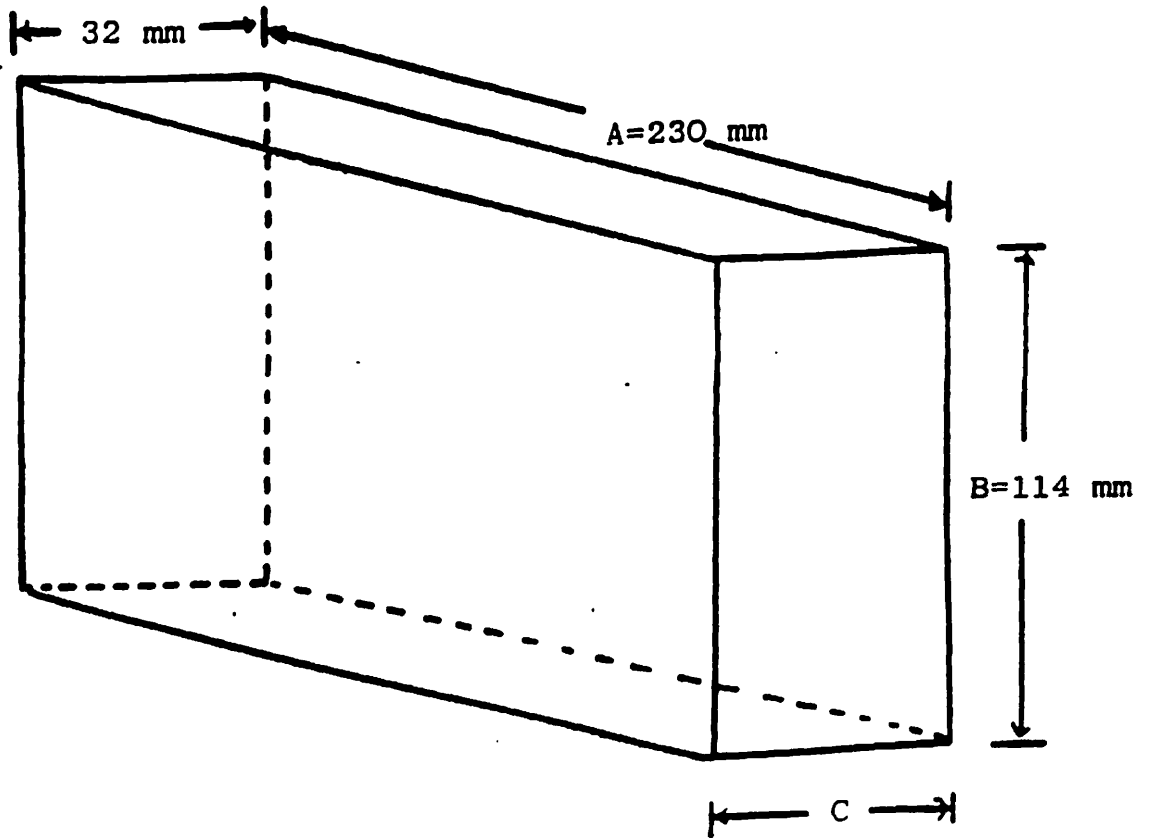


FIGURE 4.2: STANDARD SPLIT SIZES

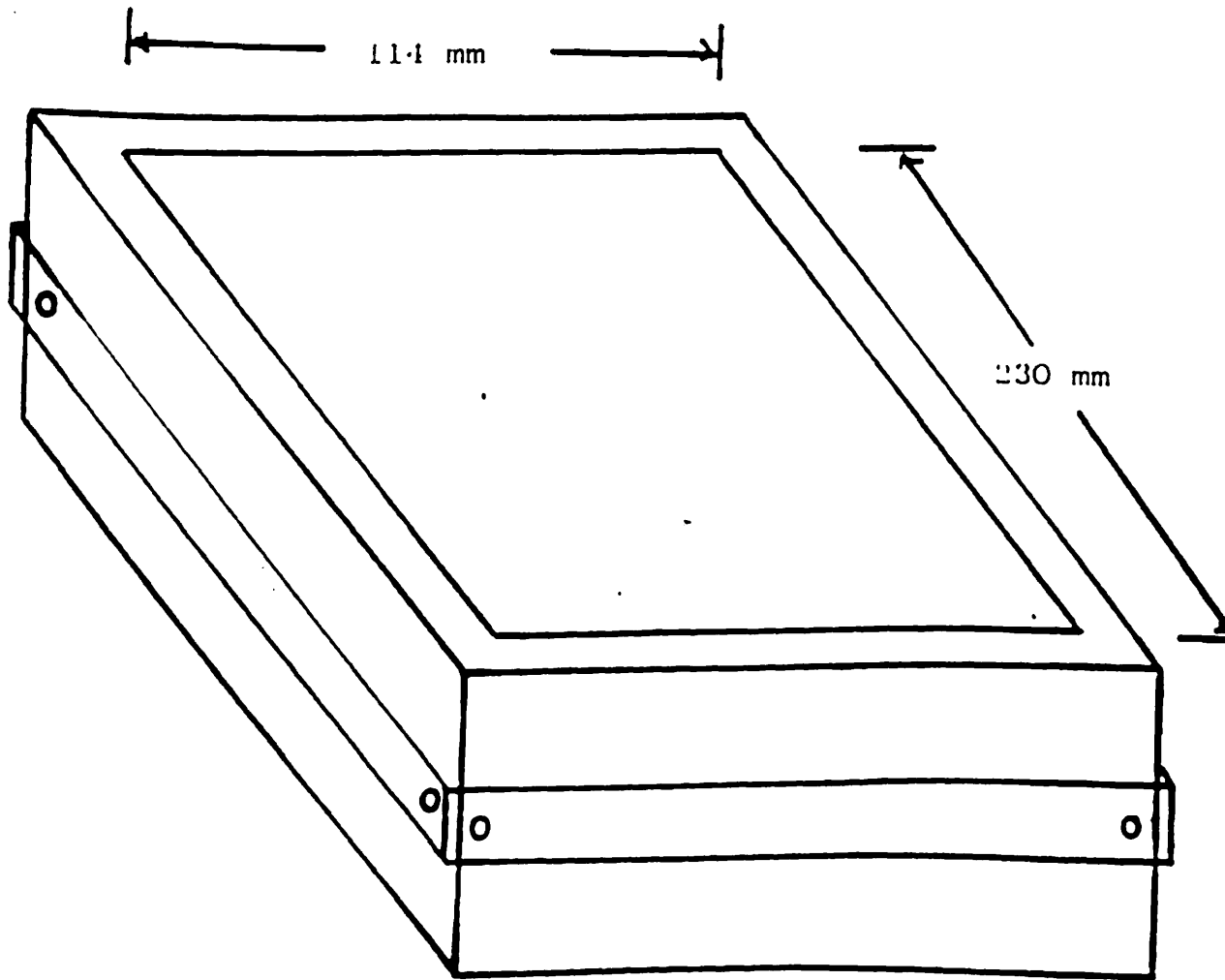


FIGURE 1.3: THE MOLD

and is the one that was used for the preparation of the bricks. The binder material was applied in the form of a twenty per cent solution prepared by boiling say 20 gms of dextrin powder in 100 mls of water.

After thorough mixing, the wet mixture is molded into cubic bricks, using the mold described in 4.3.1. The pressing was done using a Denison hydraulic pressing machine (model IIB/m/c/). A pressure of 1000 psi was applied.

#### 4.3.3. THE HEAT TREATMENT:

The last stage of the brick preparation process was the firing or baking of the refractories. After pressing and molding, the bricks in this "green" state were dried overnight in an oven maintained at a temperature of about 110°C. This is to expel the moisture which is undesirable in the firing kiln because this may spoil the heating elements.

The dry bricks were then arranged in a kiln whose temperature is gradually raised at intervals of 200°C after a duration of five hours, until a temperature of 1150°C is reached. This is the temperature at which the materials must have sintered to form the ceramic bonds.

#### 4.3.4. PREPARATION OF SAMPLES OF VARIED POROSITY:

The method that was used to vary the porosities of the bricks was by introduction of varying proportions of saw-dust in the material during mixing. The saw-dust used was first sieved to obtain fine samples using a sieve of standard gauge size number 20 (see fig. 5.5). This had the effect that during firing, the saw-dust burned off leaving behind open pores, thus increasing the porosity of the brick produced.

#### 4.4.0. THERMAL CONDUCTIVITY MEASUREMENTS:

The transient hot wire method comparison, whose theory is described in section 3.4.1.1. was employed to determine the effective thermal conductivity values of the brick materials. Fig. 4.4. shows the arrangement of the experimental apparatus. The method was initially developed to measure the thermal conductivities of solids and has been used to measure the thermal conductivity along the principal axis of orthogonal anisotropic materials such as laminated plates [53].

The hot wire is sandwiched between a plate-shaped experimental specimen and a reference material whose thermal conductivity is known. The reference material used was a plate of soda-lime glass material of thermal

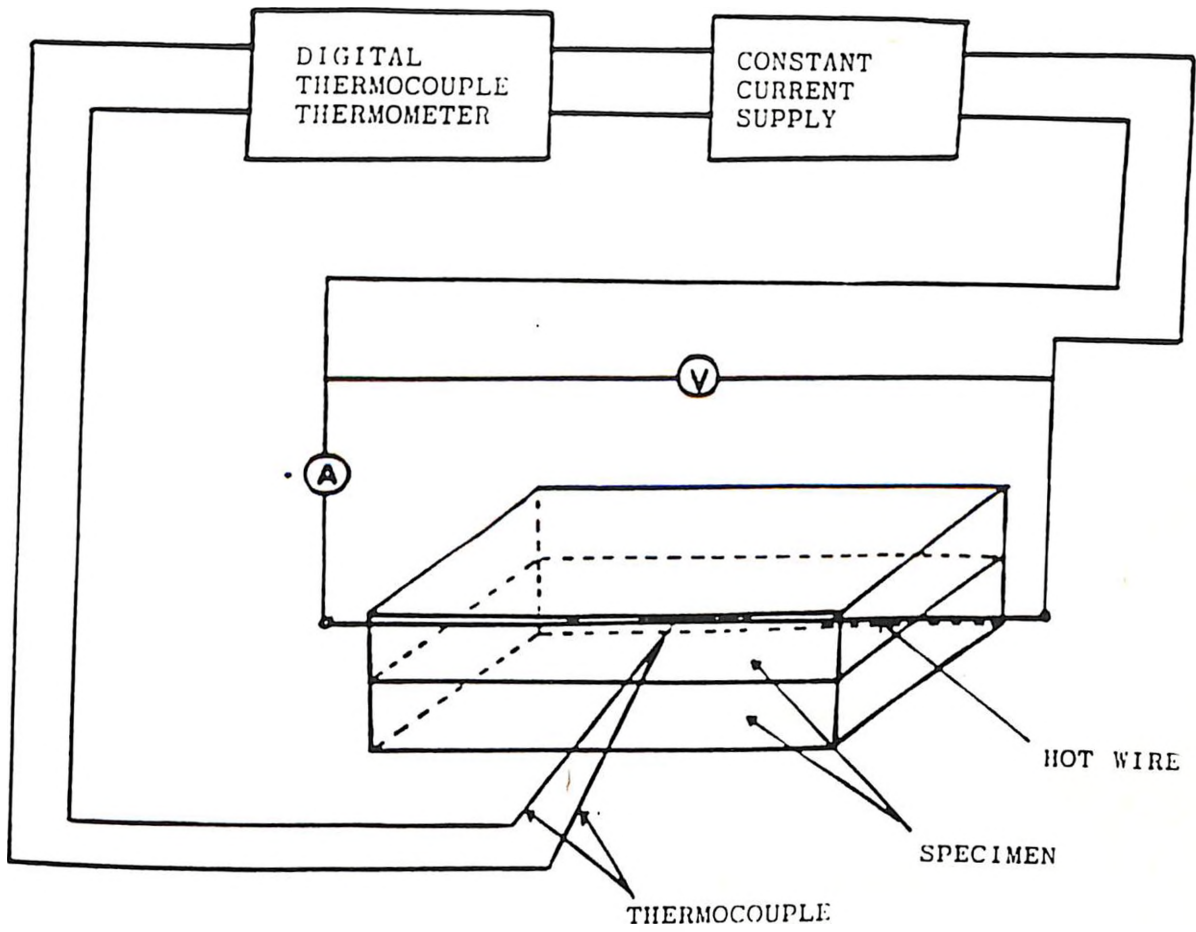


FIG. 4.4 ARRANGEMENT OF EXPERIMENTAL APPARATUS (Thermal probe and its circuitry)

conductivity values given by  $0.72 + 0.001 T_m$   $\text{Kal m}^{-1} \text{h}^{-1} \text{ } ^\circ\text{C}^{-1}$ , where  $T_m$  is the average absolute temperature of the glass plate. To ensure good contact between the two plate-type specimens and the hot wire, the specimens were pressed together by means of G-clamps. The hot wire used was of manganin material of circular cross-section of diameter 2.5 mm. The length of the hot wire was 230m the same as that of the specimen. Electrodes were then fixed at both ends of the hot wire and the electrical resistance measured in advance to ensure it exactly compares with the standard resistance.

At the middle of the hot wire, a thermocouple of nickel-constant (positive, +ve) versus nickel (negative, -ve) was fixed by means of spot welding. Care is taken so that the thermocouple wires have no gap between them. If there is a gap at the junction, voltage due to current flowing through the hot wire would be added to (or subtracted from) the e.m.f. of the thermocouple. The thermocouple leads are then fed into an electronic digital thermocouple thermometer, capable of giving temperature measurements to a precision of  $0.1^\circ\text{C}$ . The thermometer has an in-built cold junction compensator thereby eliminating the use of an external cold junction.

To determine the power input to the hot wire, the current,  $I$ , through the wire was measured by means of anammeter (A) connected in series with the hot wire, while the voltage,  $V$ , across the hot wire was measured by means of a voltmeter connected across it.

To ensure that the readings taken are free from effects of wind currents, all readings were made with the specimen inserted into the furnace. This is because the inside of the furnace is free from wind currents and therefore relatively more stable than the outside. For higher temperature measurements, the temperature of the furnace was brought to the required temperature, care being taken to ascertain that the temperature has stabilised at this temperature, which took several hours. A current is then passed through the wire by giving it a step wise voltage pulse. Readings are then taken of the time,  $t$ , from when the voltage pulse is given, by means of a digital stop watch. Also recorded is the temperature  $T$ , of the surface of the hot wire, at the corresponding time  $t$ , as measured by the thermocouple. These results are then used as described in sections 3.4.1.0 and 3.4.1.1. to calculate the thermal conductivity values.

## CHAPTER FIVE

### EXPERIMENTAL RESULTS AND DISCUSSION:

#### 5.0.0 INTRODUCTION:

The factors that affect the effective thermal conductivities of refractory materials were discussed in chapter three. In this chapter, the findings of the investigation into some of these factors are given, and the results discussed.

#### 5.1.0. SAMPLE CHARACTERISATION:

The materials used for this study are listed in section 1.0.0. In the form in which these materials were obtained, they were not characterised in terms of their chemical composition, mineralogy, grain sizes and their distribution, specific gravity and porosity. The following are results obtained from the characterisation tests.

#### 5.1.1. CHEMICAL ANALYSIS:

Tables 5.1 - 5.4 give the percentage proportions of the different compounds identified in the test samples. The percentage compositions obtained for samples collected from different sites varied slightly and therefore the values given in the tables are the



calculated averages. The percentage proportions are used in section 5.5.1. in the calculation of the theoretical effective thermal conductivity values for the purposes of comparison with experimental values obtained (see section 5.5.1)

TABLE 5.1: KAOLINITE

| Compound                       | Quantity (%) |
|--------------------------------|--------------|
| SiO <sub>2</sub>               | 44.81        |
| Al <sub>2</sub> O <sub>3</sub> | 36.79        |
| Fe <sub>2</sub> O <sub>3</sub> | 1.58         |
| MgO                            | 0.21         |
| CaO                            | 0.71         |
| Na <sub>2</sub> O              | 0.42         |
| K <sub>2</sub> O               | 0.42         |
| TiO <sub>2</sub>               | 0.97         |
| Loss on ignition               | 13.89        |

TABLE 5.2: FIRE CLAY

| Compound                       | Quantity (% age) |
|--------------------------------|------------------|
| SiO <sub>2</sub>               | 66.60            |
| Al <sub>2</sub> O <sub>3</sub> | 21.02            |
| Fe <sub>2</sub> O <sub>3</sub> | 2.85             |
| TiO <sub>2</sub>               | 0.01             |
| P <sub>2</sub> O <sub>5</sub>  | 0.24             |
| CaO                            | 0.01             |
| MgO                            | 0.01             |
| MnO                            | 0.01             |
| Na <sub>2</sub> O              | 0.87             |
| K <sub>2</sub> O               | 0.10             |
| Moisture content at 105°C      | 0.70             |
| Loss on ignition               | 7.46             |

TABLE 5.3: KISII SOAP STONE

| Compound                       | Quantity (% age) |
|--------------------------------|------------------|
| SiO <sub>2</sub>               | 46.42            |
| Al <sub>2</sub> O <sub>3</sub> | 35.73            |
| Fe <sub>2</sub> O <sub>3</sub> | 0.29             |
| MgO                            | 0.05             |
| CaO                            | 0.04             |
| Na <sub>2</sub> O              | 0.64             |
| K <sub>2</sub> O               | 3.81             |
| H <sub>2</sub> O               | 7.70             |
| TiO <sub>2</sub>               | 1.67             |
| Loss on ignition               | 3.65             |

TABLE 5.4: SIAYA CLAY

| Compound                       | Quantity (% age) |
|--------------------------------|------------------|
| SiO <sub>2</sub>               | 60.43            |
| Al <sub>2</sub> O <sub>3</sub> | 16.61            |
| P <sub>2</sub> O <sub>5</sub>  | 0.54             |
| Fe <sub>2</sub> O <sub>3</sub> | 5.18             |
| MgO                            | 0.27             |
| Na <sub>2</sub> O              | 0.69             |
| K <sub>2</sub> O               | 0.10             |
| CaO                            | 0.09             |
| TiO <sub>2</sub>               | 0.25             |
| Moisture content               | 5.74             |
| Loss on ignition               | 11.29            |

5.1.2: MINERALOGICAL ANALYSIS

Table 5.5 gives the mineralogical analysis of the materials tested. The tables give the physical description of the samples and also the mineral identified in the sample.

TABLE: 5.5a: Mineralogy

|                       |                       |   |
|-----------------------|-----------------------|---|
| Sample                | Kaolin                | Fire Clay   |
| Description of Sample | White-greyish powder  | Brownish Clay   |
| Mineralogy            | Kaolinite             | Fire Clay   |
| Formula               | $Al_2(Si_2O_5)(OH)_4$ | $Al_2O_3 \cdot 2SiO_2 \cdot 2H_2O$<br>+ $Fe_2O_3$ 2.85% |

TABLE 5.5b: Mineralogy

|             |  |                                    |
|-------------|--|------------------------------------|
| Sample      | Siayaclay                                  | Kisii Soap Stone                   |
| Description | Reddish brown clay                         | Grey Stone                         |
| Mineralogy  | Common Clay                                | China Clay                         |
| Formula     | $Al_2(Si_2O_5)(OH)_4$<br>+ 5.18% $Fe_2O_3$ | $Al_2O_3 \cdot 2SiO_2 \cdot 2H_2O$ |

The chemical composition tests and the mineralogy tests show that both kaolin and the Kisii soap stone mainly consists of granite which has decayed without

much movement from its original site. The two are compounds of silica, alumina and water, plus traces of lime and the alkalis. The brownish colour present in fireclay is due to the presence of iron oxide of about 2.85%, in this case. Siaya clay was observed to be the common clay containing a percentage of iron oxide ( $\text{Fe}_2\text{O}_3$ ) of over 4%, which makes it look reddish.

### 5.1.3. OPTICAL CHARACTERISATION

The optical characterisation of the materials was done using a Carl-Zeiss transmission microscope. The results show that kaolinite is composed of an approximately uniform distribution of particles that have shapes close to spherical ones (Fig. 5.1). Fireclay has a similar distribution of particles but here the grains are much larger Fig. 5.2. This means that it is easier to make bricks of lower porosities for the case of kaolin. This is due to the fact that, the larger the particles, the larger the interparticulate pores. Fig. 5.3. shows an agglomeration of small particles to form large ones in the Siaya clay material. This shows that it is possible to obtain molded bricks of very low porosity from this material. The naturally occurring Kisii stone was crushed and the powdered material thus obtained observed as before under a polarising

microscope (Fig. 5.4). The particles arrange themselves in a thread-like fashion. This type of arrangement would enhance conduction along the threads while reducing conduction in any direction that crosses the threads.

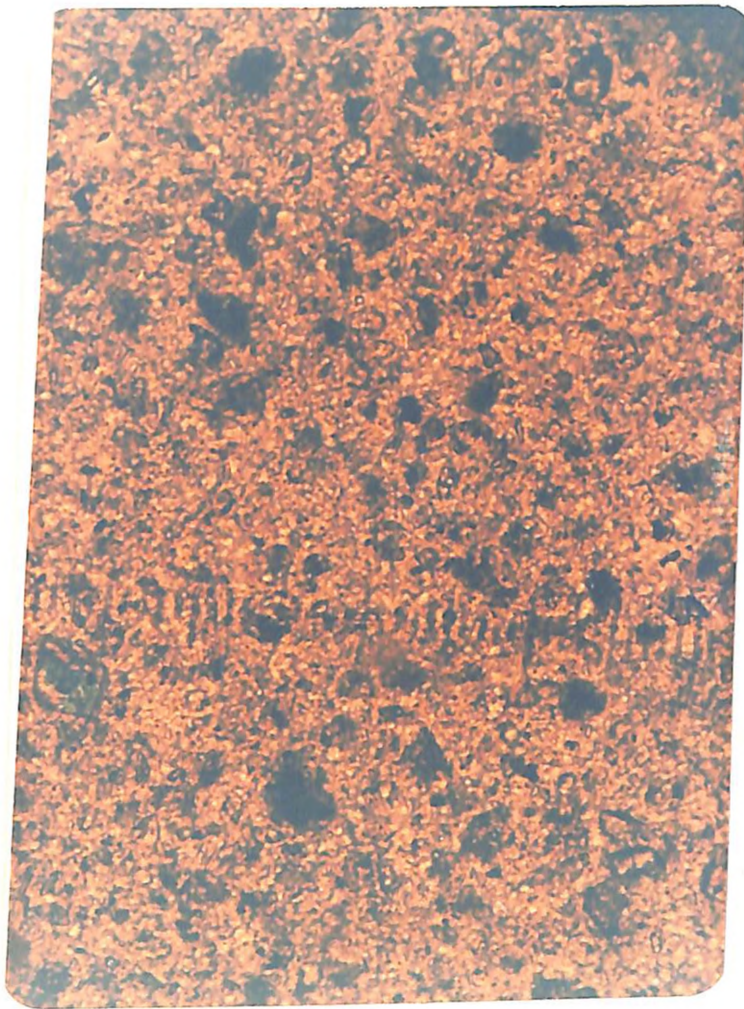


FIGURE 5.1: A PHOTO MICROGRAPH OF THE KAOLINITE MATERIAL X 80. It shows an almost uniform distribution of almost spherical particles or agglomeration of particles.

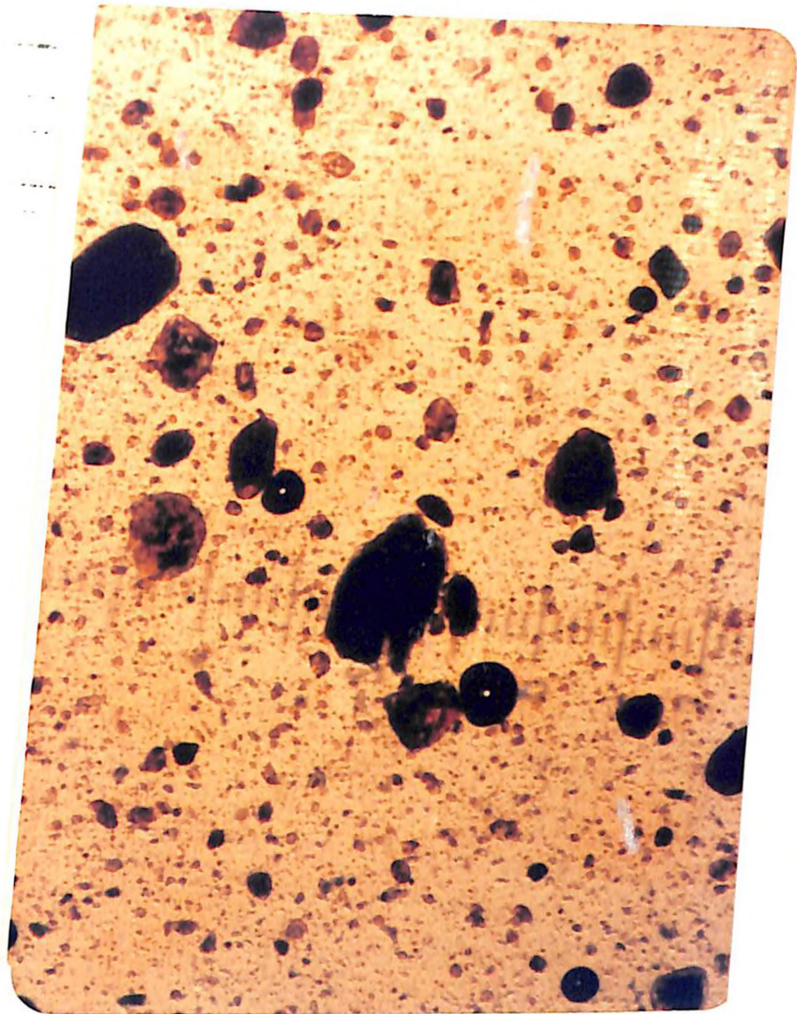


FIGURE 5.2: A PHOTOMICROGRAPH OF FIRECLAY X 20. It Shows relatively large particles which implies the presence of large interparticulate pores in molded material.



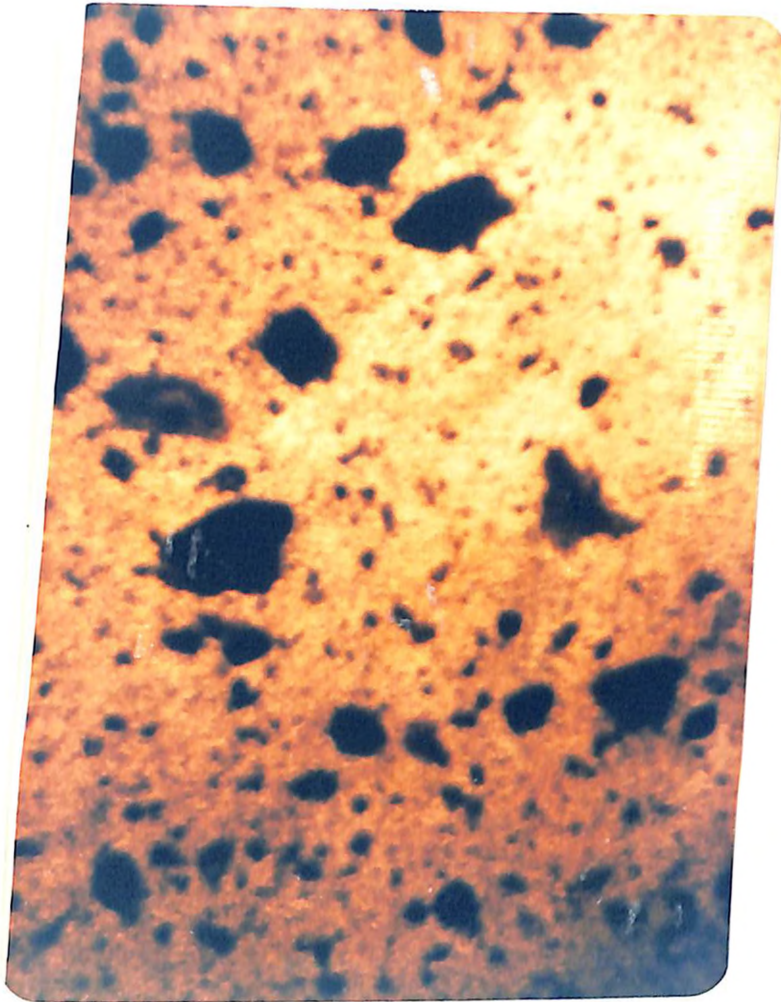


FIGURE 5.3: A PHOTOMICROGRAPH OF SIAYACLAY X 20. It shows agglomeration of small particles to form large ones. This predicts low porosities in the molded materials.

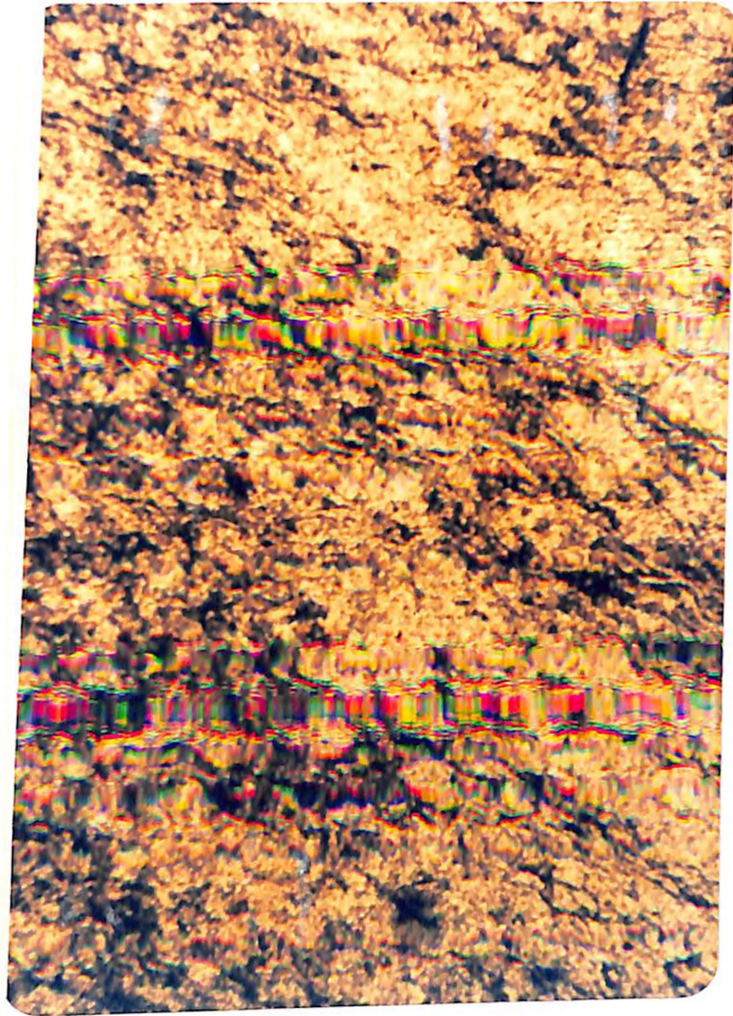


FIGURE 5.4: A PHOTOMICROGRAPH OF POWDERED KISII SOAP STONE. It shows thread-like patterns of grains. This pattern predicts an enhanced conductivity along the grain threads and a relatively low conductivity along any direction that crosses the grain-threads.

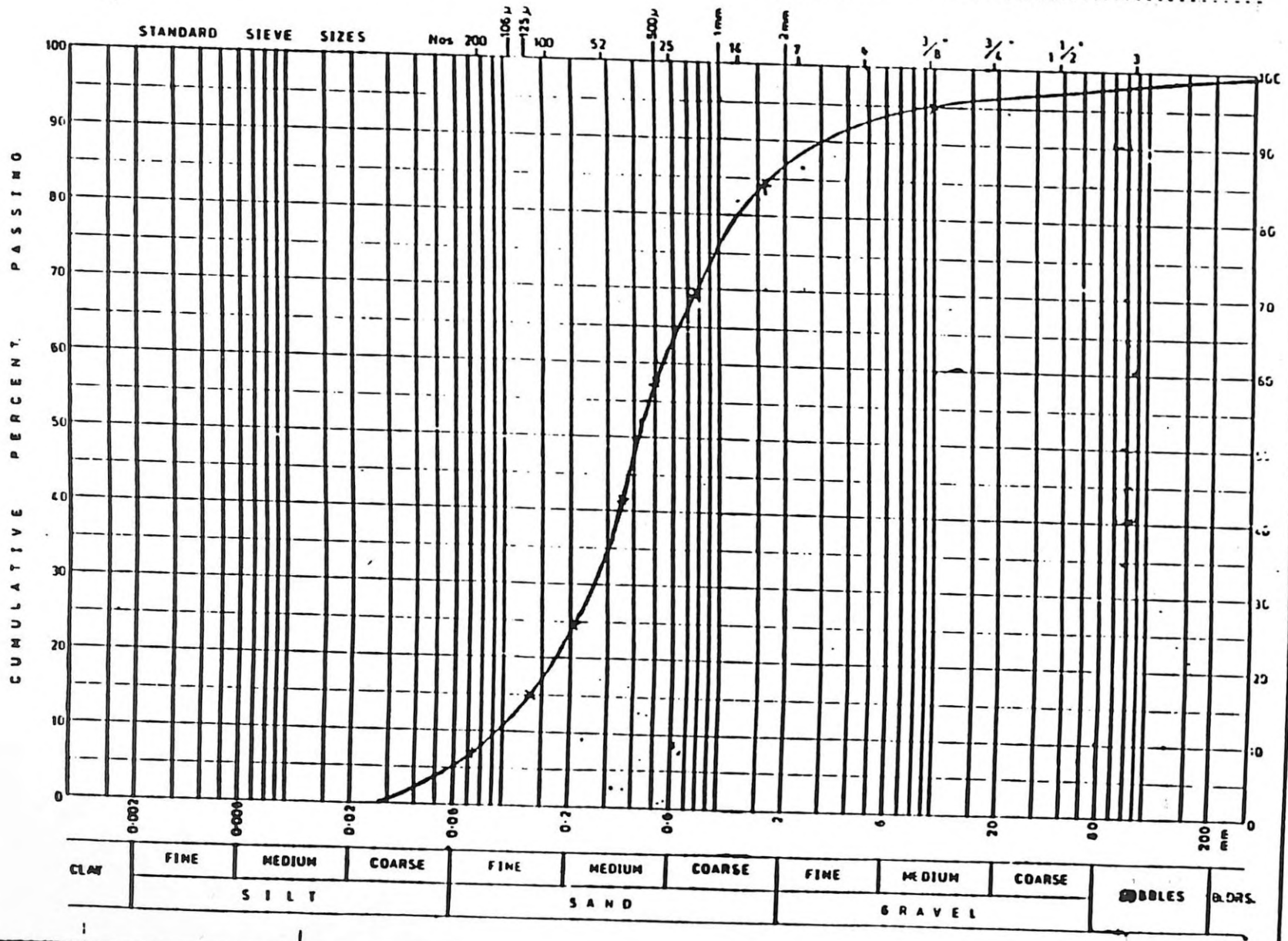
#### 5.1.4. PARTICLE SIZE DISTRIBUTION

For the fire clay material, the sieving method [see section 4.2.1.1] was used to size the samples due to the presence of particles of relatively large sizes. For kaolin and Siaya clay, the sedimentation method [see section 4.2.1.2] was used because the two were essentially powders. The Kisii stone was obtained in the form of the naturally occurring consolidated material. This material was just cut to the required shape and fired in the same form. Since the material was never in the granular form, no particle size analysis was performed on it.

Figs 5.5 - 5.7 shows the distribution curves for the particle sizes of the above three materials. For each of these materials, the particle sizes at the first quartile, the median and the third quartile marks are listed in table 5.6. For a given sample, the median particle size is considered as the representative characteristic size for the sample.

**PARTICLE SIZE DISTRIBUTION**

**FIRECLAY**



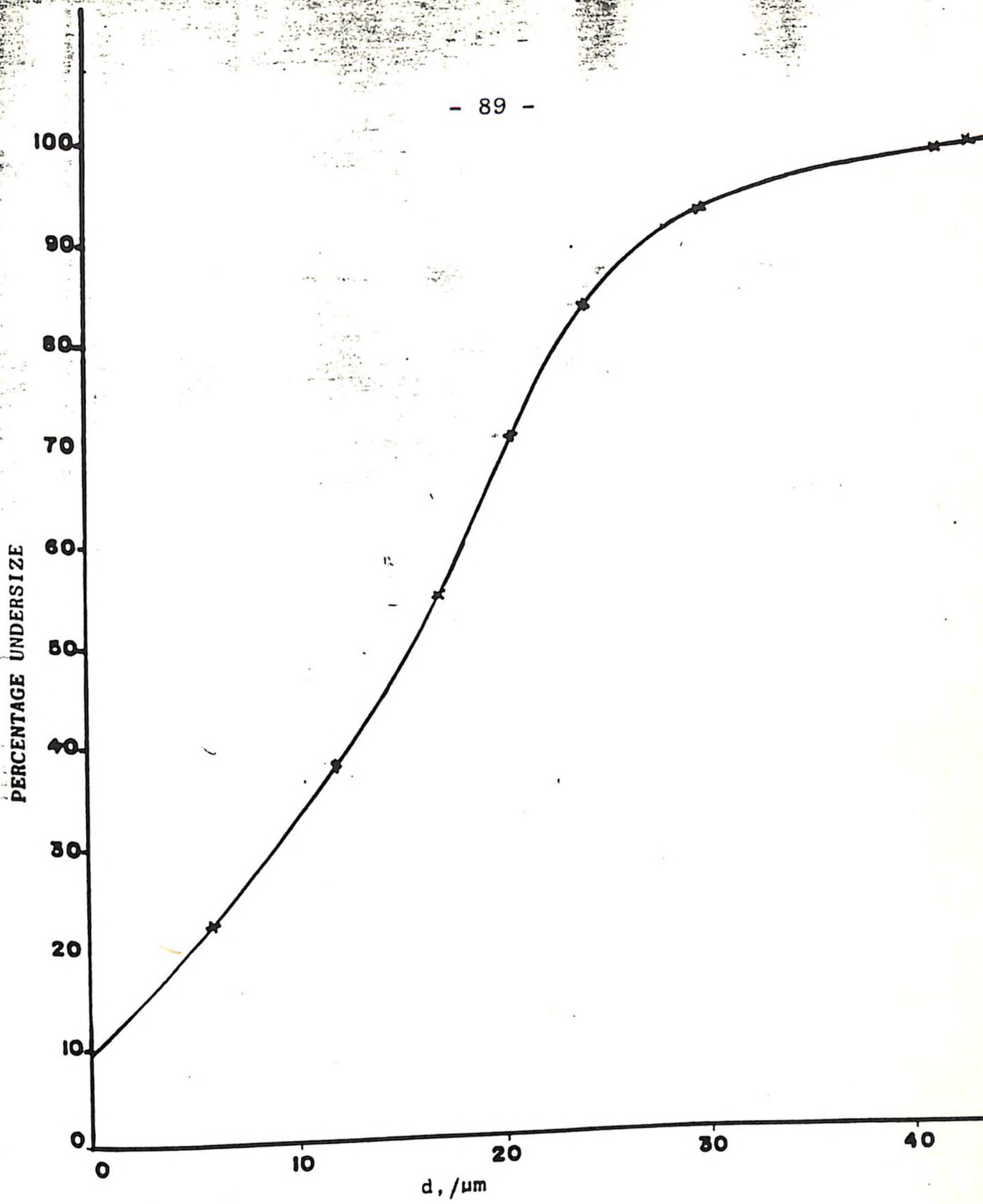


FIGURE 5.6: PERCENTAGE UNDERSIZE AGAINST PARTICLE DIAMETER  
FOR KAOLIN

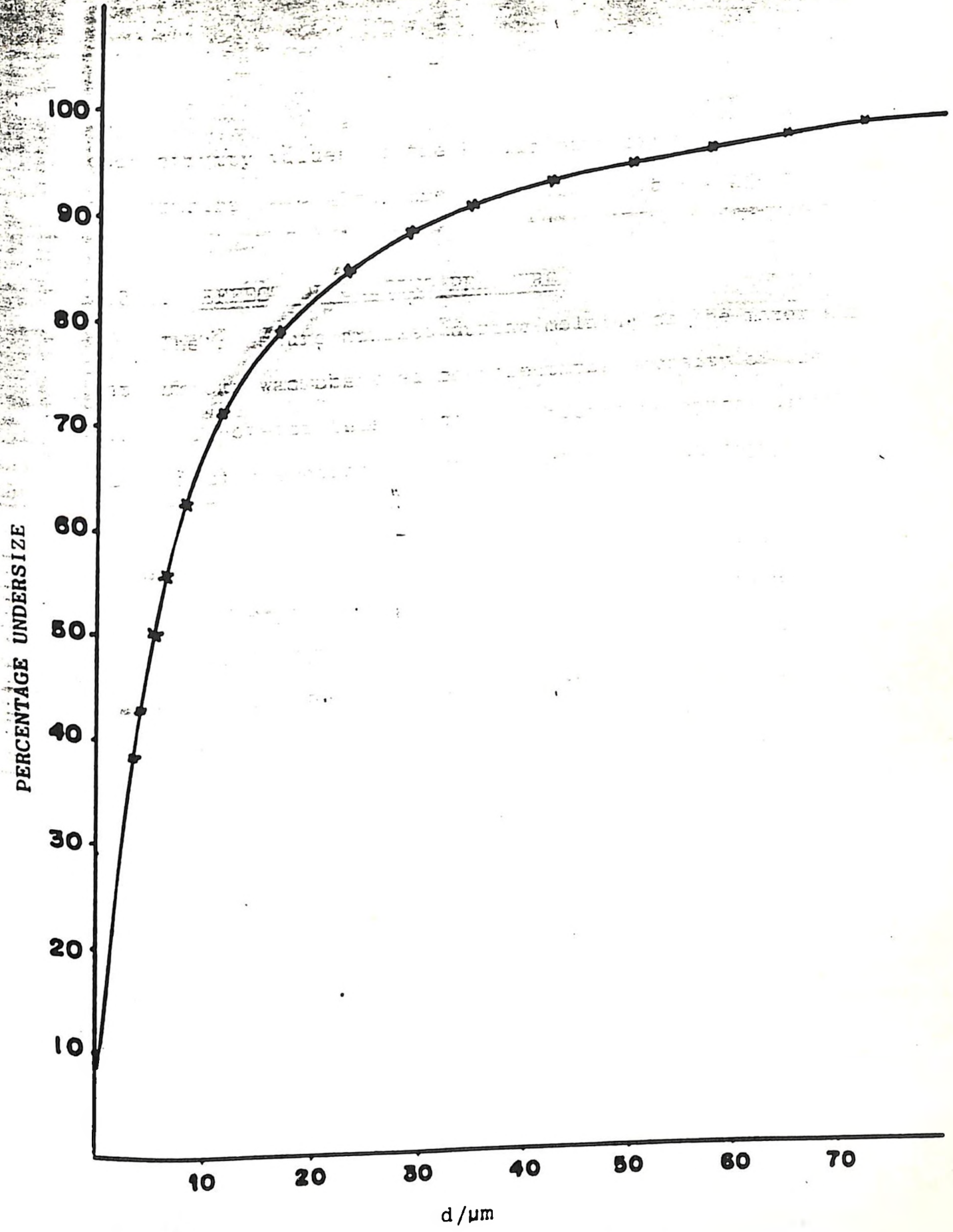


FIGURE 5.7: PERCENTAGE UNDERSIZE AGAINST PARTICLE DIAMETER  
FOR SIAYA CLAY

TABLE 5.6. Mean Particle Sizes at the first Quartile, the median and the third quartile marks.

| Sample        | First Quartile (mm)   | Median Size (mm)       | Third Quartile (mm)    |
|---------------|-----------------------|------------------------|------------------------|
| Fire Clay     | 0.22                  | 0.52                   | 0.95                   |
| <u>Kaolin</u> | $7.25 \times 10^{-6}$ | $1,575 \times 10^{-5}$ | $2.175 \times 10^{-5}$ |
| Siaya Clay    | $1.75 \times 10^{-6}$ | $5.5 \times 10^{-6}$   | $1.35 \times 10^{-5}$  |

5.1.5. SPECIFIC GRAVITY AND POROSITY MEASUREMENTS  
FOR THE MATERIALS IN GRANULAR FORM

The specific gravities and the porosities of the materials in granular form were determined as described in section 4.2.6. The results are presented in table (5.7).

TABLE 5.7. Specific gravities and porosities of the materials in Granular form.

| Sample     | Specific gravity of material in granular form | Porosity of the material in granular form |
|------------|---|---|
| Kaolin     | 2.65  | 0.837                                     |
| Fire Clay  | 2.50  | 0.898                                     |
| Siaya Clay | 2.55  | 0.859                                     |

The large grain sizes found in fire clay Fig. 5.5 explains the high porosity observed in the materials in this granular form. This predicts bricks of high porosity for those prepared from this material (see also section 5.1.4) Kaolin and Siaya clay have lower porosities in the granular form. Thus it will be easier to make bricks of low porosities from these materials.

#### 5.2.0. EFFECT OF FIRING THE MATERIALS TO DIFFERENT TEMPERATURES

Though changes that take place during firing of less perfectly crystalline kaolinite or fire clay are somewhat different from those of pure well-crystallized kaolin, the observations are quite similar.

When crystalline kaolin is slowly heated, nothing happens until 450°C is reached, at which point there is a loss in weight of about 14 per cent and a heat absorption of 170 Cal per gram. Beyond this temperature, the structure changes from kaolinite  $\text{OH}_4\text{Si}_2\text{O}_5\text{Al}_2$  to meta-kaolin  $\text{Si}_4\text{Al}_4\text{O}_{14}$ . At about 950°C there is a sharp evolution of heat and a new crystal phase appears having a spinel ( $\text{Al}_4\text{Si}_3\text{O}_{12}$ ) shape (see Fig. 5.8). Above 1050°C, this structure gradually breaks down into an amorphous or glassy phase. Fig. 5.8 shows the variation of thermal



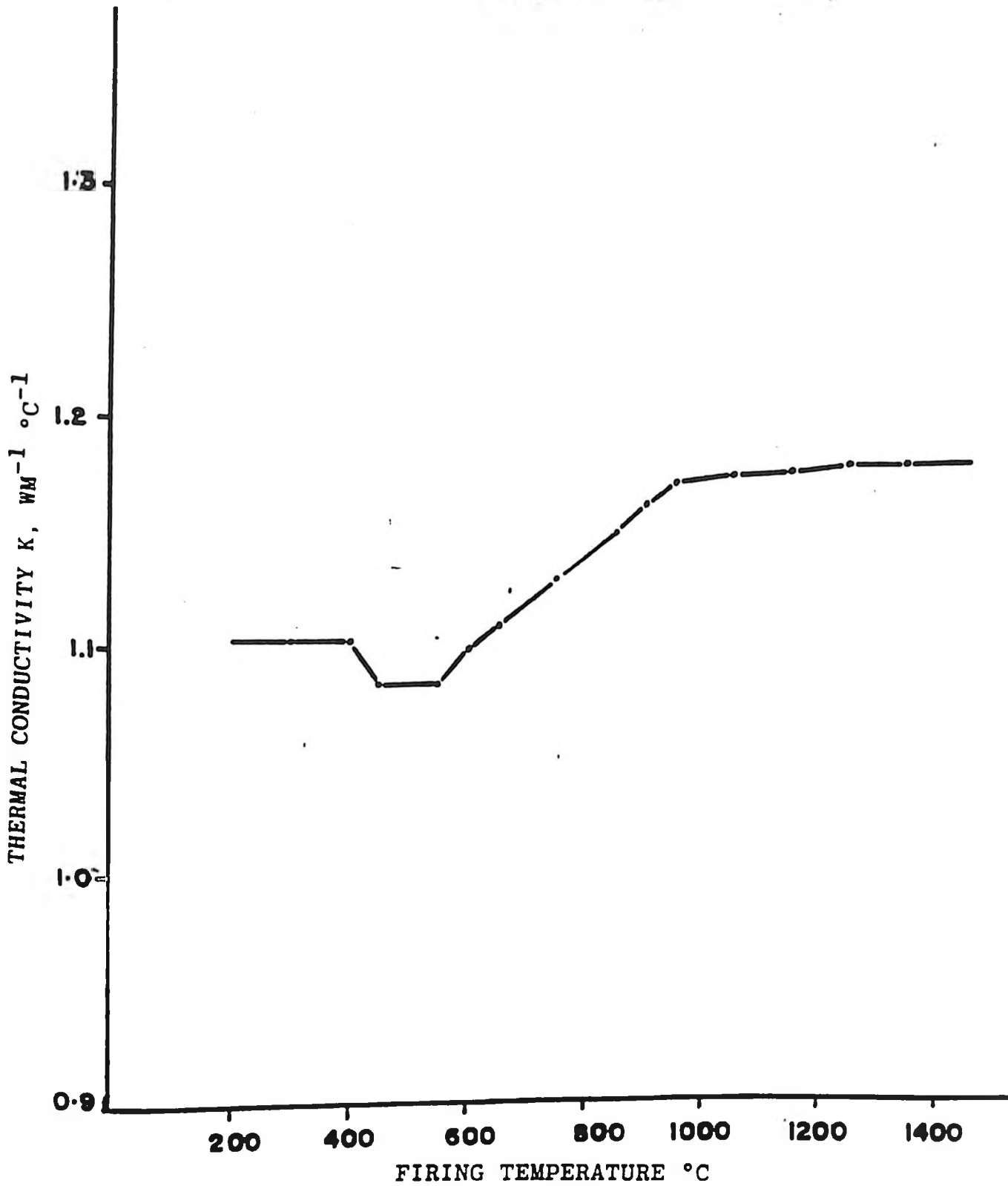


FIGURE 5.8: VARIATION OF THERMAL CONDUCTIVITY WITH FIRING TEMPERATURE FOR KAOLIN MATERIAL (The measurements were made at  $100^\circ\text{C}$ , Porosity = 38.5%)

conductivity values of the kaolin material with firing temperature (see also appendixes Figs. A 5.1 - A 5.3).

5.3.0. EFFECT OF CASTING PRESSURE

The pressure applied during molding of the materials into bricks was observed to affect the porosity of the bricks. However this is not an effective way of varying the porosity because a large variation in casting pressure produced a very small change in porosity. The more effective way of varying the porosities of the bricks was by using saw-dust (sec. 4.3.4). For pressure to affect the porosity appreciably, may be it would have to be applied throughout the firing process.

Table 5.8. shows the values of the porosities and the thermal conductivities for two fireclay bricks, one which was prepared by hand-pressing and the other one by machine pressing at 1000 psi. This difference in casting pressure brought about a porosity difference of 0.1 per cent only. The resulting difference in thermal conductivity was  $0.001 \text{ wm}^{-1} \text{ }^{\circ}\text{C}^{-1}$ .

|                       | PERCENTAGE POROSITY | THERMAL CONDUCTIVITY AT 155°C (WM <sup>-1</sup> °C <sup>-1</sup> ) |
|-----------------------|---------------------|--|
| Hand pressed brick    | 44.5                | 0.865 ± 0.043  |
| Machine pressed brick | 44.2                | 0.866 ± 0.043  |

TABLE 5.8: THERMAL CONDUCTIVITY AND POROSITY VALUES FOR TWO FIRECLAY BRICKS; ONE PREPARED BY HAND PRESSING AND THE OTHER ONE BY MACHINE PRESSING AT 1000 psi.

#### 5.4.0. EFFECT OF POROSITY VARIATION

The variation of the thermal conductivity with the percentage porosity for the fired bricks followed patterns shown in Fig. (5.9) and also in the appendices Figs. A5.4 - A5.5. The percentage porosity for Kisii soap stone could not be varied because this was only available in the form of the naturally occurring stone which was cut to size and fired in the same form. Each of the figures show the variation of the thermal conductivity with the percentage porosity for two temperatures, one below 200°C and the other one above 600°C. The values of thermal conductivity were observed to decrease with increasing values of percentage porosity. It may be pointed out here that the method of varying the porosity of the bricks as described in section (4.3.4) could only give porosity ranges of between 20 per cent and 50 per cent. Bricks of low porosity were not easy to make while those with very high porosities became too weak and very hard to handle.

#### 5.4.1. EFFECT OF MOISTURE ON THERMAL CONDUCTIVITY AT DIFFERENT PERCENTAGE POROSITIES

The effect of moisture on the effective thermal conductivity of the bricks was investigated, by measuring the thermal conductivities of dump bricks

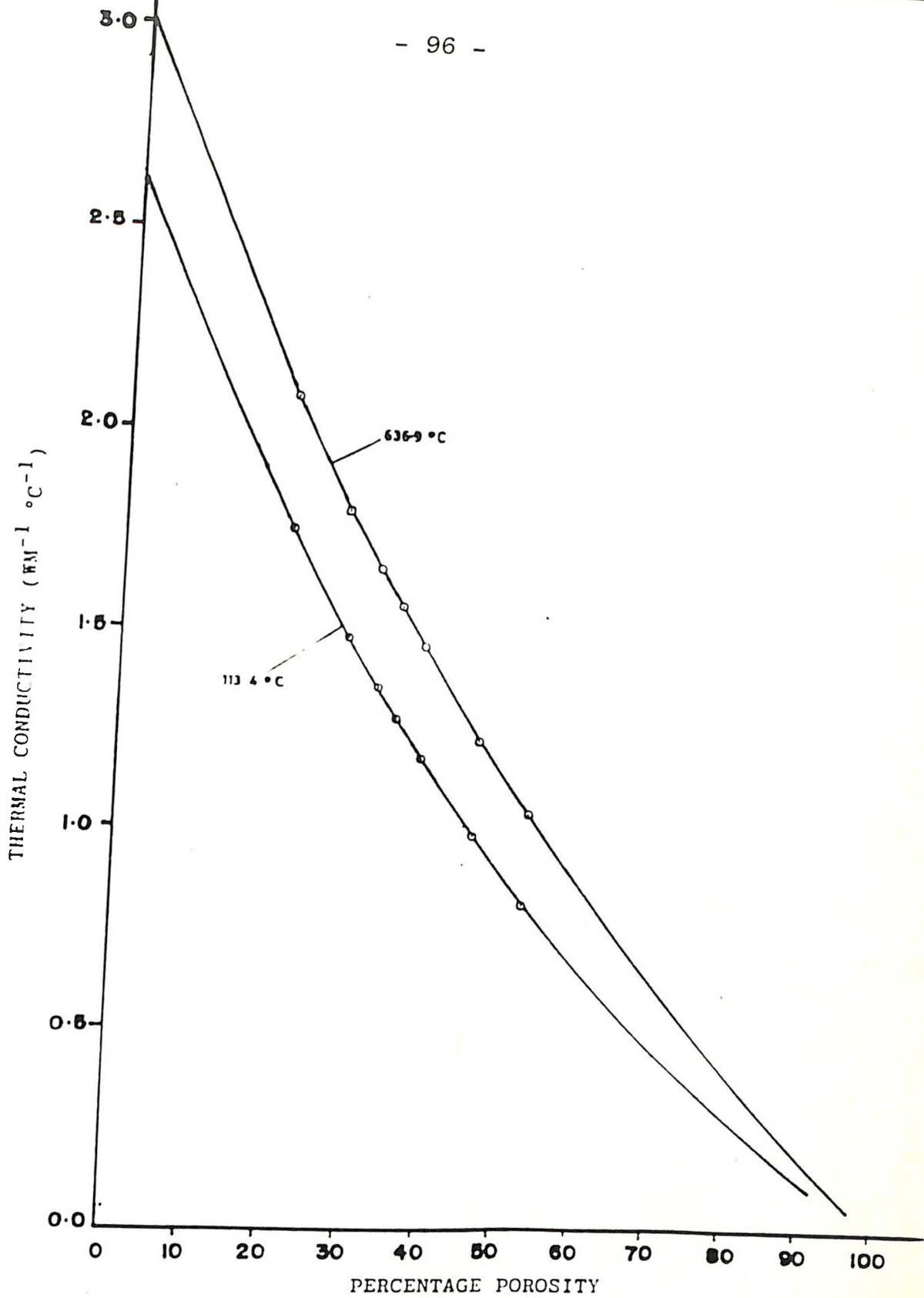


FIGURE 5.9: THERMAL CONDUCTIVITY AGAINST PERCENTAGE POROSITY  
FOR KAOLIN AT TEMPERATURES A = 113.4 °C and  
B = 636.7 °C

of different percentage porosities at room temperature. It can be seen from figure (5.10) and also from appendices Figs. A5.6 - A5.7 that the effective thermal conductivity of moist bricks is higher than that of the dry sample. The increase of thermal conductivity by the presence of moisture may be explained by the fact that the presence of water in the pores of the material increases the mean free path,  $\lambda$ , of the Debye expression Eqn. 3.9 thus increasing the effective thermal conductivity.

#### 5.4.2. COMPARISON BETWEEN EXPERIMENTAL RESULTS WITH THEORETICAL PREDICTION OF THE VARIATION OF THERMAL CONDUCTIVITY WITH POROSITY

As it was pointed out in chapter two, very little has been reported in the literature on the thermal conductivity of sintered refractory bricks. Even less work has been reported on the theoretical calculations for thermal conductivity of such materials. More attention has been given to the thermal conductivity of pure crystalline or amorphous materials or for mixtures of either consolidated or unconsolidated two or three phase systems which are well defined in terms of manner of mixing and nature of the mixture [6, 7, 8, 10, 13, 14, 17, 27, 51, 63 - 66]. Brailsford and

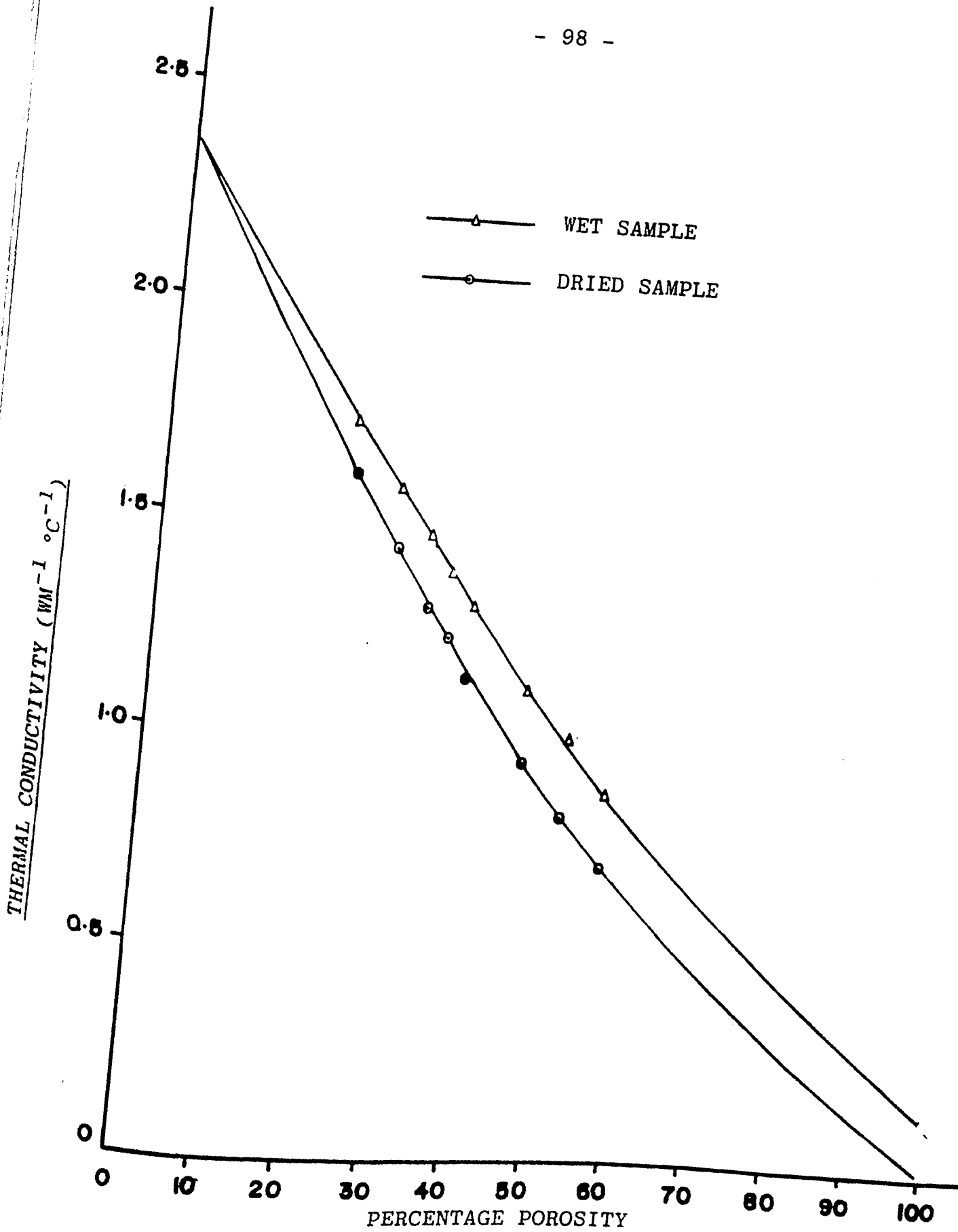


FIGURE 5.10: THERMAL CONDUCTIVITY AGAINST PERCENTAGE POROSITY FOR KAOLIN DRY AND WET SAMPLES AT 30°C OF PERCENTAGE MOISTURE CONTENT OF 24.5%

Major [13] have derived an expression for the effective thermal conductivity,  $K_e$ , of a three phase mixture of constituents of known thermal conductivity values  $K_0$ ,  $K_1$  and  $K_2$  and of volumetric proportions  $V_0$ ,  $V_1$  and  $V_2$ , as;

$$K_e = \frac{K_0 V_0 + K_1 V_1 \frac{3K_0}{2K_0 + K_1} + K_2 V_2 \frac{3K_0}{2K_0 + K_1}}{V_0 + V_1 \frac{3K_0}{2K_0 + K_1} + V_2 \frac{3K_0}{2K_0 + K_2}} \quad \text{----- (5.1)}$$

assuming that the phase with thermal conductivity  $K_0$  is the continuous phase.

Figs. (5.11, A5.8, A5.9) show the comparison of the theoretically obtained values with those obtained from experiment. The experimental values are in general lower than those obtained from theory. This difference may be attributed to differences between the assumptions made during the derivation of the theoretical expressions and the actual situation in the refractory brick. In the derivations, for example, the particles that make up the system are assumed to be arranged as a random distribution of solid spheres in a continuous medium which is not exactly the case for the materials used in this study as may be seen from Figs. 5.1 - 5.4.

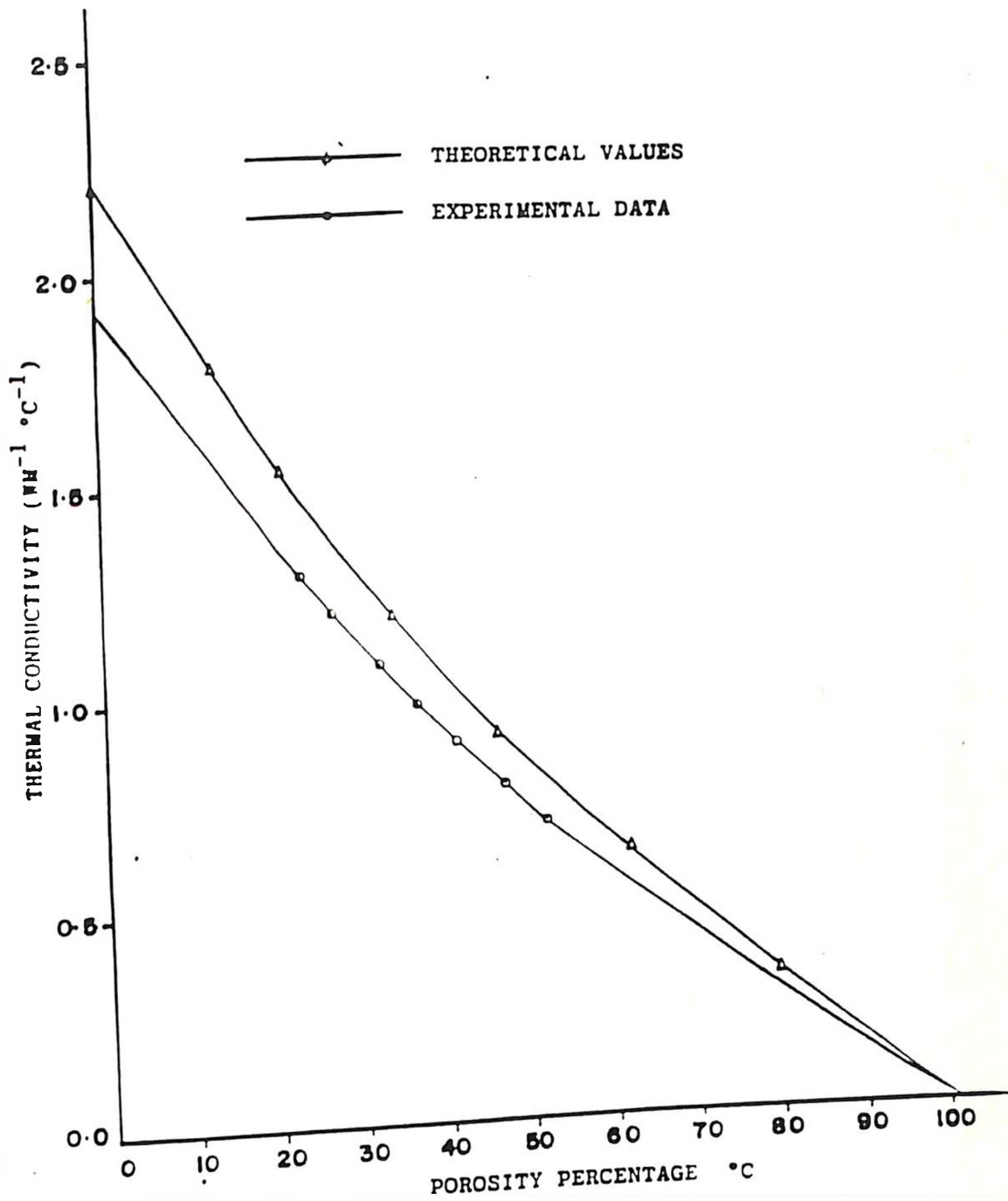


FIGURE 5.11: COMPARISON BETWEEN THEORETICAL PREDICTION AND EXPERIMENTAL DATA FOR FIRECLAY AT 110.7°C



THERMAL CONDUCTIVITY ( $WM^{-1} \text{ } ^\circ C^{-1}$ )

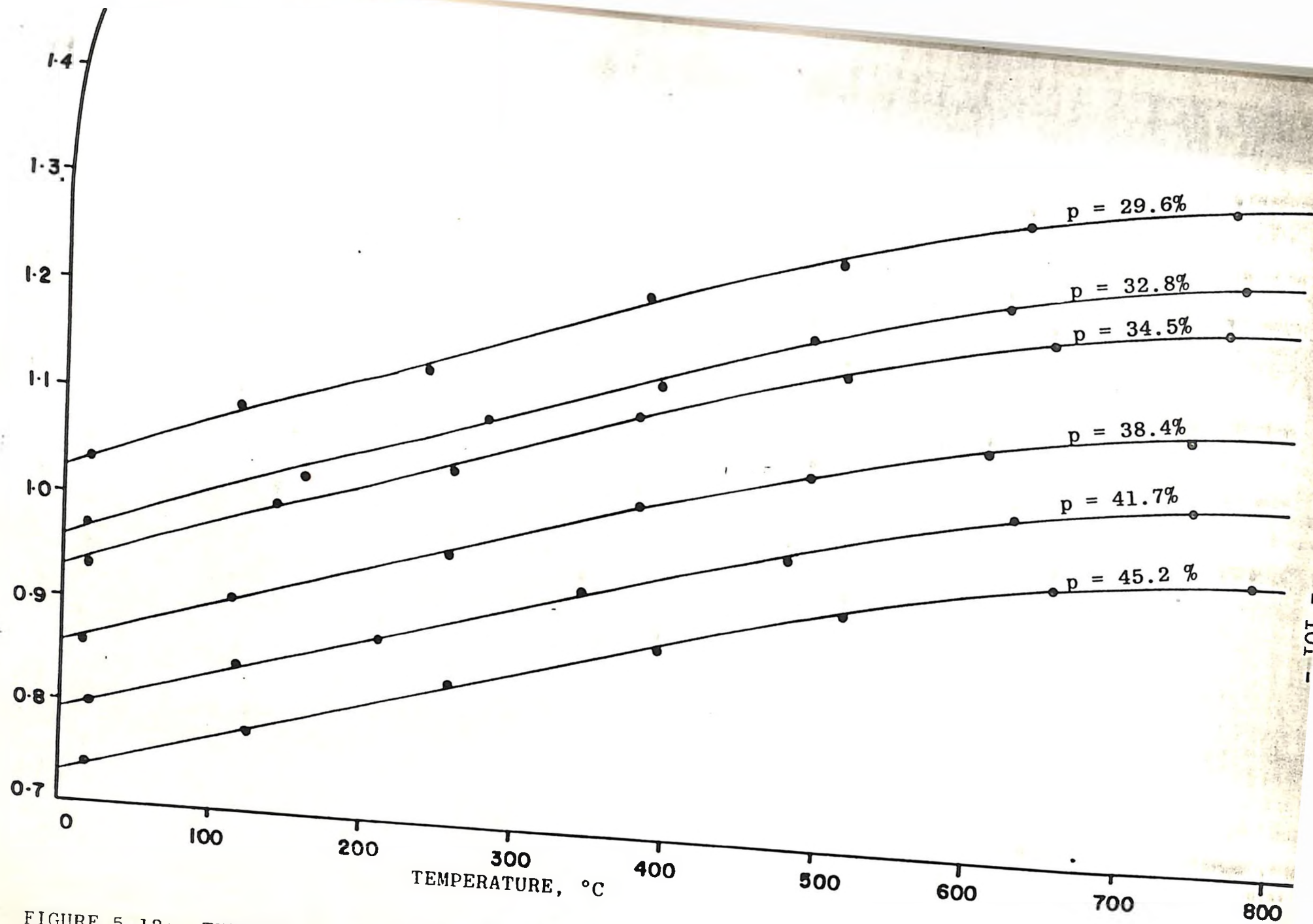


FIGURE 5.12: THERMAL CONDUCTIVITY AGAINST TEMPERATURE FOR SIAYA CLAY SAMPLES OF DIFFERENT PERCENTAGE POROSITIES

#### 5.5.0. EFFECT OF TEMPERATURE ON THERMAL CONDUCTIVITY

The variation of the effective thermal conductivity of the refractory bricks with temperature is shown in Figs. (5.12, A5.10, A5.11, A5.12). A family of curves for thermal conductivity values for each material for given porosities is shown, except for Kisii soap stone where the porosity could not be varied.

For temperatures below 500°C the values of thermal conductivity are observed to increase with temperature at a steady rate. At higher temperature, the rate of increase of thermal conductivity with temperature reduces. This could be attributed to the fact that at higher temperatures, there is more vigorous vibration of particles making up the material. This would result in the reduction of the mean free path of the heat wave transmitting the heat, resulting to a decrease in the rate of increase of heat conduction.

#### 5.5.1. COMPARISON BETWEEN EXPERIMENTAL RESULTS WITH THOSE THEORETICALLY PREDICTED FOR THE VARIATION OF THERMAL CONDUCTIVITY WITH TEMPERATURE

To compare experimental values with those calculated from theory [6], the admixtures of  $Fe_2O_3$ ,  $TiO_2$  and other components that make up negligible fraction in the volume were neglected so as to

consider the solid basis (skeleton) as a two-phase system consisting of silicon dioxide ( $\text{SiO}_2$ ) and aluminium oxide ( $\text{Al}_2\text{O}_3$ ). It is then assumed that the component greater in volume in this case  $\text{SiO}_2$ , forms a continuous medium in which particles of the second, smaller in volume phase are dispersed.

The temperature dependence of thermal conductivity of this two phase system was calculated using the relationship of Odelevskiy [8]:

$$K_s = K_{\text{SiO}_2} \left[ 1 - \frac{V_{\text{Al}_2\text{O}_3} \left( \frac{1}{K_{\text{Al}_2\text{O}_3} - 1} - \frac{1 - V_{\text{Al}_2\text{O}_3}}{3} \right)}{1 - \frac{V_{\text{Al}_2\text{O}_3}}{K_{\text{SiO}_2}}} \right] \quad \text{--- (5.2)}$$

where  $K_s$  is the thermal conductivity of the solid skeleton of the brick,  $V_{\text{Al}_2\text{O}_3}$  and  $V_{\text{SiO}_2}$  are the volume proportions of  $\text{Al}_2\text{O}_3$  and  $\text{SiO}_2$  respectively,  $K_{\text{Al}_2\text{O}_3}$  the thermal conductivity of crystalline  $\text{Al}_2\text{O}_3$  whose appropriate data is obtained from ref [20] and  $K_{\text{SiO}_2}$  is the thermal conductivity of amorphous  $\text{SiO}_2$  whose data is found in ref [6].

The results obtained by expression 5.2 were compared and found to be quite similar to those given by the Maxwell-Eucken [6] relation which is given as:

$$K_s = \left[ \frac{1 + 2V_{Al_2O_3} \frac{1 - K_{SiO_2}/K_{Al_2O_3}}{2K_{SiO_2}/K_{Al_2O_3} + 1}}{1 - V_{Al_2O_3} \frac{1 - K_{SiO_2}/K_{Al_2O_3}}{2K_{SiO_2}/K_{Al_2O_3} + 1}} \right] K_{SiO_2} \quad \text{----- (5.3)}$$

where  $K_s$ ,  $K_{SiO_2}$ ,  $K_{Al_2O_3}$ ,  $V_{Al_2O_3}$  and  $V_{SiO_2}$  have the same meaning as in Eqn. 5.2.

The next step in the calculation was the determination of the effective thermal conductivity of the brick. Since the material has connecting pores, Dulnev's relation [8] obtained for the determination of the thermal conductivity of a two-component disperse system with connecting pores (see section 3.5.0) was used in the following form:

$$K_{ef} = K_s \left[ \left(\frac{h}{L}\right)^2 + V_g \left(1 - \frac{h}{4}\right)^2 + \frac{2V_g \frac{h}{L} \left(1 - \frac{h}{L}\right)}{1 - \frac{h}{L} - V_g} \right] \quad \text{----- (5.4)}$$

where  $K_s$  has the same meaning as in Eqn. 5.2,  $L$  is the characteristic size of an elementary cell (particle diameter, see section 3.5.0) and  $V_g$  is the ratio  $K_g/K_s$  and  $K_g$  is the total molecular and radiative thermal conductivities of the gas contained in the cavities of the brick.

The effect of radiation in the pores of the materials may be best estimated using the relation in Ref [13].

$$K_g = 2 \epsilon^2 C T^3 \lambda \quad \text{-----} \quad (5.5)$$

$\lambda$  being the characteristic pore size and  $\epsilon$  the emissivity of pore surface. Calculations using this formula for the temperature ranges considered under this study showed that the coefficient of radiative heat conduction in the pores was not more than 1.5 percent of the molecular heat conduction.

In tables (5.9 - 5.12), data is presented on the temperature dependence of the heat conduction coefficients of the skeleton components of the bricks i.e.  $K_{Al_2O_3}$  and  $K_{SiO_2}$  obtained from refs [5, 20], of the air filling the pores  $K_o$ , the calculated values of the temperature dependence of the heat conduction coefficients of the skeleton  $K_s$ , and the effective thermal conductivity of the materials.

Figs. (5.13, A5.13, A5.14, A5.15) show the comparison between the experimental and theoretically calculated values for the variation of the thermal conductivity with temperature. In general, the experimental values are lower than the theoretically calculated ones except for Kisii soap stone Fig. A5.13 where the calculated

| $K_o$<br>$Wm^{-1}^{\circ}C^{-1}$ | Temperature<br>$^{\circ}C$ | $K_{Al_2O_3}$<br>$Wm^{-1}^{\circ}C^{-1}$ | $K_{SiO_2}$<br>$Wm^{-1}^{\circ}C^{-1}$ | $K_s$<br>$Wm^{-1}^{\circ}C^{-1}$ | $K_{Calc}$<br>$Wm^{-1}^{\circ}C^{-1}$ | $K_{expt}$<br>$Wm^{-1}^{\circ}C^{-1}$ |
|----------------------------------|----------------------------|--|--|----------------------------------|---------------------------------------|---------------------------------------|
| 0.0265                           | 27.0                       | 32.5                                     | 1.28                                   | 3.638                            | 1.180                                 | $1.140 \pm 0.057$                     |
| 0.0305                           | 82.2                       | 27.5                                     | 1.43                                   | 3.916                            | -                                     | $1.160 \pm 0.058$                     |
| 0.0340                           | 127.0                      | 23.6                                     | 1.53                                   | 4.042                            | 1.267                                 | $1.193 \pm 0.060$                     |
| 0.0370                           | 183.0                      | 19.0                                     | 1.61                                   | 4.070                            | -                                     | -                                     |
| 0.0395                           | 222.3                      | 17.9                                     | 1.65                                   | 4.060                            | -                                     | $1.260 \pm 0.063$                     |
| 0.0460                           | 327.0                      | 14.3                                     | 1.72                                   | 4.823                            | 1.350                                 | $1.319 \pm 0.066$                     |
| 0.0530                           | 444.0                      | 11.5                                     | 1.85                                   | 3.916                            | -                                     | $1.383 \pm 0.069$                     |
| 0.0574                           | 527.0                      | 10.0                                     | 2.05                                   | 4.002                            | 1.482                                 | $1.424 \pm 0.071$                     |
| 0.0649                           | 654.6                      | 8.6                                      | 2.54                                   | 4.319                            | 1.581                                 | $1.487 \pm 0.074$                     |
| 0.0684                           | 727.0                      | 7.7                                      | 2.91                                   | 4.467                            | 1.649                                 | $1.489 \pm 0.075$                     |
| 0.0725                           | 810.0                      | 6.9                                      | 3.40                                   | 4.650                            | -                                     | $1.500 \pm 0.075$                     |

Table 5.9: Comparison between thermal conductivity values obtained from experiment and those from theoretical prediction for a kaolin brick of porosity,  $P = 38.5$  per cent.

| $K_o$<br>$Wm^{-1} \cdot ^\circ C^{-1}$ | Tempe-<br>rature<br>$^\circ C$ | $K_{Al_2O_3}$<br>$Wm^{-1} \cdot ^\circ C^{-1}$ | $K_{SiO_2}$<br>$Wm^{-1} \cdot ^\circ C^{-1}$ | $K_s$<br>$Wm^{-1} \cdot ^\circ C^{-1}$ | $K_{Calc}$<br>$Wm^{-1} \cdot ^\circ C^{-1}$ | $K_{expt}$<br>$Wm^{-1} \cdot ^\circ C^{-1}$ |
|--|--------------------------------|--|--|--|---|---|
| 0.0265                                 | 27.0                           | 32.5   | 1.28   | 2.254                                  | 0.921                                       | $0.905 \pm 0.045$                           |
| 0.0310                                 | 90.0                           | 26.8   | 1.45   | 2.496                                  | 0.963                                       | $0.951 \pm 0.047$                           |
| 0.0340                                 | 127.0                          | 23.6   | 1.53   | 2.593                                  | 0.990                                       | $0.972 \pm 0.049$                           |
| 0.0395                                 | 223.4                          | 17.9   | 1.65   | 2.694                                  | 1.065                                       | $1.043 \pm 0.052$                           |
| 0.0460                                 | 327.0                          | 14.3   | 1.77   | 2.711                                  | 1.130                                       | $1.107 \pm 0.055$                           |
| 0.0529                                 | 443.3                          | 11.5   | 1.85   | 2.785                                  | 1.210                                       | $1.178 \pm 0.059$                           |
| 0.0574                                 | 527.0                          | 10.0   | 2.05   | 2.953                                  | 1.265                                       | $1.236 \pm 0.062$                           |
| 0.0637                                 | 633.4                          | 8.8  | 2.44   | 3.304                                  | 1.335                                       | $1.295 \pm 0.065$                           |
| 0.0684                                 | 727.0                          | 7.7  | 2.91   | 3.674                                  | 1.425                                       | $1.338 \pm 1.067$                           |
| 0.0744                                 | 840.0                          | 6.4  | 3.57   | 4.104                                  | 1.526                                       | $1.377 \pm 0.069$                           |

Table 5.10: Comparison between thermal conductivity values obtained from experiment and those from theoretical predictions for a fireclay brick of porosity  $P = 39.5$  per cent.

| $K_o$<br>$Wm^{-1} \cdot ^\circ C^{-1}$ | Temperature<br>$^\circ C$ | $K_{Al_2O_3}$<br>$Wm^{-1} \cdot ^\circ C^{-1}$ | $K_{SiO_2}$<br>$Wm^{-1} \cdot ^\circ C^{-1}$ | $K_s$<br>$Wm^{-1} \cdot ^\circ C^{-1}$ | $K_{Calc}$<br>$Wm^{-1} \cdot ^\circ C^{-1}$ | $K_{expt}$<br>$Wm^{-1} \cdot ^\circ C^{-1}$ |
|--|---------------------------|--|--|--|---|---|
| 0.0265                                 | 27.0                      | 32.5   | 1.28   | 2.113                                  | 0.885                                       | $0.868 \pm 0.043$                           |
| 0.0340                                 | 127.0                     | 23.6   | 1.53   | 2.442                                  | 0.930                                       | $0.913 \pm 0.046$                           |
| 0.0460                                 | 327.0                     | 14.3   | 1.72   | 2.574                                  | 1.020                                       | $1.002 \pm 0.050$                           |
| 0.0574                                 | 527.0                     | 10.0   | 2.05   | 2.833                                  | 1.125                                       | $1.078 \pm 0.054$                           |
| 0.0684                                 | 727.0                     | 7.7  | 2.91   | 3.576                                  | 1.239                                       | $1.144 \pm 0.057$                           |

**Table 5.11:** Comparison between thermal conductivity values from experiments and from theoretical predictions for a Siayaclay brick of porosity  $P = 38.4$  per cent.



| $K_o$<br>$Wm^{-1} \cdot C^{-1}$ | Temperature<br>$^{\circ}C$ | $K_{Al_2O_3}$<br>$Wm^{-1} \cdot C^{-1}$ | $K_{SiO_2}$<br>$Wm^{-1} \cdot C^{-1}$ | $K_s$<br>$Wm^{-1} \cdot C^{-1}$ | $K_{Calc}$<br>$Wm^{-1} \cdot C^{-1}$ | $K_{expt}$<br>$Wm^{-1} \cdot C^{-1}$ |
|---------------------------------|----------------------------|---|---------------------------------------|---------------------------------|--------------------------------------|--------------------------------------|
| 0.0265                          | 27.0                       | 32.5                                    | 1.28                                  | 3.429                           | 2.290                                | $2.206 \pm 0.110$                    |
| 0.0340                          | 127.0                      | 23.6                                    | 1.53                                  | 3.827                           | 2.428                                | $2.365 \pm 0.118$                    |
| 0.0400                          | 230.0                      | 17.6                                    | 1.65                                  | 3.849                           | 2.548                                | $2.518 \pm 0.126$                    |
| 0.0460                          | 327.0                      | 14.3                                    | 1.72                                  | 3.869                           | 2.667                                | $2.682 \pm 0.134$                    |
| 0.0525                          | 436.7                      | 11.0                                    | 1.84                                  | 3.754                           | -                                    | $2.830 \pm 0.147$                    |
| 0.0574                          | 527.0                      | 10.0                                    | 2.05                                  | 3.858                           | 2.953                                | $2.990 \pm 0.150$                    |
| 0.0625                          | 613.3                      | 9.0                                     | 2.36                                  | 4.076                           | -                                    | $3.100 \pm 0.155$                    |
| 0.0667                          | 693.4                      | 8.1                                     | 2.73                                  | 4.286                           | -                                    | $3.220 \pm 0.161$                    |
| 0.0684                          | 727.0                      | 7.7                                     | 2.91                                  | 4.364                           | 3.309                                | -                                    |
| 0.0700                          | 700.0                      | 7.4                                     | 3.10                                  | 4.458                           | -                                    | $3.302 \pm 0.165$                    |
| 0.0729                          | 819.6                      | 6.7                                     | 3.46                                  | 4.561                           | -                                    | $3.343 \pm 0.167$                    |

Table 5.12: Comparison between thermal conductivity values obtained from experiment and those from theoretical prediction for a Kisii soap stone brick of porosity  $p = 7.64$  per cent.

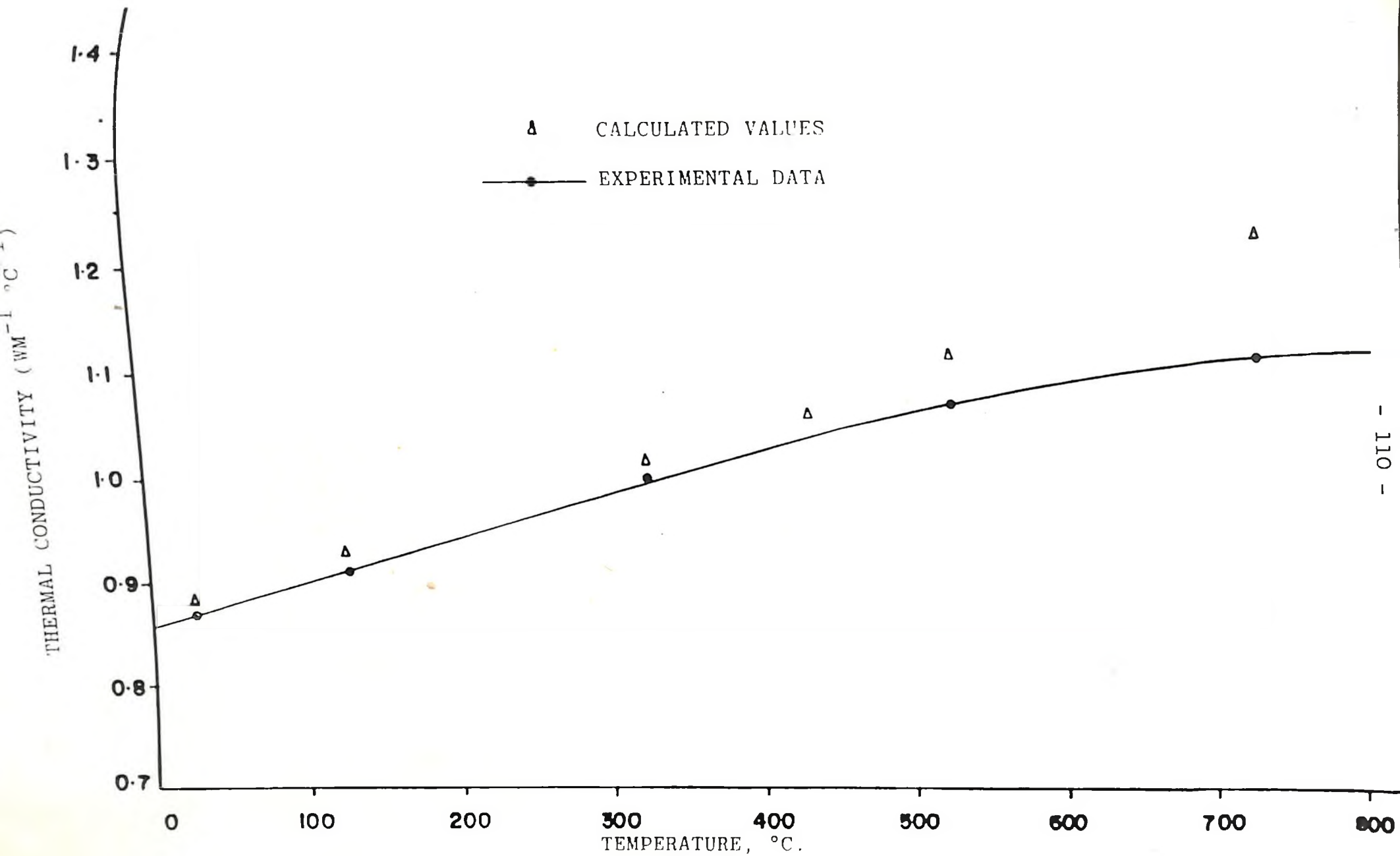


FIGURE 5.13: THERMAL CONDUCTIVITY AGAINST TEMPERATURE FOR SIAYA CLAY OF POROSITY  $p = 38.4\%$

values fall below the experimental ones between about 300°C and 650°C.

At low temperatures, below 600°C both the experimental and the theoretical curves increase at the same rate and the difference between the two was less than 10 per cent. The deviation became only marked at higher temperatures, above 700°C. This may be explained by attributing the deviation of the theoretical curve to the large contribution of the radiation term, which depends on  $T^3$ , to the total heat transfer for higher values of  $T$ , in the theoretical calculation.

To explain the difference further one should consider the point that has been raised by Imura et al. [28]. These authors have pointed out that in order to calculate the thermal conductivity of materials that have sintered on firing you need to know the nature and therefore the thermal conductivity of the sintered-glassy bond that is formed during maturing of the brick to hold the particles together. In this study, it is likely that the glassy ceramic bonds that are formed are such that they make the material more amorphous, since the less crystalline a material, the lower is its thermal conductivity.

## C H A P T E R   S I X

### CONCLUSIONS AND RECOMMENDATIONS:

#### 6.1.0. CONCLUSIONS:

The study has been carried out to investigate the thermal conductivity of refractory bricks made from Kaolin, Fireclay, Siayaclay and Kisii soap stone under different experimental conditions.

The measurements were made in air at atmospheric pressure within a temperature range of about 15°C to 800°C using the transient hot wire method of comparison.

The following conclusions were made:

1. The transient hot wire method of comparison is satisfactory for the determination of the effective thermal conductivity of refractory bricks provided good thermal contact is ensured between the hot wire and the materials. This is as it may be observed from the results of the measurements that were carried out for the two glass plates of the same material and shape as the reference specimen. An experimental error less than 5 per cent was confirmed.
2. For all the materials tested, the values of thermal conductivity were observed to decrease with increase

in percentage porosity Figs. 5.9 - 5.10, A5.4 - A5.7. This variation of experimental data was in good agreement with observations made by Brailsford et al. [13].

3. Comparison between experimental data and values predicted by Dulnev's relation for the determination of thermal conductivities of two component disperse systems with connecting pores for different porosities showed the theoretical predictions giving slightly higher values than those obtained from experiment, Figs. 5.11, A5.8, A5.9. The difference may be attributed to the increase of thermal conductivity values predicted by theory at elevated temperatures due to the contribution of the radiant heat transmission. This increase is nevertheless somehow offset by the lowering of thermal conductivity due to increased anharmonicity of the vibration at these temperatures.
4. In all the cases considered, the values of the thermal conductivity for the refractory bricks were increased by the presence of moisture in them. (Figs. 5.10, A5.6, A5.7). This means that moist bricks become better heat conductors and may therefore not serve well in heat insulation applications.

5. The thermal conductivities for the bricks of all the materials studied were observed to increase with increasing temperature, (Figs. 5.12, A5.10 - A5.12). The rate of increase of these values with temperature was observed to be higher at temperatures below 500°C than at higher temperatures where the rate decreased with rise in temperature. This observation of variation of thermal conductivity with temperature is in good agreement with those obtained by Luikov et al. [6] for the chamotte ceramics and also with those obtained by Kingery and McQuarrie [4] for fireclay bricks.
6. A comparison between theoretical predictions of variation of thermal conductivity with temperature and the experimental findings show that for most part of the temperature range considered in the study, the theoretically predicted values were slightly higher than the experimental ones, (Figs 5.13, A5.13 - A5.15). It was only for the case of Kisii soap stone (Fig. A5.13) in the temperature range 300°C - 660°C that the theoretical values fell lower than the experimental values as predicted by the variation of the solid phase thermal conductivity for zero porosity,  $K_s$ , with temperature. The difference between the

experimental values and the theoretically predicted values may be explained by considering two factors. One, it has been shown by Imura et al. [28] that the effective thermal conductivity of a sintered material is greatly influenced by the thermal conductivity of the bond formed to hold the particles together during sintering. Since the nature and therefore the thermal conductivities of the ceramic bonds formed were not established in this study, it could be that their values are such that they lower the effective thermal conductivity of the entire brick. The other possibility could be that the radiant heat transmission considered in the theoretical prediction gives higher values than those observed in the practical situation. As it has been explained in section 3.1.0. (see eqn. 3.2), if the radiant heat transmission is considered, the thermal conductivity coefficient,  $K$ , is observed to vary with  $T^3$ .

7. The theoretical predictions may be used to deduce the expected thermal conductivity for the refractory bricks. This can be argued from the fact that in all the cases reported in this study the difference between the theoretically predicted

values and those experimentally obtained was always less than ten per cent. The difference in these values is small at low temperatures below 500°C and becomes bigger as the temperature increases.

8. The thermal conductivity values obtained gives us an indication that the materials; Siaya clay, Kaolin, Kisii soap stone and fireclay could be put to thermal insulation uses in the refractory brick form. The Kisii soap stone in the form in which it was investigated gave higher thermal conductivity values than the other three materials. This is attributed to the low value of its porosity.

9. When used as insulators, the materials must be kept dry and free from the influence of moisture, otherwise their insulating power has been observed to deteriorate with the presence of moisture in them. (see Figs. 5.10, A5.6, A5.7)

#### G.2.0. RECOMMENDATIONS FOR FUTURE WORK:

More investigations should be carried out on these materials and other locally obtainable materials such as silica, magnesite, alumina etc. to establish the



nature and therefore the thermal conductivity values of the ceramic bond that form to hold the brick particles together during sintering at the maturing temperature of the refractory bricks. This will not only enable us to predict more surely the thermal conductivity values of the refractory bricks made from these materials but will also point more clearly to their applicability in different uses.

More work should also be carried out on these refractory brick materials to establish more clearly the way the transfer of heat in each of them is influenced by the radiant heat transmission through the voids and also by the gas molecules in them. This may be done by way of establishing accurately the pore sizes, shapes and lengths to enable us to estimate the conduction lengths more accurately.

Further research work should be done to determine the values of other factors that determine the applicability of the refractory bricks made from these materials to several uses. There are such factors as the mechanical strength of the bricks, that is their load bearing capacities when subjected to different modes of stress, the resistance to thermal stresses, the fusion points, resistance to slags and other chemical effects among others.

6. Luikov, A.V., Shaskov, A.G., Vasiliev, L.L. and Fraiman Y.E.; Thermal conductivity of porous systems; International Journal of Heat Mass Transfer II 117 - 140, (1968).
7. Dulnev, G.N.; Thermal conductivity of mixtures with Interpenetrating components, Heat Transfer, Soviet Research, 3, 2, (1971).
8. Dulnev, G.N., and Zarichnyak, Yu.P.; A study of the Generalized Conductivity Coefficients in Heterogenous systems; Heat Transfer, Soviet Research, 2, 4, 89, (1970).
9. Aduda, B.O.C.; 'Thermal Conductivity Porous Insulators, Wood-Ash and Vermiculite' M.Sc. Thesis, University of Nairobi. (1987)
10. Zumbrunnen, D.A., Viskanta, R. and Incropera, F.P. 'Heat Transfer through Porous Solids with Complex Internal Pores,' International Journal of Heat and Mass Transfer, 29 2, 275 - 284, (1986).

11. Newman, D.R.; 'Woodstoves Materials Testing at Kenyatta University College'.  
Appropriate Technology Centre, Nairobi,  
Kenyatta University, (1983).
12. Negussie, A.; 'Fracture Behaviour of Ceramic  
Cylinders due to Thermal Stress'.  
M.Sc. Thesis, University of Nairobi,  
(1987).
13. Brailsford, A.D., and Major, K.G.; 'The Thermal  
Conductivity of Aggregates of several  
phases, Including Porous Materials'.  
British Journal of Applied Physics,  
15, 313 - 319, (1964).
14. Woodside, W. and Messmer, J.H.; 'Thermal Conductivity  
of Porous Media. I. Unconsolidated  
Sands'. Journal of Applied Physics  
Physics 32 9 1688 - 1699  
(1961).
15. Maxwell, J.C.. 'A Treatise on Electricity and Magnetism'  
Third Edition, 1. 440. Clarendon  
Press Oxford (1892).
16. Takegoshi, L., Imura, S., Harasawa, Y., and Takenaka, T.;  
'A Method of Measuring the Thermal

conductivity of Solid Materials by  
transient Hot Wire Method of Comparison'.  
Bulletin of the Japanese Society of  
Mechanical Engineers, 25, 201, 395, (1982).

- 16a. Schleiermacher, A.L.E.F., Wiedmann AnnalenPhysics.  
31, 623, (1888).
17. Woodside, W. and Messmer, J.H.; 'Thermal Conductivity  
of Porous Media. II. Consolidated  
Rocks'. Journal of Applied Physics  
32, 9, 1699 - 1906 (1961).
18. Norton C.L. Jr.; Apparatus of Measuring Thermal  
Conductivity of Refractories. Journal  
of American Ceramic Society. 25,  
451, (1942).
19. Potton, T.C., and C.L. Norton, Jr.. Measurement  
of Thermal Conductivity of fireclay  
refractories. Journal of American  
Ceramic Society, 26, 350, (1943).
20. McQuarrie, M.; 'Thermal Conductivity: VII. Analysis  
of variation of conductivity with  
temperature for  $Al_2O_3$ ,  $B_2O_3$ , and  $MgO$ .  
Journal of American Ceramic Society.  
37 (2, pt II), 91, (1954).

21. Kingery, W.D., France, J., Coble, R.L., and Vasilos, T.;  
'Thermal Conductivity: X, Data for  
several pore oxide materials corrected  
to zero porosity. Journal of American  
Ceramic Society. 37, (2, Pt II),  
107,(1954).
22. Vasilos, T., and Kingery, W.D.; 'Thermal Conductivity:  
XI, Conductivity of some Refractory  
Carbides and Nitrides'. Journal of  
American Ceramic Society. 37,  
9, 409.(1954).
24. Grimshaw, R.W., The chemistry and Physics of Clays  
and Allied Ceramic Materials. (4th  
Edition), Ernest Benn Limited, London,  
1229-1231, (1971).
25. Kingery, W.D.; Introduction to Ceramics. John  
Wiley, New York,18-57 (1960).
26. Gilchrist J.D.; Fuel, Furnaces and Refractories.  
Pergamon Press Ltd. Oxford, 237-303 (1977)
27. Loeb, A.L.; 'Thermal Conductivity: VIII, A Theory  
of Thermal Conductivity of Porous  
Material', Journal of American Ceramic  
Society. 37, (2, pt. II), 96,  
(1954).

28. Imura, S., Takegoshi, S. and Nagamoto, T.; 'An experimental study of the effective Thermal Conductivities of Sintered Porous Materials such as Grinding Wheels', Heat Transfer, Japanese Research. 7, 3, 78. (1978).
29. Jakob, M. Heat Transfer, Volume II. Wiley, New York. 530 - 560, (1957).
30. Ozisik, N.M.; Basic Heat Transfer, McGraw Hill Book Company, New York, 59-61. (1977)
31. Holman, J.P.; Heat Transfer (4th Edition) McGraw Hill Book Company, New York, 45-48 (1972)
32. Carslaw, H.S. and Jaeger, J.C.; Conduction of Heat in Solids (2nd Edition) Oxford University Press, New York, 1-3 (1959).
33. Kittel, C.; Introduction to Solid State Physics 5th Edition - Wiley, New York. 199-235 (1976)
34. Kittel, C.; Thermal Physics, Wiley, New York 212 - 215, (1969).
35. Mokoto, N., Sugiyama, S., Inaba Yoshihiro, and M. Hasatani.; 'Heat transfer in static packed beds. Effects of

Radiation on Temperature Distribution,  
Heat Transfer, Japanese Research 1,  
3, 1, (1972).

36. Norio, Y., Y. Sasaki, t. Okada, and O. Shigemori;  
Effective thermal conductivity of  
moist Granular beds'. Heat Transfer,  
Japanese Research. 2, 2, 77, (1973).
38. Takegoshi, E.; Imura, S., and Nirasawa, Y.; 'A  
Method of Measuring the Thermal  
Conductivity of Orthogonal Anisotropic  
Materials by a Transient Hot Wire  
Method'. Heat Transfer Japanese  
Research. 11, 3 74 - 89. (1982)
39. Loeb, A.L.; 'A Theory of the Envelop type of Thermal  
Conductivity Test'. Journal of Applied  
Physics, 22, 282, (1951)
40. Milton A.; 'Thermal Conductivity: III, Prolate  
Spheroidal Envelope method; Data  
for  $Al_2O_3$   $BeO$   $MgO$   $ThO_2$  and  $ZrO_2$ , '  
Journal of American Ceramic Society,  
37 [2, Part II] 74 - 79 (1954).
41. Ramiir, S., Saxena, N.S. and Chaudlary, D.R.;  
Simultaneous Measurement of Thermal

Conductivity and Thermal Diffusivity of some building materials using Hot-Shi Method'. Journal of Applied Physics, 18, 1 - 8, (1985).

42. Gustafsson, S.E.; Karawacki, E., and Khan, M.M.; The Hot-Strip Method for simultaneously measuring thermal conductivity and thermal diffusivity of solids and fluids. Journal of Physics, (D. Applied Physics). 12, 1411 - 1421, (1979).
43. Van Der Held, E.F.M. and Van Drunen, F.C.; 'A Method of Measuring the Thermal Conductivity of Liquids'. Physica, 15, 10, 865 - 881, (1949).
44. De Groot, J.J., Kestin, J. and Sookratnan, H.; 'Instrument to measure the Thermal Conductivity of gases'. Physica, 75, 454 - 482, (1974).
45. Nieto De Castro, C.A., Calado, J.C.G., Wakeham, W.A., and Dix, M.; 'An apparatus to measure the thermal conductivity of liquids'. Journal of Physics and Scientific Instrumentation. 1073 - 1082, 9 (1976).



46. Haran, E.N., and Wakeham, W.A.; 'A Transient hot wire cell for Thermal Conductivity Measurements over a wide range. Journal of Physics and Scientific Instrumentation, 15, 839 - 842 (1982).
47. Blackwell, J.H.; 'A Transient Flow Method for Determination of Thermal constants of Insulating Materials. Journal of Applied Physics, 25, No. 2, 137 - 144, (1954).
49. Kestin, J., and Wakeham, W.A.; 'A Contribution to the theory of the transient hot wire technique for thermal conductivity measurements. Physica. 92A, 102 - 116. (1978).
50. Knibbe, P.G.; 'The End-Effect Error in the Determination of Thermal Conductivity using a Hot-wire Apparatus'. International

Journal Heat Mass Transfer. 29,  
3, 463 - 473, (1986).

51. Oleynikova, N.M. and Dushenko V.P.; 'Calculation of Heterogeneous Matrix Heat Transfer', Heat Transfer, Soviet Research, 8, 4, 133, (1970).
52. Lee, D.W. and W.D. Kingery; 'Radiation Transfer and Thermal Conductivity of Ceramic oxides. Journal of American Ceramic Society, 43, 594, (1960).
53. Beterkhtin, A.G.; A Course in Mineralogy, Translated by V. Agol. Peace Publishers, Moscow (ND), 532 - 542, (1965).
54. Stockham, J.D., and E.G. Fochtman; Particle Size Analysis, Ann Arbor Science Publishers Inc. Michigan, 14 - 34 (1977).
55. Allen, T.; Particle Size Measurements. Chapman and Hall, London, 5 - 26 (1975).
56. Wilcard, N.N., L.L. Merritt, Jr., J.A. Dean and F.A. Settle, Jr.; Instrumental Methods of Analysis. Sixth Edition, CBS Publishers, India, 53 - 78, (1976).

57. Kenner, C.T., and K.W. Busch; Quantitative Analysis.  
MacMillan Publishing Co., Inc. New York,  
1 - 47, (1979).
58. Ewing, G.W. (Editor); Topics in Chemical Instrumentation.  
Chemical Education Publication Co.  
Eaton, 3 - 35, (1971).
59. British Standard B.S.S: No. 1902 Part 1A, (1966).
60. Washburn, E.W., Journal of American Ceramic Society  
4, 918 (1921).
61. British Standards B.S.S: No. 3921, (1965).
62. British Standards (B.S.S.); 'Sizes of refractory  
bricks part one'. Specifications  
for multipurpose bricks. BS. 3056:  
Part 1: (1985).
63. Bjurstrom, H., Karawacki, E. and Carlsson, B.;  
'Thermal conductivity of microporous  
particulate medium: Moist Silica  
Gel,' International Journal of Heat  
and Mass Transfer, 27, 11, 2025 -  
2036, (1984).
64. Holman, J.P.; Heat Transfer (4th Edition) McGraw  
Hill Book Company, New York,  
45 - 48, (1972).

65. Prakouras, A.G., Vachon, R., Crane, R.A. and Khader, S.M.; 'Thermal Conductivity of Heterogenous Mixtures'. International Journal of Heat and Mass Transfer, 21, 1157 - 1166, (1975).
66. Russell, M.W.; 'Principle of Heat, Flow in Porous Insulators', Journal of American Ceramic Society, 18, 1, (1935).
67. Opolo, M.; A review of the production and sales of improved Jiko Stoves in Kenya, Kenya Renewable Energy Development Project (REDP). Prepared by Energy/Development International for Ministry of Energy and Regional Development.
68. Norton, F.B.; Refractories. McGraw Hill Book Company, New York (4th Edition), 295 - 314, (1968).
69. Ringery, W.D., and Franel J.; 'Thermal Conductivity: IX. Experimental investigation of effect of porosity on thermal conductivity'. Journal of American Ceramic Society, 37, (2, pt II), 99 - 107, (1954).
70. Parker, W.J., Jenkins, R.J., Butter, C.P. and Abbot, G.L.; Flash method of

Determining Thermal Conductivity.  
Journal of Applied Physics,  
32, No. 9, 1679 - 1684, (1961).

71. Harmathy, T.A.; 'Variable-state methods of measuring Thermal Properties of Solids'. Journal of Applied Physics 36, 1, 1190 - 1200, (1961).
72. Tamarin, A.J.; The effective thermal conductivity of beds of unconsolidated particles. Heat Transfer, Soviet Research, 2, 5, 190, (1970).
73. Jackson, K.W., and Black, W.Z.; A unit cell model for Predicting the Thermal Conductivity of a Granular medium containing an Adhesive Binder. International Journal of Heat and Mass Transfer, 26, 1 87 - 99, (1983).
74. Kaganer, M.G.; 'Heat Transfer by the combined effect of conduction and radiation in absorbing and scattering media'. Heat Transfer, Soviet Research, 1, 3, 176 - 182, (1969).

75. Burn, R.N., Stem, R.D. and Knock, J.; INSTAT  
Introductory Guide. Statistical  
Service Centre, University of Reading,  
(1986).
76. Nikitin, V.S., Zabrodskiy, S.S. and Antonishin, N.V.;  
'Thermal Conductivity of Dispersed  
material in various gases at Elevated  
Temperatures'. Heat Transfer - Soviet  
Research, 1. 3, 39 - 42,  
(1969).
77. Godbee, H.W. and Ziegler, W.T.; Thermal conductivities  
of MgO, Al<sub>2</sub>O<sub>3</sub>, and ZrO<sub>2</sub> Powders to  
850°C. II. Theoretical. Journal  
of Applied Physics. 37, 37  
1, 56 - 65. (1966).
78. Mellown, E.J.; 'The Clay Mineral' Ceramic Review  
40, 1, (1976).
79. Kenny, J.B.; The Complete Book of Pottery Making  
Sir Isaac Pitman. London. 184-195, (1965).
80. Hanson, W.C., and A.F. Livovich, 'Thermal Conductivity  
of Refractory Insulating Concrete',  
Journal of American Ceramic Society  
36, 359, (1953).

81. Ruh, e., and J. Spotts McDowell; Thermal Conductivity of Refractory Brick, Journal of American Society, 45, 189, (1962).
82. Clements, J.F., and J. Vyse; 'Thermal Conductivity of some Refractory Materials', Transactions of British Ceramic Society, 56, 296, (1957).
83. Barret, L.R.; 'Heat Transfer in Refractory Insulators, I', Transactions of British Ceramic Society, 48, 235, (1949).

APPENDIX A.1.

ANALYSIS OF THERMAL DATA

A typical thermal probe temperature-time data and the necessary transformations is given in table A1.1. From these, the values of the natural logarithm of the corrected time ( $\lambda nt$ ) are plotted against the temperature as shown in Fig. A.1.1. The slope of the curve thus obtained is then used in equation 3.17 to calculate the thermal conductivity value. The power per unit length,  $Q$ , of the hot wire is calculated from the input voltage,  $V$ , the input current,  $I$ , and the length,  $L$ , of the hot wire as  $Q = \frac{VI}{L}$ . The slope of the  $\lambda nt$  versus  $T$  curve gives the value  $d(\lambda nt)/dT$  of equation 3.20. Since the value  $K_1$ , is the thermal conductivity of the reference material is known, then the thermal conductivity,  $K_2$  of the specimen is calculated from eqn. 3.17 as:

$$K_2 = \frac{VI}{2\pi k} \cdot (\text{Slope of } \lambda nt \text{ versus } T \text{ Curve}) - K_1$$

$$Q = \frac{V(I \times 1000)}{L \times 10^3}$$

$$K_2 = \frac{VI}{2\pi L} \text{ Grad} - K_1$$



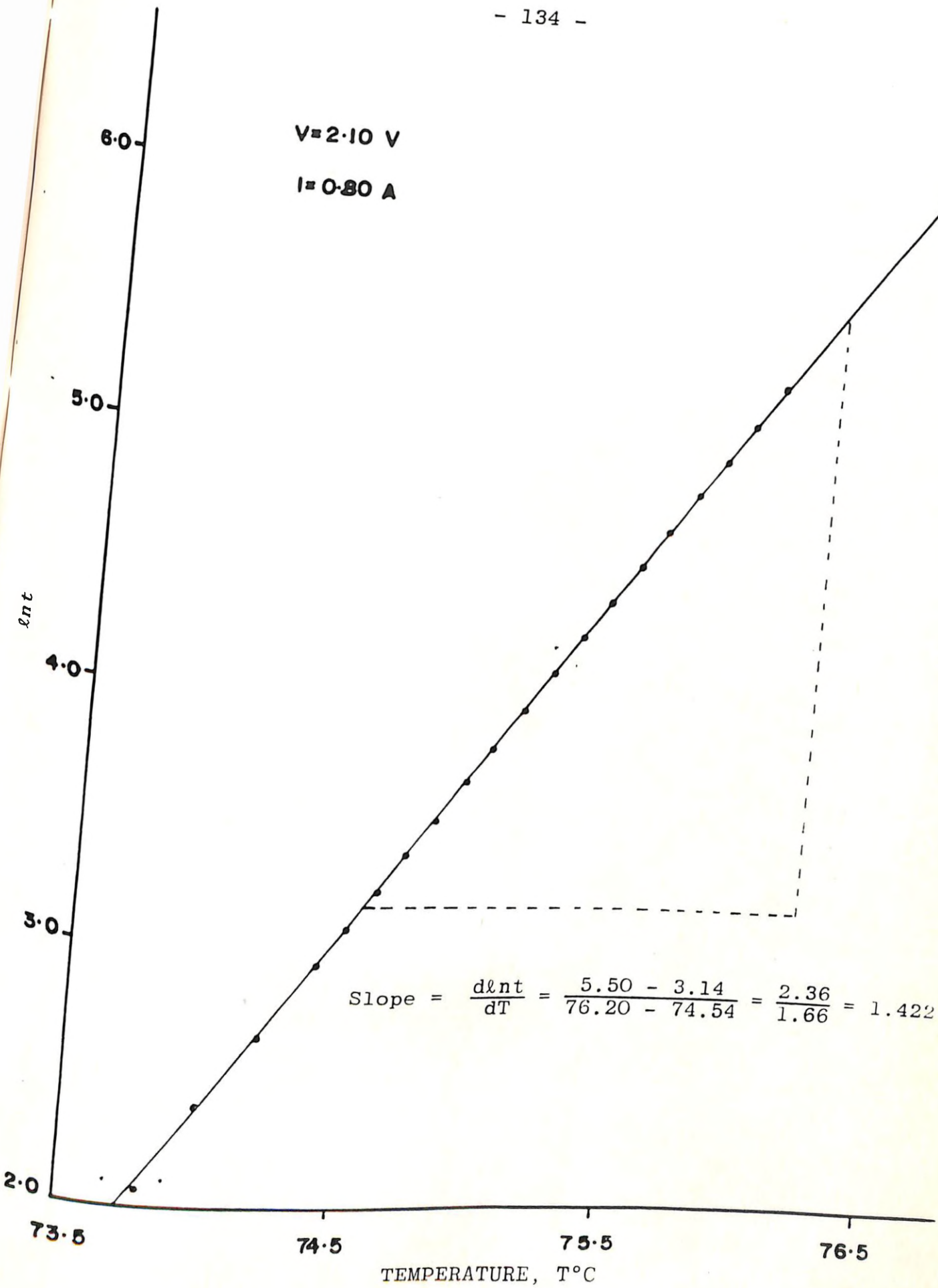


FIGURE A 1.1: NATURAL LOGARITHM OF TIME AGAINST TEMPERATURE FOR FIRECLAY SAMPLE NO. III AT 71.7°C

| TIME<br>(Sec.) | CORRECTED TIME<br>(Sec.) | TEMPERATURE (°C) | ln t  |
|----------------|--------------------------|------------------|-------|
| 06             | 09                       | 74.2             | 2.708 |
| 07             | 13                       | 74.4             | 2.944 |
| 10             | 16                       | 74.5             | 2.091 |
| 13             | 19                       | 74.6             | 3.219 |
| 17             | 23                       | 74.7             | 3.367 |
| 21             | 27                       | 74.8             | 3.497 |
| 26             | 32                       | 74.9             | 3.638 |
| 32             | 38                       | 75.0             | 3.784 |
| 39             | 45                       | 75.1             | 3.931 |
| 47             | 53                       | 75.2             | 4.078 |
| 56             | 62                       | 75.3             | 4.220 |
| 66             | 72                       | 75.4             | 4.357 |
| 78             | 84                       | 75.5             | 4.500 |
| 90             | 96                       | 75.6             | 4.625 |
| 108            | 114                      | 75.7             | 4.787 |
| 125            | 131                      | 75.8             | 4.920 |
| 147            | 153                      | 75.9             | 5.069 |
| 171            | 177                      | 76.0             | 5.09  |

Table A. 1.1. Probe temperature = Time data  
Input voltage (V) = 2.30V  
Current (I) = 0.81A

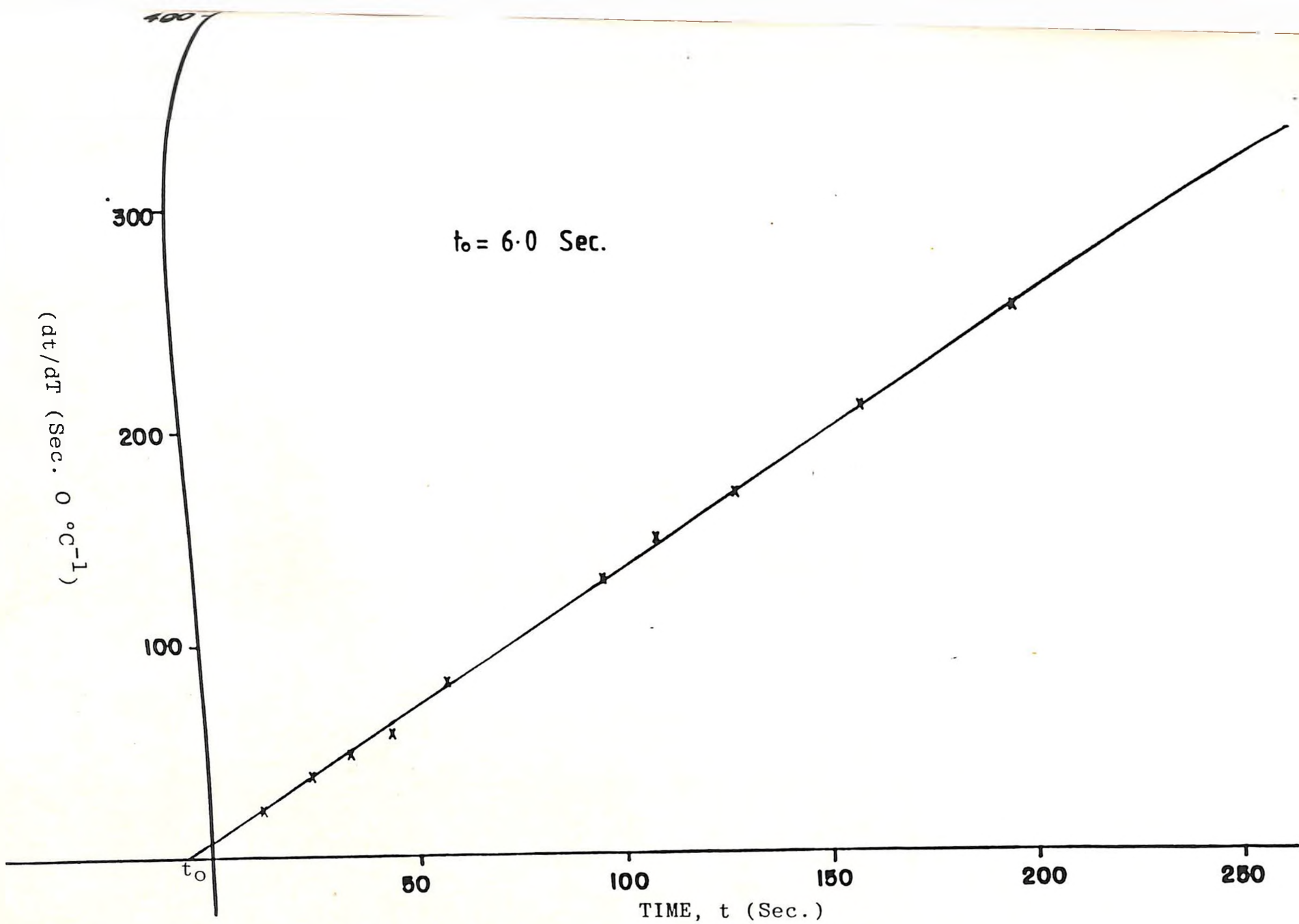


FIGURE A 2.1: DETERMINATION OF THE CORRECTION TIME  $t_0$ : GRAPH OF  $dt/dT$  VERSUS TIME,  $t$ .

APPENDIX A.2

DETERMINATION OF THE CORRECTION TIME  $t_o$ :

The data required for the determination of the correction time for the probe used is given in table A 2.1. The value  $dt$  was obtained from times  $t_{i+1} - t_i$  and similarly  $dT$  from temperatures  $T_{o+1} - T_i$ . From these, the value  $dt/dT$  of equation 3 is calculated. These values are then plotted against their correspond averages of time  $t_{av}$  which is obtained from:

$$t_{av} = (t_{i+1} + t_i)/2, i = 1, 2, 3, \dots, n$$

A plot of  $dt/dT$  versus  $t_{av}$  is given in Fig. A.2.1. From this plot, the value  $t_o$  is obtained from the intercept on the  $t_{av}$  - axis, as shown.

|                                |      |      |      |      |      |       |       |       |       |       |
|--------------------------------|------|------|------|------|------|-------|-------|-------|-------|-------|
| $dT \ 5^{\circ}C^{-1}$<br>$dT$ | 20.0 | 38.8 | 50.0 | 60.0 | 82.5 | 130.0 | 150.0 | 170.0 | 210.0 | 255.0 |
| Time, $t$<br>Sec.              | 12.0 | 25.0 | 34.5 | 45.0 | 38.5 | 97.5  | 111.5 | 131.3 | 162.5 | 200.0 |

Table A. 2.1: Data required for the determination of the correction time,  $t_o$

APPENDIX A. 3

CALCULATION OF THERMAL CONDUCTIVITY OF SOLID PHASE  $K_s$

To estimate the thermal conductivity of the solid phase of the materials from the characteristic thermal conductivities of the components obtained from the chemical analysis tests, the following was assumed:

- (i) That components forming less than 8 per cent of the total percentage of volume for the materials are neglected (see tables 5.1, 5.2, 5.3, and 5.4.)
- (ii) That the components are geometrically equivalent, that is, interchanging their locations does not alter the thermal properties of the matrix. Thus the multicomponent mixture was reduced to a three-component one enabling the use of Equ. 3. the Maxwell-Eucken relation to calculate  $K_s$ . The thermal conductivity of solid phase  $K_s$  for kaolin at a temperature of 127.0°C was given by:

$$K_s = K_{SiO_2} \frac{(1 + 2V_{Al_2O_3}) \frac{1 - K_{SiO_2}/K_{Al_2O_3}}{2 K_{SiO_2}/K_{Al_2O_3} + 1}}{(1 - V_{Al_2O_3}) \frac{1 - K_{SiO_2}/K_{Al_2O_3}}{2 K_{SiO_2}/K_{Al_2O_3} + 1}}$$

From the chemical analysis data and taking the values of the thermal conductivity of the constituents as

$$k_{\text{Al}_2\text{O}_3} = 23.6 \text{ W m}^{-1} \text{ } ^\circ\text{C}^{-1}$$

$$k_{\text{SiO}_2} = 1.53 \text{ W m}^{-1} \text{ } ^\circ\text{C}^{-1}$$

The appropriate data for amorphous  $\text{SiO}_2$  were taken from [6.52] and for crystal  $\text{Al}_2\text{O}_3$ , from [5, 6, 20, 21]. We then obtain:

$$k_s = 1.53 \left[ \frac{1 + 2 \times \frac{36.78}{86.11} \frac{1 - 1.53 : 23.6}{2 \times 1.53 : 23.6 + 1}}{1 - \frac{36.79}{86.11} \frac{1 - 1.53 : 23.6}{2 \times 1.53 : 23.6 + 1}} \right]$$
$$= 4.043 \text{ W m}^{-1} \text{ } ^\circ\text{C}^{-1}$$

The same procedure but for different thermal conductivity values for the components at different temperatures was used to obtain the solid phase thermal conductivity values.

APPENDIX A. 4

THERMAL CONDUCTIVITY DATA:

[The original time-temperature data is obtainable at the Physics Department, University of Nairobi].

| PERCENTAGE POROSITY | THERMAL CONDUCTIVITY $Wm^{-1} \text{ } ^\circ C^{-1}$ |                    |
|---------------------|---|--------------------|
|                     | EXPERIMENTAL DATA                                     | THEORETICAL VALUES |
| 0.00                | -   | $3.038 \pm 0.152$  |
| 8.40                | -   | $2.644 \pm 0.132$  |
| 16.70               | -   | $2.275 \pm 0.114$  |
| 23.60               | $1.666 \pm 0.083$                                     | -                  |
| 27.0                | -   | $1.866 \pm 0.093$  |
| 27.9                | $1.519 \pm 0.076$                                     | -                  |
| 33.3                | $1.338 \pm 0.067$                                     | -                  |
| 37.0                | -   | $1.491 \pm 0.075$  |
| 39.0                | $1.175 \pm 0.059$                                     | -                  |
| 43.0                | $1.069 \pm 0.053$                                     | -                  |
| 48.0                | $0.938 \pm 0.047$                                     | $1.150 \pm 0.058$  |
| 52.7                | $0.819 \pm 0.041$                                     | -                  |
| 60.0                | -   | $0.840 \pm 0.042$  |
| 77.0                | -   | $0.431 \pm 0.021$  |

Table A.4.1: Comparison between values of thermal conductivity from experimental data with those predicted by theory for kaolin at 113.4°C.

| PERCENTAGE POROSITY | THERMAL CONDUCTIVITY $Wm^{-1} \text{ } ^\circ C^{-1}$ |                    |
|---------------------|---|--------------------|
|                     | EXPERIMENTAL DATA                                     | THEORETICAL VALUES |
| 00.0                | -   | 2.200              |
| 10.4                | -   | 1.850              |
| 23.5                | $1.285 \pm 0.064$                                     | -                  |
| 29.0                | $1.156 \pm 0.058$                                     | 1.303              |
| 35.3                | $1.010 \pm 0.051$                                     | -                  |
| 38.7                | -   | 1.063              |
| 41.0                | $0.962 \pm 0.048$                                     | -                  |
| 47.4                | $0.775 \pm 0.039$                                     | -                  |
| 50.6                | -   | 0.812              |
| 52.9                | $0.675 \pm 0.034$                                     | -                  |
| 64.0                | -   | 0.575              |
| 81.5                | -   | 0.285              |

Table A. 4.2: Comparison between thermal conductivity values obtained from experiment with those predicted by theory for Siayaclay at 105.6°C.



| PERCENTAGE POROSITY | THERMAL CONDUCTIVITY $Wm^{-1} \text{ } ^\circ C^{-1}$ |                   |
|---------------------|---|-------------------|
|                     | EXPERIMENTAL DATA                                     | THEORETICAL VALUE |
| 00.3                | -   | 2.210             |
| 13.3                | -   | 1.788             |
| 21.5                | -   | 1.537             |
| 23.5                | 1.300 $\pm$ 0.065                                     | -                 |
| 27.2                | 1.212 $\pm$ 0.061                                     | -                 |
| 32.7                | 1.084 $\pm$ 0.054                                     | -                 |
| 34.3                | -   | 1.200             |
| 37.1                | 0.987 $\pm$ 0.049                                     | -                 |
| 41.7                | 0.898 $\pm$ 0.045                                     | -                 |
| 46.6                | -   | 0.912             |
| 47.3                | 0.787 $\pm$ 0.039                                     | -                 |
| 52.0                | 0.708 $\pm$ 0.035                                     | -                 |
| 62.3                | -   | 0.625             |
| 80.0                | -   | 0.325             |

Table A.4.3: Comparison between values of thermal conductivity from experimental data and those predicted by theory for fire clay at 100°C

| PERCENTAGE POROSITY | THERMAL CONDUCTIVITY $Wm^{-1} \text{ } ^\circ C^{-1}$ |                   |
|---------------------|---|-------------------|
|                     | DRIED SAMPLE  | WET SAMPLE        |
| 23.3                | $1.262 \pm 0.063$                                     | $1.353 \pm 0.068$ |
| 30.0                | $1.106 \pm 0.055$                                     | $1.219 \pm 0.061$ |
| 35.3                | $0.993 \pm 0.050$                                     | $1.117 \pm 0.056$ |
| 39.4                | $0.906 \pm 0.045$                                     | $1.038 \pm 0.052$ |
| 44.4                | $0.813 \pm 0.041$                                     | $0.956 \pm 0.048$ |
| 47.7                | $0.750 \pm 0.038$                                     | $0.900 \pm 0.045$ |
| 56.0                | $0.613 \pm 0.031$                                     | $0.755 \pm 0.038$ |

Table A.4.4: Variation of thermal conductivity with percentage porosity for Fireclay dried and wet samples. Moisture content for the wet samples was 25.6%.

| PERCENTAGE POROSITY | THERMAL CONDUCTIVITY $Wm^{-1} \text{ } ^\circ C^{-1}$ |                   |
|---------------------|---|-------------------|
|                     | DRIED SAMPLE  | WET SAMPLE        |
| 21.7                | $1.198 \pm 0.060$                                     | $1.275 \pm 0.064$ |
| 29.7                | $1.043 \pm 0.052$                                     | $1.124 \pm 0.056$ |
| 34.5                | $0.950 \pm 0.048$                                     | $1.035 \pm 0.052$ |
| 38.3                | $0.872 \pm 0.044$                                     | $0.969 \pm 0.049$ |
| 41.8                | $0.809 \pm 0.041$                                     | $0.913 \pm 0.046$ |
| 45.0                | $0.745 \pm 0.037$                                     | $0.858 \pm 0.043$ |
| 50.7                | $0.642 \pm 0.032$                                     | $0.764 \pm 0.038$ |
| 57.6                | $0.525 \pm 0.026$                                     | $0.650 \pm 0.033$ |

Table A.4.5: Variation of thermal conductivity with percentage porosity for Siayaclay dried and moist samples of moisture content of 25.2%.

| PERCENTAGE POROSITY | THERMAL CONDUCTIVITY |               |
|---------------------|----------------------|---------------|
|                     | AT 105.6°C           | AT 632.9°C    |
| 21.3                | 1.271 ± 0.064        | 1.538 ± 0.077 |
| 29.7                | 1.081 ± 0.054        | 1.319 ± 0.066 |
| 32.8                | 1.015 ± 0.051        | 1.244 ± 0.062 |
| 34.5                | 0.983 ± 0.049        | 1.205 ± 0.060 |
| 38.3                | 0.908 ± 0.045        | 1.112 ± 0.056 |
| 41.7                | 0.840 ± 0.042        | 1.041 ± 0.052 |
| 45.2                | 0.775 ± 0.039        | 0.909 ± 0.049 |
| 50.0                | 0.686 ± 0.034        | 0.869 ± 0.044 |

Table A4.6: Variation of thermal conductivity with percentage porosity for Siayaclay for two temperatures A = 105.6°C and B = 632.9°C

| PERCENTAGE POROSITY | THERMAL CONDUCTIVITY |               |
|---------------------|----------------------|---------------|
|                     | DRIED SAMPLE         | WET SAMPLE    |
| 22.7                | 1.613 ± 0.081        | 1.729 ± 0.087 |
| 28.4                | 1.444 ± 0.072        | 1.584 ± 0.079 |
| 32.3                | 1.316 ± 0.066        | 1.480 ± 0.074 |
| 35.3                | 1.240 ± 0.062        | 1.400 ± 0.070 |
| 38.3                | 1.144 ± 0.057        | 1.319 ± 0.066 |
| 46.0                | 0.950 ± 0.048        | 1.119 ± 0.056 |
| 51.3                | 0.819 ± 0.044        | 0.991 ± 0.050 |
| 56.7                | 0.704 ± 0.035        | 0.875 ± 0.044 |

Table A.4.7: Variation of thermal conductivity with percentage porosity for kaolin dried and wet sample. Moisture content for the wet sample was 24.5%.

| PERCENTAGE POROSITY | THERMAL CONDUCTIVITY $Wm^{-1} \text{ } ^\circ C^{-1}$ |                     |
|---------------------|---|---------------------|
|                     | AT 113.4 $^\circ C$                                   | AT 636.7 $^\circ C$ |
| 21.1                | 1.763 $\pm$ 0.088                                     | 2.085 $\pm$ 0.104   |
| 28.5                | 1.494 $\pm$ 0.075                                     | 1.806 $\pm$ 0.090   |
| 32.6                | 1.3.63 $\pm$ 0.068                                    | 1.663 $\pm$ 0.083   |
| 35.3                | 1.288 $\pm$ 0.064                                     | 1.563 $\pm$ 0.078   |
| 38.5                | 1.188 $\pm$ 0.059                                     | 1.463 $\pm$ 0.073   |
| 46.0                | 0.988 $\pm$ 0.049                                     | 1.231 $\pm$ 0.062   |
| 52.7                | 0.819 $\pm$ 0.041                                     | 1.050 $\pm$ 0.053   |

Table A.4.8: Variation of thermal conductivity with percentage porosity for kaolin at two different temperatures A 0 113.4 $^\circ C$  and B = 636.7 $^\circ C$ .

| PERCENTAGE POROSITY | THERMAL CONDUCTIVITY $Wm^{-1} \text{ } ^\circ C^{-1}$ |                     |
|---------------------|---|---------------------|
|                     | AT 110.7 $^\circ C$                                   | AT 620.4 $^\circ C$ |
| 23.3                | 1.325 $\pm$ 0.066                                     | 1.706 $\pm$ 0.085   |
| 35.2                | 1.053 $\pm$ 0.053                                     | 1.400 $\pm$ 0.070   |
| 39.6                | 0.956 $\pm$ 0.049                                     | 1.290 $\pm$ 0.065   |
| 44.5                | 0.860 $\pm$ 0.043                                     | 1.168 $\pm$ 0.058   |
| 47.8                | 0.798 $\pm$ 0.040                                     | 1.090 $\pm$ 0.055   |
| 52.0                | 0.724 $\pm$ 0.036                                     | 0.995 $\pm$ 0.050   |

Table A.4.9: Variation of thermal conductivity with percentage porosity for fireclay at two different temperatures A = 110.7 $^\circ C$  and B = 620.4 $^\circ C$

| TEMPERATURE OF FIRING | THERMAL CONDUCTIVITY $Wm^{-1} \text{ } ^\circ C^{-1}$ |
|-----------------------|---|
| 300                   | $0.830 \pm 0.042$                                     |
| 400                   | $0.828 \pm 0.041$                                     |
| 450                   | $0.813 \pm 0.041$                                     |
| 550                   | $0.818 \pm 0.041$                                     |
| 650                   | $0.830 \pm 0.042$                                     |
| 700                   | $0.837 \pm 0.042$                                     |
| 800                   | $0.851 \pm 0.043$                                     |
| 850                   | $0.862 \pm 0.043$                                     |
| 900                   | $0.870 \pm 0.044$                                     |
| 950                   | $0.895 \pm 0.045$                                     |
| 1050                  | $0.898 \pm 0.045$                                     |
| 1150                  | $0.901 \pm 0.045$                                     |
| 1200                  | $0.902 \pm 0.045$                                     |
| 1350                  | $0.903 \pm 0.045$                                     |

Table A.4.10: Variation of thermal conductivity with temperature of firing for Siayaclay material (measurements are made at 100°C. Porosity = 38.5 per cent).

| TEMPERATURE OF FIRING | THERMAL CONDUCTIVITY<br>$Wm^{-1} \text{ } ^\circ C^{-1}$ |
|-----------------------|--|
| 300                   | 2.193 ± 0.110  |
| 400                   | 2.190 ± 0.110  |
| 450                   | 2.171 ± 0.109  |
| 550                   | 2.175 ± 0.109  |
| 600                   | 2.199 ± 0.110  |
| 700                   | 2.210 ± 0.111  |
| 800                   | 2.224 ± 0.111  |
| 900                   | 2.237 ± 0.112  |
| 950                   | 2.257 ± 0.113  |
| 1050                  | 2.259 ± 0.113  |
| 1150                  | 2.262 ± 0.113  |
| 1250                  | 2.263 ± 0.113  |
| 1350                  | 2.264 ± 0.113  |

Table A.4.11: Variation of thermal conductivity with temperature of firing for Kisii soap stone material (measurements are made at 100°C, porosity = 7.64%)

| TEMPERATURE OF FIRING °C | THERMAL CONDUCTIVITY<br>$W m^{-1} °C^{-1}$ |
|--------------------------|--|
| 300                      | 0.876 ± 0.044                              |
| 400                      | 0.875 ± 0.044                              |
| 450                      | 0.858 ± 0.043                              |
| 500                      | 0.862 ± 0.043                              |
| 550                      | 0.880 ± 0.044                              |
| 650                      | 0.891 ± 0.045                              |
| 750                      | 0.900 ± 0.045                              |
| 850                      | 0.915 ± 0.046                              |
| 900                      | 0.925 ± 0.046                              |
| 950                      | 0.945 ± 0.047                              |
| 1050                     | 0.950 ± 0.048                              |
| 1150                     | 0.952 ± 0.048                              |
| 1250                     | 0.953 ± 0.048                              |
| 1350                     | 0.953 ± 0.048                              |

Table A. 4.12: Variation of thermal conductivity with temperature of firing for fireclay material (measurements were made at 100°C and porosity = 39.5 %).

| TEMPERATURE OF FIRING °C | THERMAL CONDUCTIVITY<br>$Wm^{-1} °C^{-1}$ |
|--------------------------|---|
| 300                      | 1.103 ± 0.055                             |
| 400                      | 1.103 ± 0.055                             |
| 450                      | 1.083 ± 0.054                             |
| 550                      | 1.083 ± 0.054                             |
| 600                      | 1.098 ± 0.055                             |
| 650                      | 1.108 ± 0.055                             |
| 750                      | 1.128 ± 0.056                             |
| 850                      | 1.148 ± 0.057                             |
| 900                      | 1.160 ± 0.058                             |
| 950                      | 1.170 ± 0.059                             |
| 1050                     | 1.174 ± 0.059                             |
| 1150                     | 1.175 ± 0.059                             |
| 1250                     | 0.179 ± 0.059                             |
| 1350                     | 0.179 ± 0.059                             |

Table A. 4.13: Variation of thermal conductivity with temperature of firing for kaolin material. (Measurements were made at 100°C. Porosity = 38.5 per cent).



| TEMPERATURE °C | THERMAL CONDUCTIVITY<br>$Wm^{-1} °C^{-1}$ |
|----------------|---|
| 17.7           | 1.035 ± 0.052                             |
| 115.0          | 1.091 ± 0.055                             |
| 235.6          | 1.139 ± 0.057                             |
| 378.7          | 1.221 ± 0.061                             |
| 502.0          | 1.266 ± 0.063                             |
| 620.3          | 1.315 ± 0.066                             |

Table A. 4.14: Variation of thermal conductivity with temperature for a Siavaclay brick of Porosity of 29.6 per cent.

| TEMPERATURE °C | THERMAL CONDUCTIVITY<br>$Wm^{-1} °C^{-1}$ |
|----------------|---|
| 15.0           | 1.072 ± 0.054                             |
| 158.2          | 1.030 ± 0.052                             |
| 275.3          | 1.048 ± 0.053                             |
| 387.6          | 1.140 ± 0.057                             |
| 485.0          | 1.195 ± 0.060                             |
| 612.0          | 1.236 ± 0.062                             |
| 763.2          | 1.270 ± 0.064                             |

Table A. 4.15: Variation of thermal conductivity with temperature for Siavaclay brick of porosity of 32.8 per cent.

| TEMPERATURE °C | THERMAL CONDUCTIVITY<br>$Wm^{-1} °C^{-1}$ |
|----------------|---|
| 16.7           | 0.935 ± 0.047                             |
| 141.6          | 1.002 ± 0.050                             |
| 255.0          | 1.045 ± 0.052                             |
| 375.3          | 1.111 ± 0.056                             |
| 508.2          | 1.163 ± 0.058                             |
| 625.3          | 1.205 ± 0.060                             |
| 755.0          | 1.228 ± 0.061                             |

Table A. 4.16: Variation of thermal conductivity with temperature for a Siyacylay brick of porosity of 34.5 per cent.

| TEMPERATURE °C | THERMAL CONDUCTIVITY<br>$Wm^{-1} °C^{-1}$ |
|----------------|---|
| 14.6           | 0.835 ± 0.042                             |
| 112.2          | 0.911 ± 0.046                             |
| 286.7          | 0.965 ± 0.048                             |
| 377.2          | 1.026 ± 0.051                             |
| 488.3          | 1.066 ± 0.053                             |
| 602.2          | 1.100 ± 0.055                             |
| 735.3          | 1.125 ± 0.056                             |

Table A. 4.17: Variation of thermal conductivity with temperature for a Siyacylay brick of porosity of 38.4 per cent.

| TEMPERATURE °C | THERMAL CONDUCTIVITY<br>$Wm^{-1} °C^{-1}$ |
|----------------|---|
| 18.00          | 0.800 ± 0.040                             |
| 115.3          | 0.845 ± 0.042                             |
| 208.2          | 0.880 ± 0.044                             |
| 341.3          | 0.941 ± 0.047                             |
| 476.0          | 0.985 ± 0.049                             |
| 620.4          | 1.040 ± 0.052                             |
| 738.0          | 1.059 ± 0.053                             |

Table A. 4.18: Variation of thermal conductivity with temperature for a Siyaclay brick of porosity of 41.7 per cent.

| TEMPERATURE °C | THERMAL CONDUCTIVITY<br>$Wm^{-1} °C^{-1}$ |
|----------------|---|
| 15.0           | 0.741 ± 0.037                             |
| 123.7          | 0.780 ± 0.039                             |
| 256.0          | 0.840 ± 0.042                             |
| 393.4          | 0.890 ± 0.045                             |
| 514.0          | 0.936 ± 0.047                             |
| 650.0          | 0.975 ± 0.049                             |
| 780.0          | 0.990 ± 0.050                             |

Table A. 4.19: Variation of thermal conductivity with temperature for a Siyaclay brick of porosity of 45.2 per cent.

| TEMPERATURE °C | THERMAL CONDUCTIVITY<br>$Wm^{-1} °C^{-1}$ |
|----------------|---|
| 17.0           | 0.991 ± 0.050                             |
| 124.7          | 1.035 ± 0.052                             |
| 257.3          | 1.167 ± 0.058                             |
| 354.2          | 1.220 ± 0.061                             |
| 416.0          | 1.271 ± 0.064                             |
| 613.3          | 1.395 ± 0.070                             |
| 746.2          | 1.460 ± 0.073                             |

Table A. 4.20: Variation of thermal conductivity with temperature for a fireclay brick of porosity of 35.2 per cent.

| TEMPERATURE °C | THERMAL CONDUCTIVITY<br>$Wm^{-1} °C^{-1}$ |
|----------------|---|
| 14.4           | 0.894 ± 0.045                             |
| 111.0          | 0.959 ± 0.048                             |
| 235.0          | 1.050 ± 0.053                             |
| 369.3          | 1.130 ± 0.057                             |
| 495.0          | 1.215 ± 0.061                             |
| 621.7          | 1.288 ± 0.064                             |
| 721.6          | 1.335 ± 0.067                             |

Table A. 4.21: Variation of thermal conductivity with temperature for a fireclay brick of porosity of 39.5 per cent.

| TEMPERATURE °C | THERMAL CONDUCTIVITY<br>$Mw^{-1} °C^{-1}$ |
|----------------|---|
| 15.4           | 0.775 ± 0.039                             |
| 155.0          | 0.865 ± 0.043                             |
| 276.6          | 0.955 ± 0.048                             |
| 402.3          | 1.030 ± 0.052                             |
| 523.2          | 1.119 ± 0.056                             |
| 655.0          | 1.185 ± 0.059                             |
| 763.3          | 1.235 ± 0.062                             |

Table A. 4.22: Variation of thermal conductivity with temperature for a fireclay brick of porosity of 44.5 per cent.

| TEMPERATURE °C | THERMAL CONDUCTIVITY<br>$Mw^{-1} °C^{-1}$ |
|----------------|---|
| 17.1           | 0.739 ± 0.037                             |
| 118.0          | 0.800 ± 0.040                             |
| 232.3          | 0.875 ± 0.044                             |
| 358.4          | 0.950 ± 0.048                             |
| 489.2          | 1.030 ± 0.052                             |
| 602.7          | 1.090 ± 0.055                             |
| 732.6          | 1.144 ± 0.057                             |

Table A. 4.23: Variation of thermal conductivity with temperature for a fireclay brick of porosity of 47.8 per cent.

| TEMPERATURE °C | THERMAL CONDUCTIVITY<br>$Wm^{-1} °C^{-1}$ |
|----------------|---|
| 25.0           | 2.210 ± 0.111                             |
| 151.7          | 2.398 ± 0.120                             |
| 225.6          | 2.500 ± 0.125                             |
| 316.7          | 2.672 ± 0.134                             |
| 403.2          | 2.840 ± 0.142                             |
| 548.3          | 3.015 ± 0.151                             |
| 633.2          | 3.200 ± 0.160                             |
| 736.7          | 3.310 ± 0.166                             |
| 820.0          | 3.370 ± 0.169                             |

Table A. 4.24: Variation of thermal conductivity with temperature for a Kisii soap stone brick of porosity  $P = 7.64$  per cent.

| TEMPERATURE °C | THERMAL CONDUCTIVITY<br>$Wm^{-1} °C^{-1}$ |
|----------------|---|
| 18.7           | 1.440 ± 0.072                             |
| 113.2          | 1.495 ± 0.075                             |
| 225.4          | 1.561 ± 0.078                             |
| 354.6          | 1.659 ± 0.085                             |
| 482.0          | 1.710 ± 0.086                             |
| 563.2          | 1.782 ± 0.089                             |
| 637.3          | 1.805 ± 0.090                             |
| 765.0          | 1.838 ± 0.092                             |

Table A. 4.25: Variation of thermal conductivity with temperature for a kaolin brick of porosity of 28.4 per cent.

| TEMPERATURE °C | THERMAL CONDUCTIVITY<br>$Wm^{-1} \text{ } ^\circ C^{-1}$ |
|----------------|--|
| 15.6           | 1.312 ± 0.066  |
| 108.0          | 1.350 ± 0.068  |
| 254.7          | 1.465 ± 0.073  |
| 378.3          | 1.520 ± 0.076  |
| 502.7          | 1.612 ± 0.081  |
| 651.2          | 1.658 ± 0.083  |
| 764.0          | 1.698 ± 0.085  |

Table A. 4.26: Variation of thermal conductivity with temperature for a kaolin brick of porosity of 32.6 per cent.

| TEMPERATURE °C | THERMAL CONDUCTIVITY<br>$Wm^{-1} \text{ } ^\circ C^{-1}$ |
|----------------|--|
| 19.0           | 1.239 ± 0.062  |
| 118.7          | 1.239 ± 0.064  |
| 228.2          | 1.369 ± 0.069  |
| 344.3          | 1.415 ± 0.071  |
| 483.2          | 1.500 ± 0.075  |
| 562.3          | 1.548 ± 0.077  |
| 670.6          | 1.569 ± 0.079  |
| 786.2          | 1.591 ± 0.080  |

Table A. 4.27: Variation of thermal conductivity with temperature for a kaolin brick of porosity of 35.3 per cent.

| TEMPERATURE °C | THERMAL CONDUCTIVITY<br>$Wm^{-1} °C^{-1}$ |
|----------------|---|
| 14.3           | 1.135 ± 0.057                             |
| 152.4          | 1.202 ± 0.060                             |
| 283.5          | 1.301 ± 0.065                             |
| 410.7          | 1.359 ± 0.068                             |
| 546.6          | 1.432 ± 0.072                             |
| 633.2          | 1.465 ± 0.073                             |
| 778.7          | 1.498 ± 0.075                             |

Table A. 4.28: Variation of thermal conductivity with temperature for a kaolin brick of porosity of 38.5 per cent

| TEMPERATURE °C | THERMAL CONDUCTIVITY<br>$Wm^{-1} °C^{-1}$ |
|----------------|---|
| 16.6           | 0.943 ± 0.047                             |
| 131.7          | 1.001 ± 0.050                             |
| 268.0          | 1.056 ± 0.053                             |
| 386.3          | 1.132 ± 0.057                             |
| 511.7          | 1.181 ± 0.061                             |
| 758.0          | 1.238 ± 0.062                             |

Table A. 4.29: Variation of thermal conductivity with temperature for a kaolin brick of porosity of 46.0 per cent.



APPENDIX A.5: MORE FIGURES ON VARIATION OF THERMAL CONDUCTIVITY WITH THE FACTORS CONSIDERED IN THE STUDY

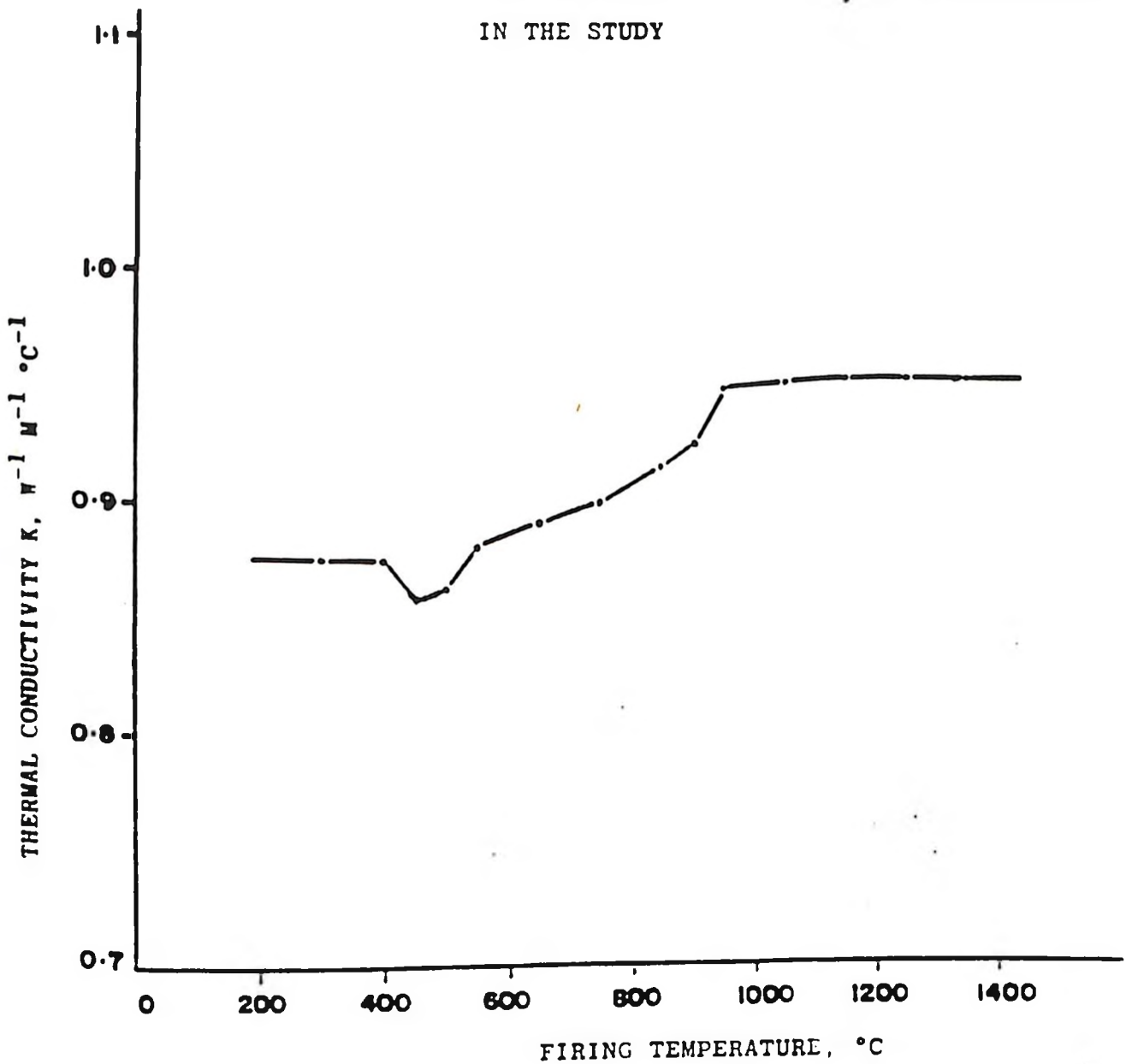


FIGURE A 5.1: VARIATION OF THERMAL CONDUCTIVITY WITH FIRING TEMPERATURE FOR FIRECLAY MATERIAL (Measurements made at  $100^{\circ}\text{C}$ . Porosity = 39.5%)

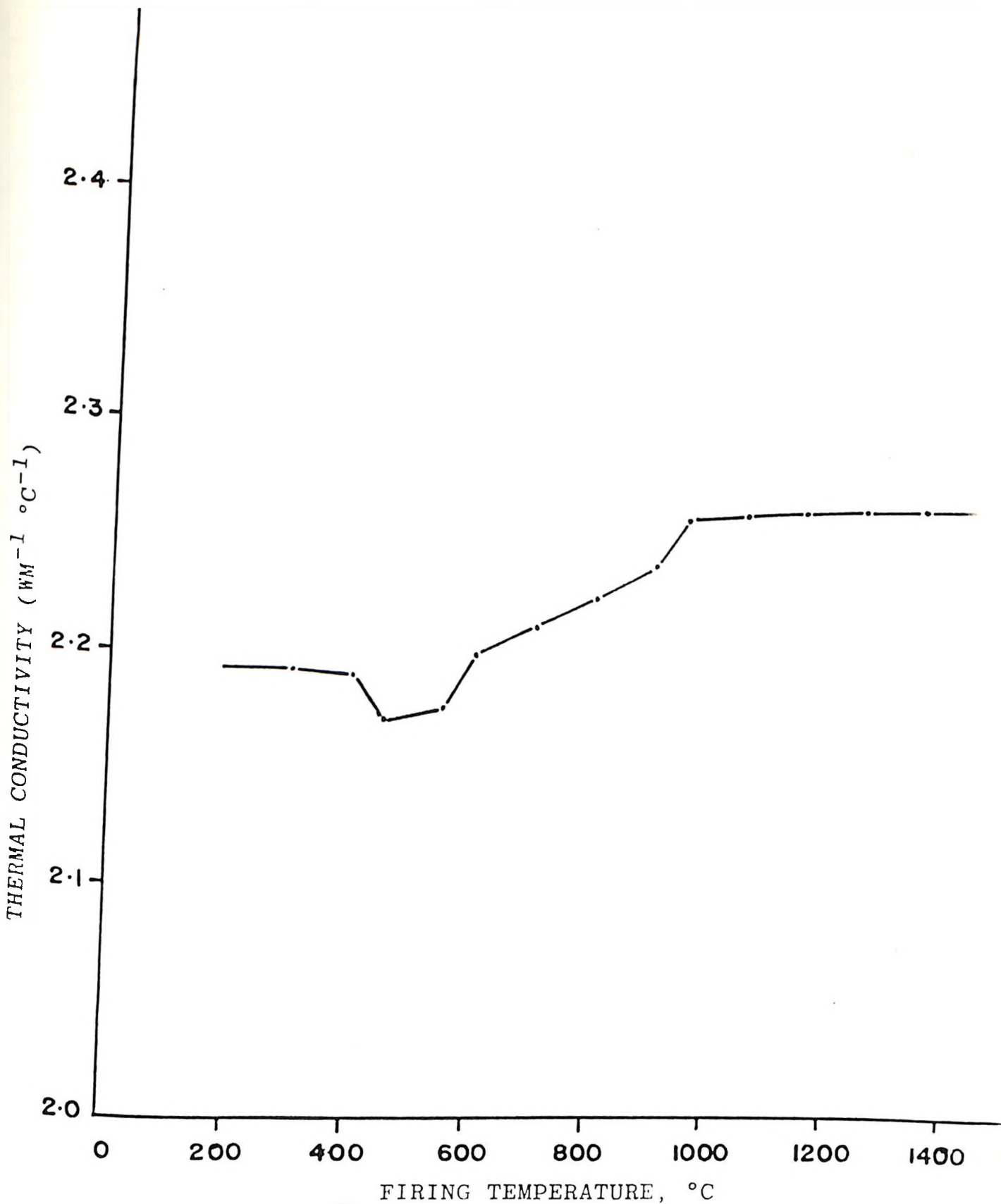


FIGURE A 5.2: VARIATION OF THERMAL CONDUCTIVITY WITH FIRING TEMPERATURE FOR KISII SOAP STONE MATERIAL (Measurements made at 100°C, Porosity = 7.64%).

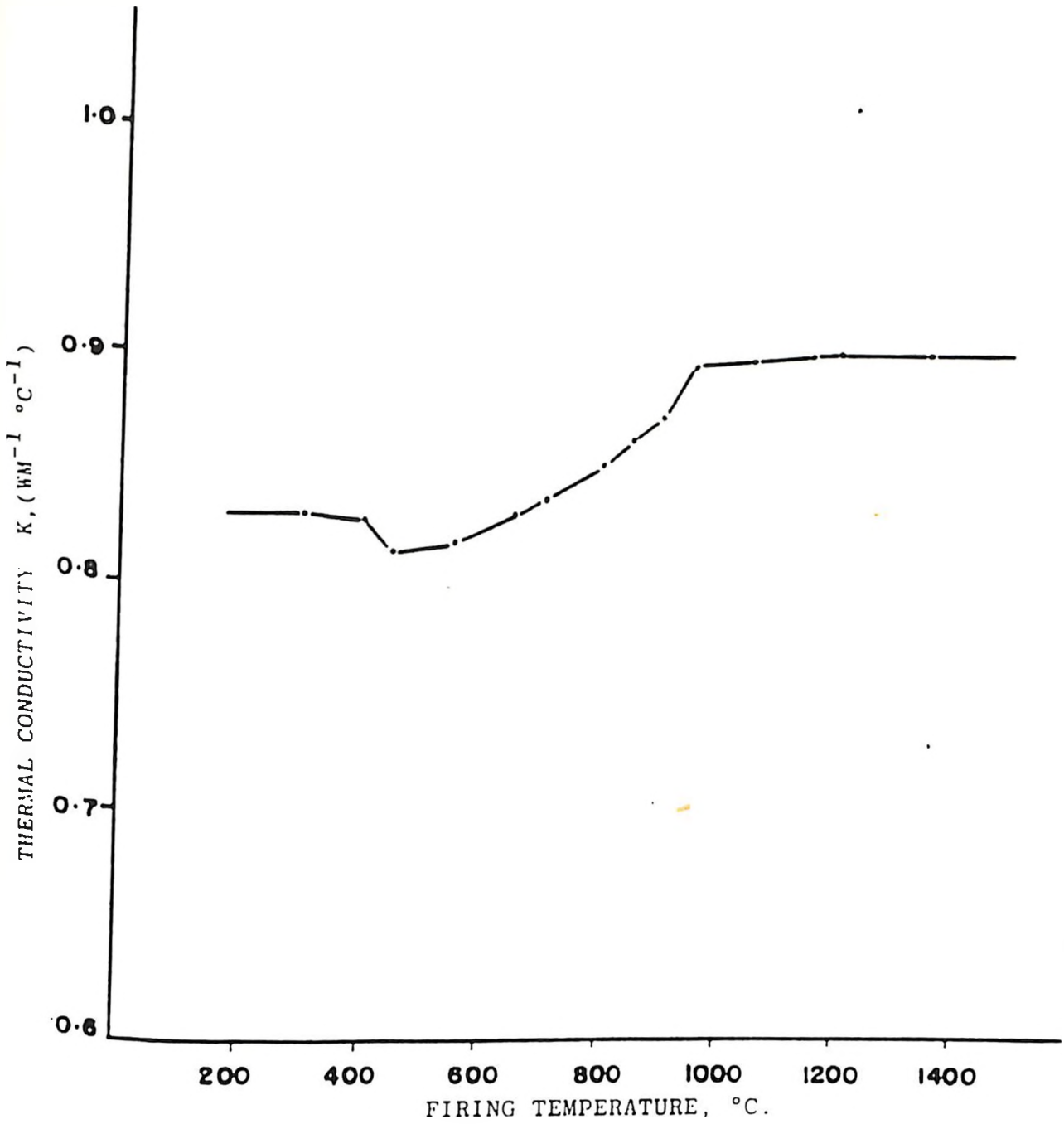


FIGURE A 5.3: VARIATION OF THERMAL CONDUCTIVITY WITH FIRING TEMPERATURE FOR SIAYA CLAY MATERIAL.

(Measurements made at 100°C. Porosity = 38.5%)

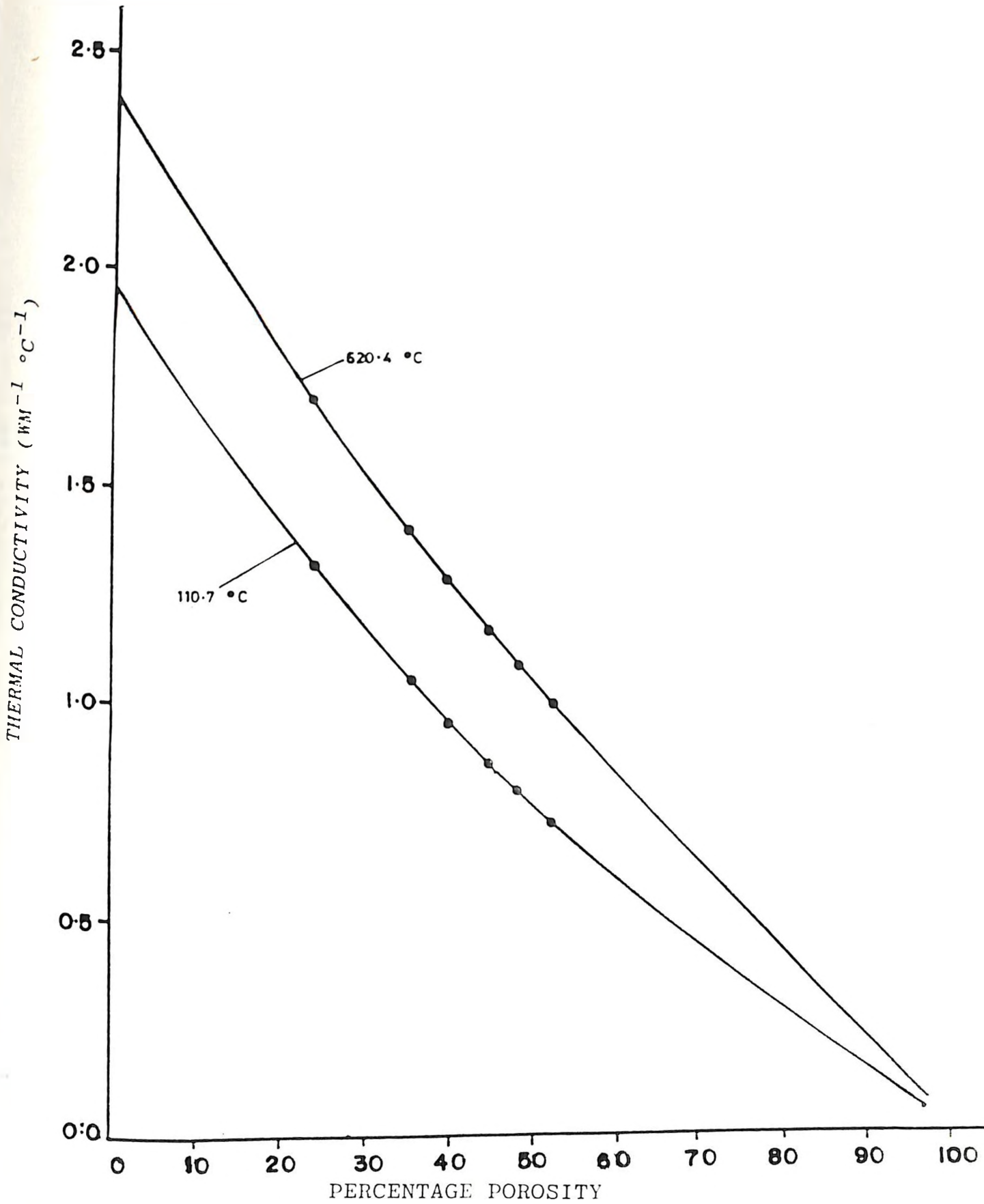


FIGURE A 5.4: THERMAL CONDUCTIVITY AGAINST PERCENTAGE POROSITY  
FOR FIRECLAY AT TEMPERATURES A = 110.7°C AND  
B = 620.4°C

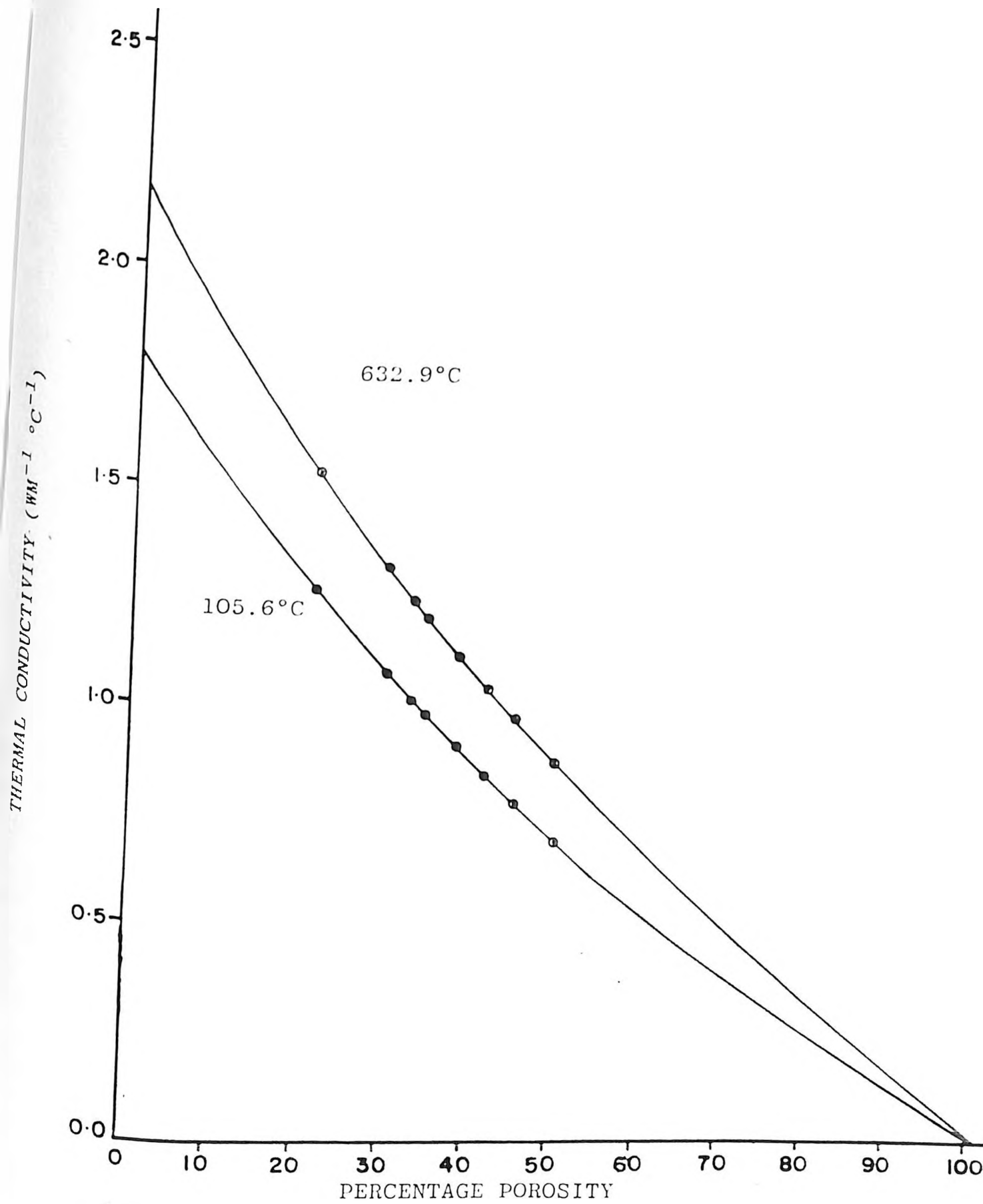


FIGURE A 5.5: THERMAL CONDUCTIVITY AGAINST PERCENTAGE POROSITY  
FOR SIAYA CLAY AT TEMPERATURES A = 105.6°C AND  
B = 632.9°C

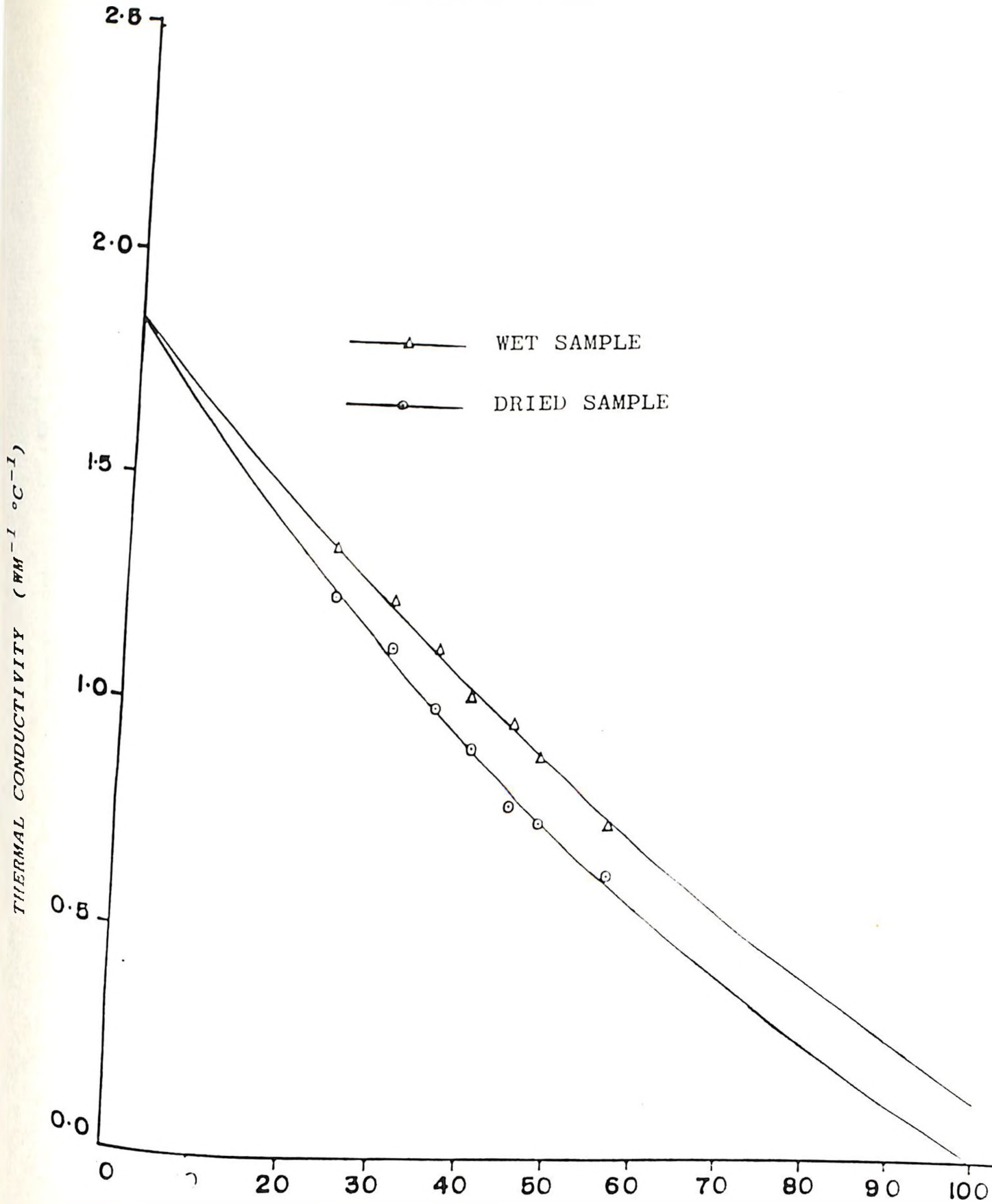


FIGURE A 5.6: THERMAL CONDUCTIVITY AGAINST PERCENTAGE POROSITY FOR A DRIED SAMPLE AND A WET SAMPLE OF FIRECLAY AT 30°C

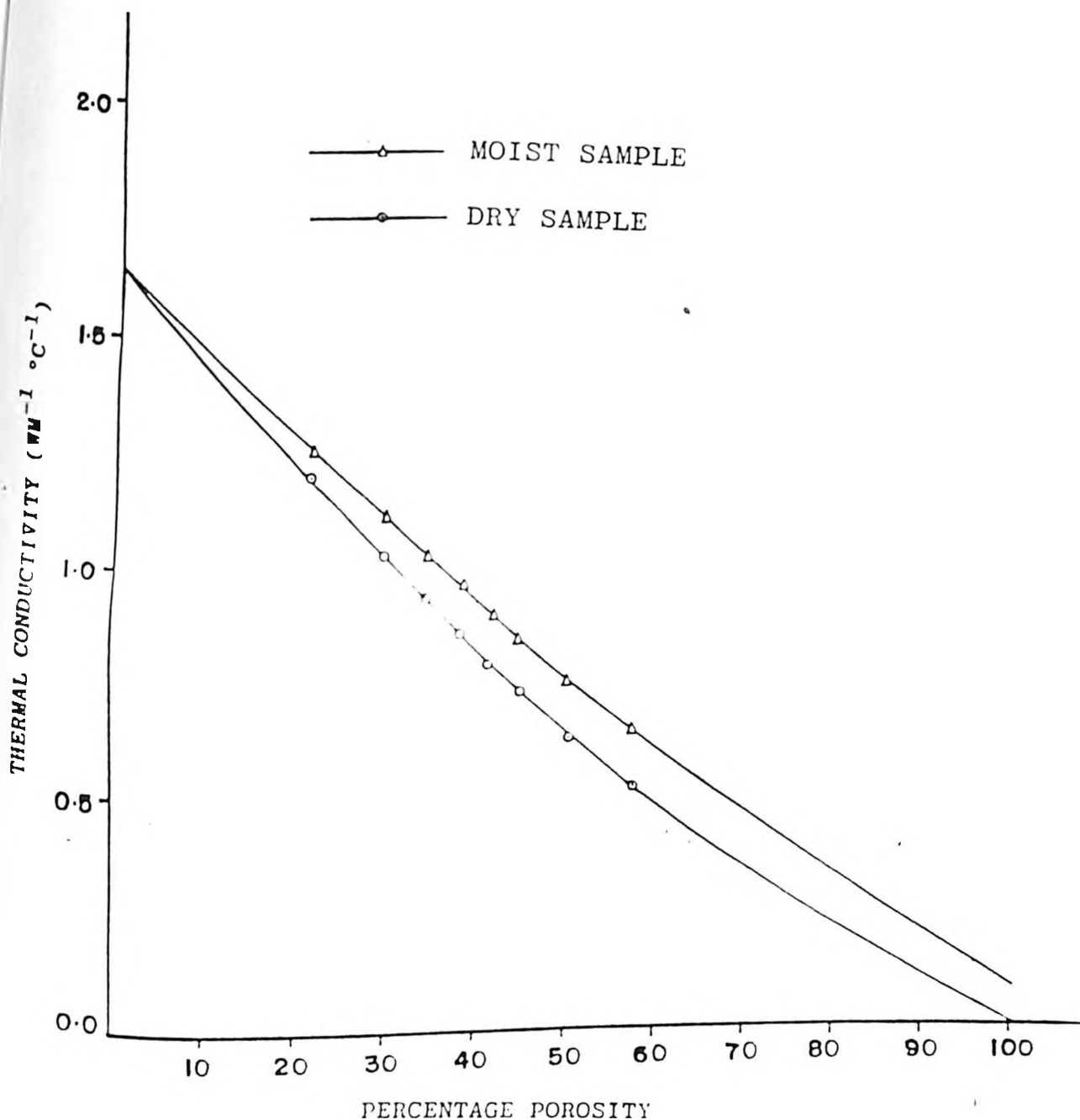


FIGURE A 5.7. THERMAL CONDUCTIVITY AGAINST PERCENTAGE POROSITY FOR SIAYA CLAY DRIED SAMPLE AND MOIST SAMPLE AT 33.3°C

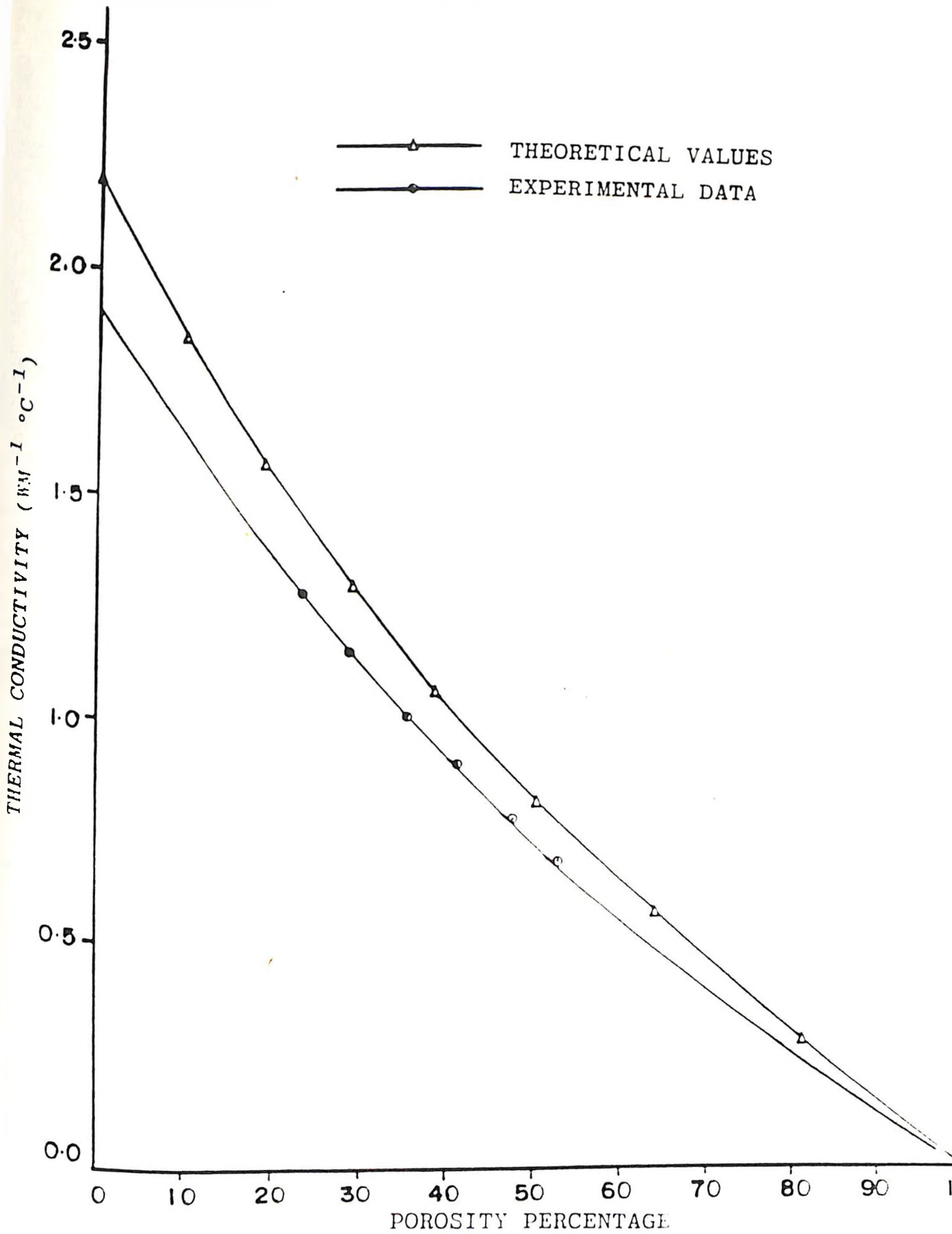


FIGURE A 5.8: COMPARISON BETWEEN THEORETICAL PREDICTION AND  
EXPERIMENTAL DATA FOR SIAYA CLAY AT 105.6°C



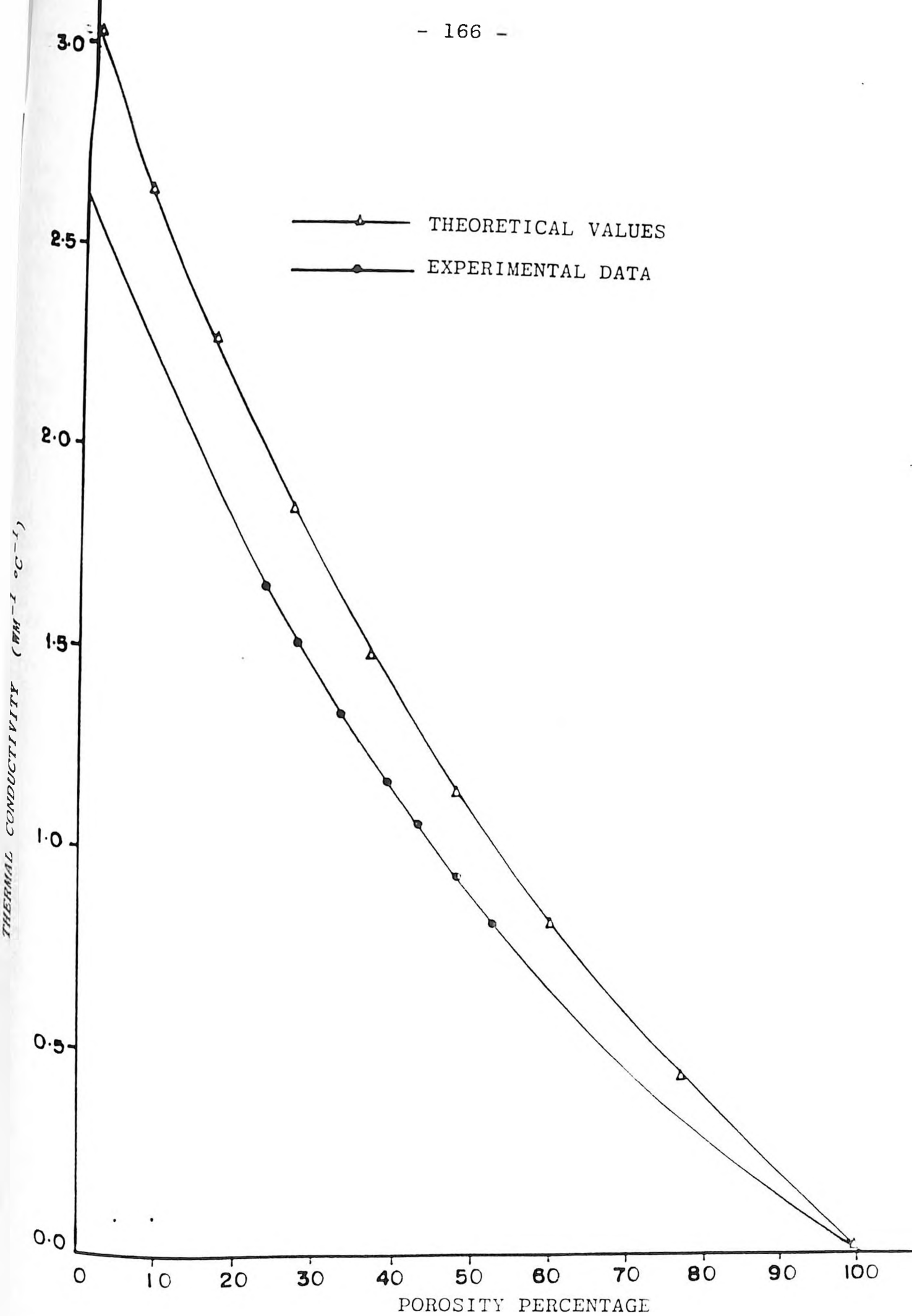


FIGURE A 5.9. COMPARISON BETWEEN THEORETICAL PREDICTION AND EXPERIMENTAL DATA FOR KAOLIN AT 113.4°C

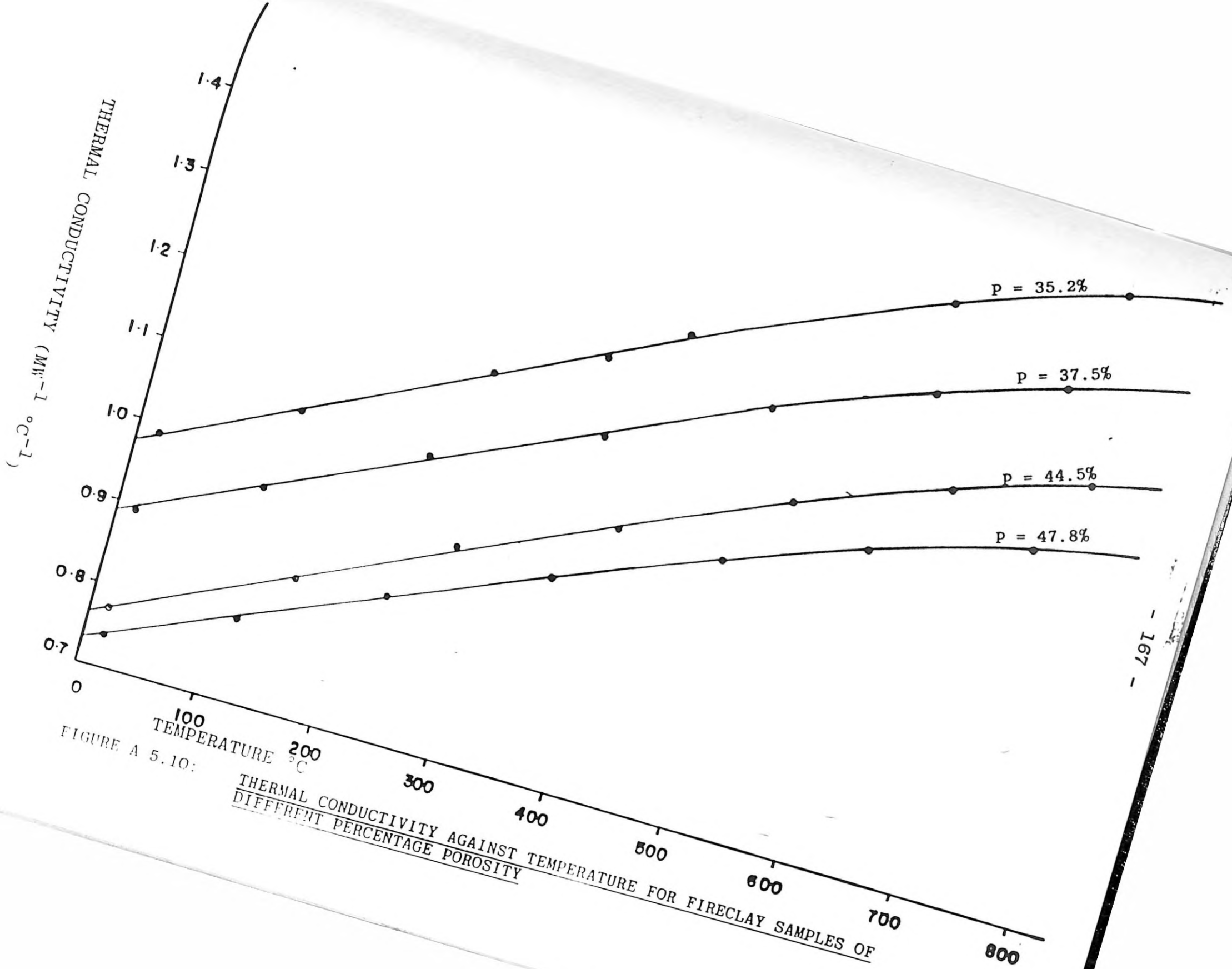


FIGURE A 5.10:

THERMAL CONDUCTIVITY AGAINST TEMPERATURE FOR FIRECLAY SAMPLES OF DIFFERENT PERCENTAGE POROSITY

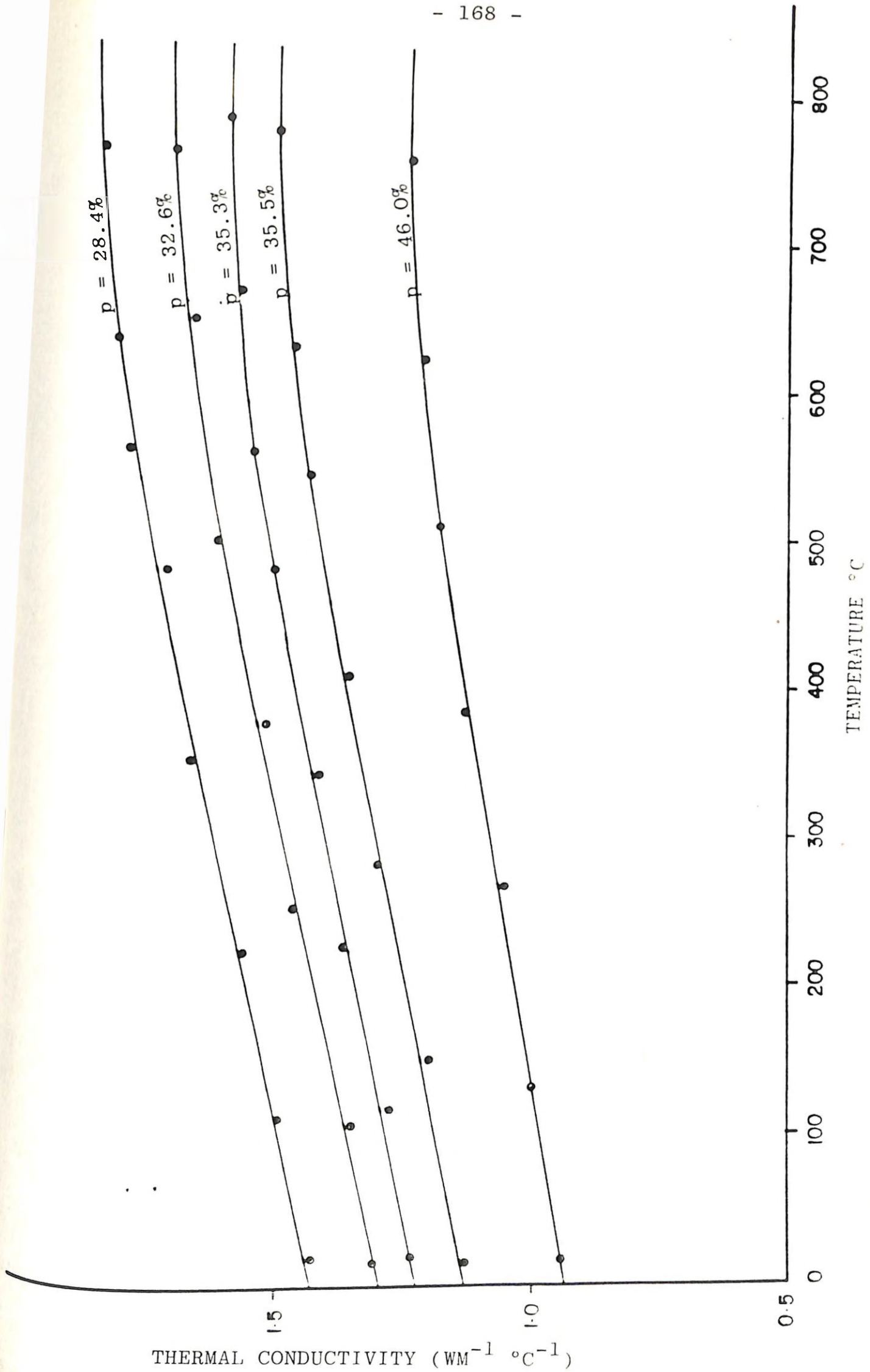


FIGURE A 5.11: THERMAL CONDUCTIVITY AGAINST TEMPERATURE FOR KAOLIN SAMPLES OF DIFFERENT PERCENTAGE MOISTURE

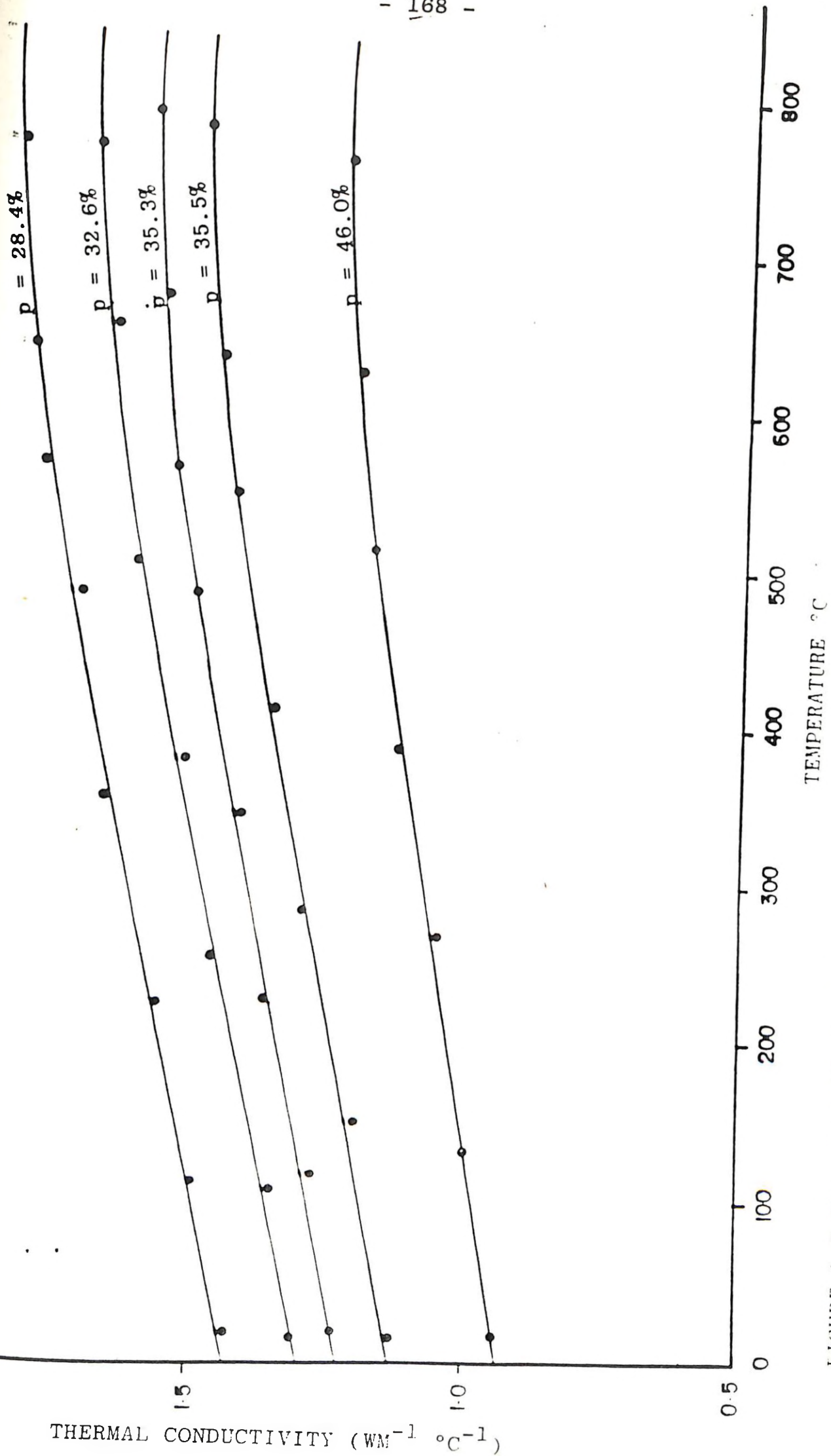


FIGURE A 5.11: THERMAL CONDUCTIVITY AGAINST TEMPERATURE FOR KAOLIN SAMPLES OF DIFFERENT PERCENTAGE POROSITY

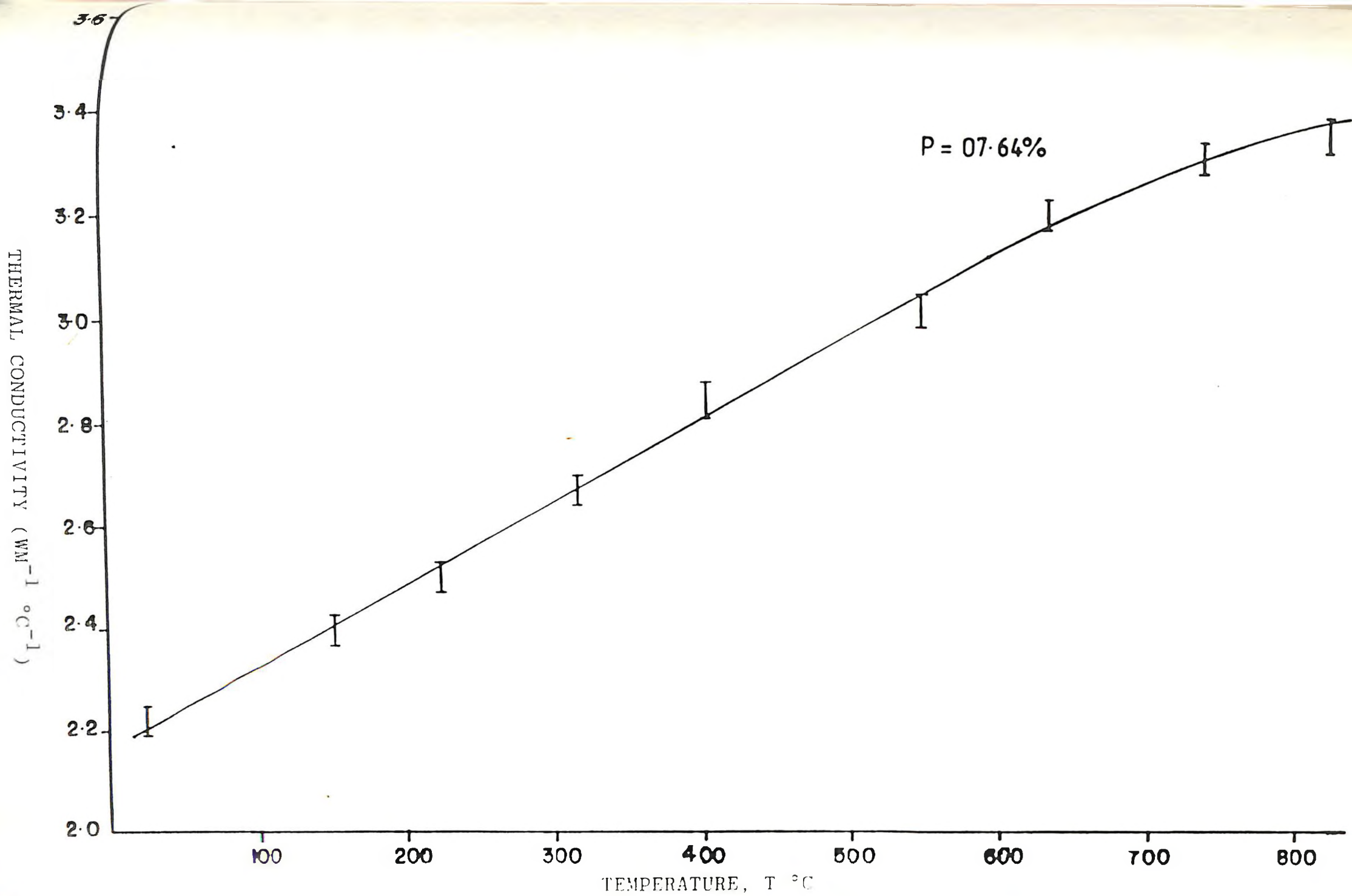


FIGURE A 5.12: THERMAL CONDUCTIVITY AGAINST TEMPERATURE FOR KISI STONE

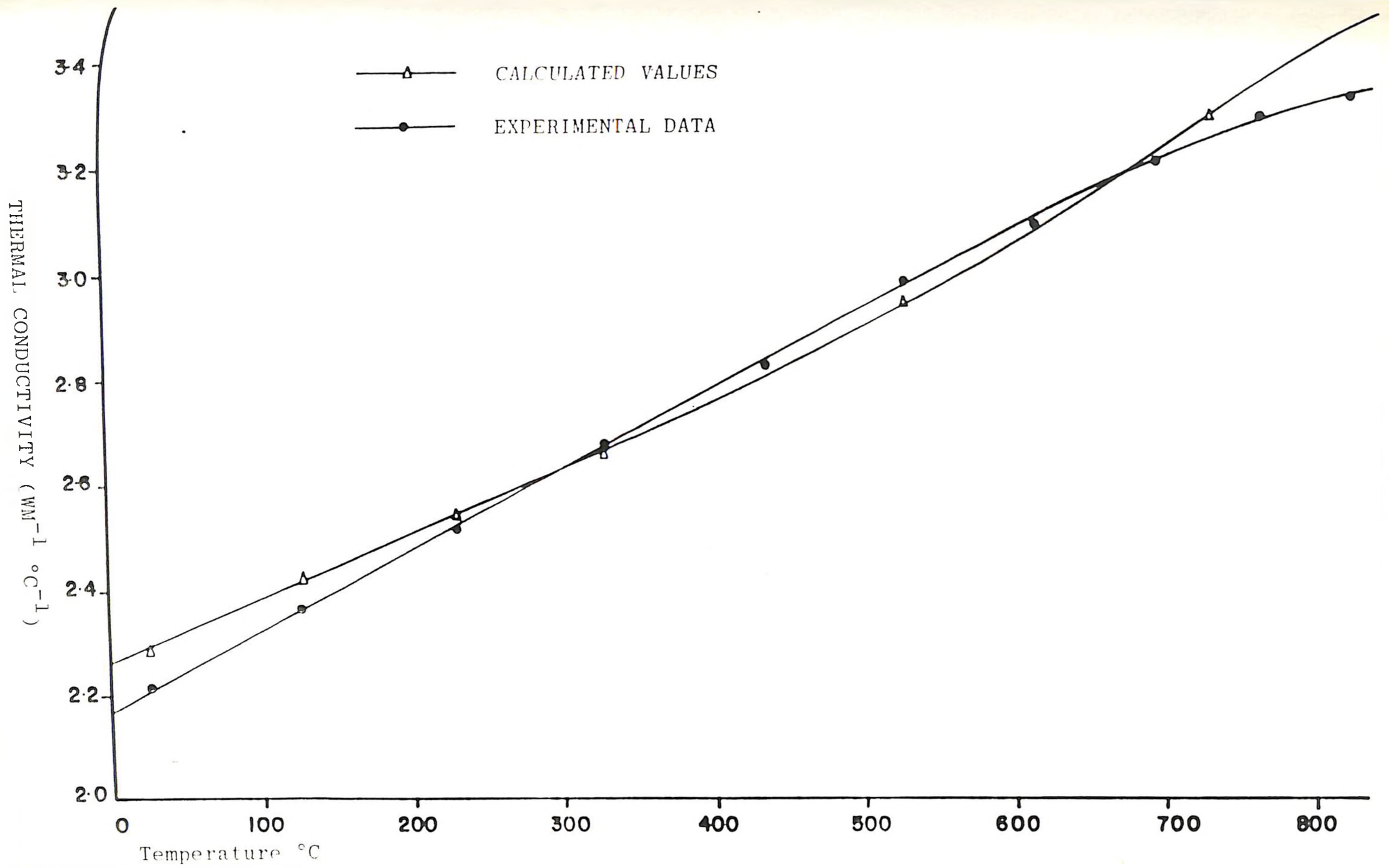


FIGURE A 5.13: THERMAL CONDUCTIVITY AGAINST TEMPERATURE FOR KISII STONE OF  
POROSITY P = 0.01

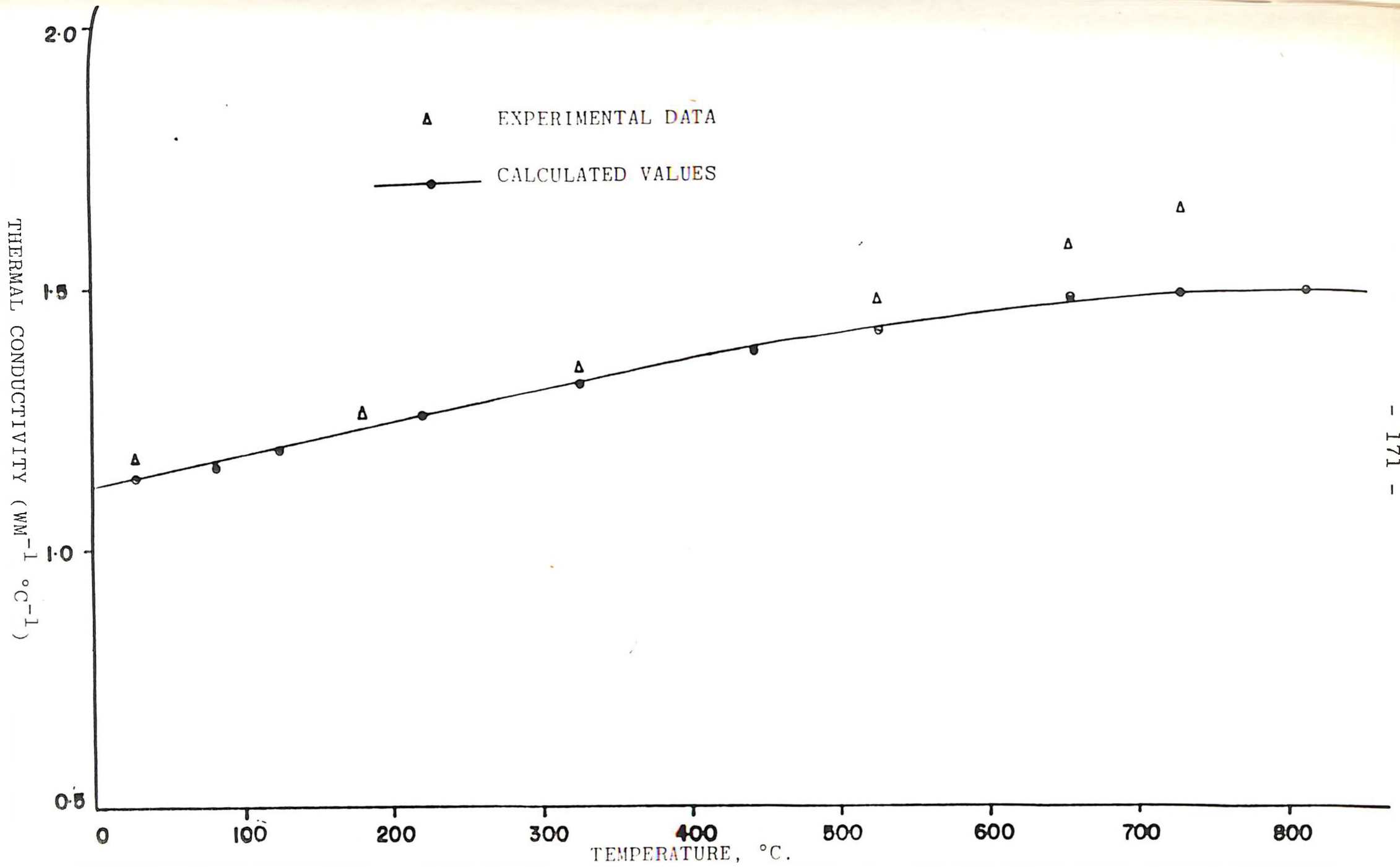


FIGURE A 5.14: THERMAL CONDUCTIVITY AGAINST TEMPERATURE (Experimental and calculated values) for kaoline of p = 38.5%

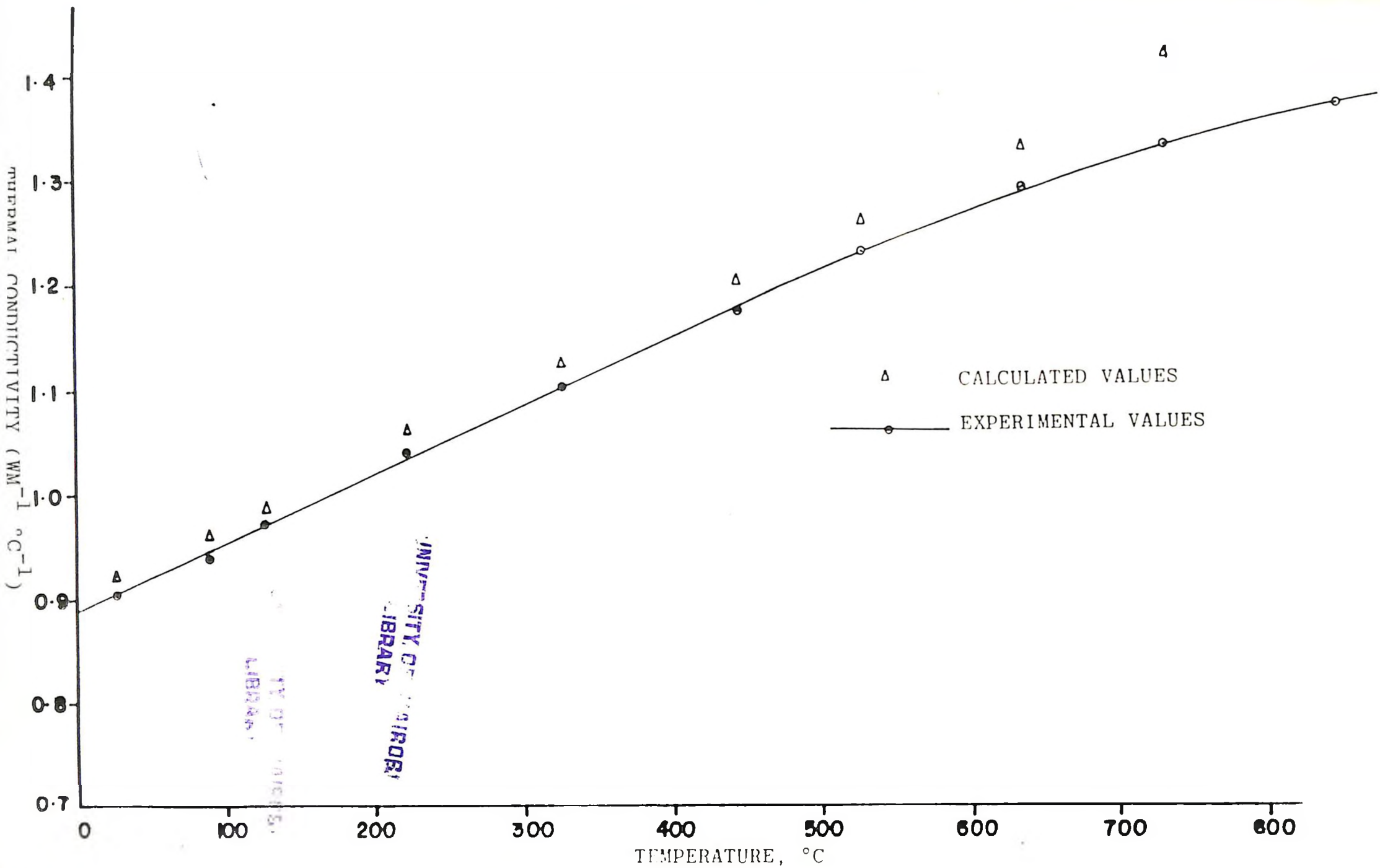


FIGURE A 5.15: THERMAL CONDUCTIVITY AGAINST TEMPERATURE FOR FIRECLAY OF POROSITY  $p = 39.5\%$